

Evaluation of Technology to Support A Heavy-Duty Diesel Vehicle Inspection And Maintenance Program

**Principal Investigators
Nigel N. Clark & Mridul Gautam**

**Department of Mechanical & Aerospace Engineering
College of Engineering and Mineral Resources
West Virginia University
Morgantown, WV.**

EXECUTIVE SUMMARY

The desire to establish a heavy-duty I&M program in the State of California is to support the California State Implementation Plan, measure M-17, "Further Emissions Reductions from Heavy-duty Engines." The thrust is to identify gross emitters, particularly high NO_x emitters, and hence reduce their contribution to the emissions inventory, leading ultimately to improvements in air quality. Objectives of this study included identification of a suitable system that would both identify high emitters and realistically quantify emissions from in-service vehicles (System 1) and of a suitable system only for detection of gross emitters (System 2).

Dynamometers

Heavy-duty vehicles are not at present certified holistically for emissions, but rather their engines are certified to meet energy-specific emissions output levels. For I&M, it will be necessary to operate a vehicle on a chassis dynamometer and to draw power from the vehicle drive wheels through rollers. These dynamometers may be equipped with flywheels, and may use a variety of power absorbers. Most suitable for both single and tandem drive axle applications is a six-roller configuration, using rollers of 16 to 20 inches in diameter, air-cooled eddy-current power absorbers, and no flywheels. Units of this type are commercially available, and include computer-managed control, data acquisition and driver's screen prompt.

Exhaust Sampling

Although raw exhaust can be sampled, dilute exhaust is preferred to avoid condensation in lines and analyzers. Exhaust can be diluted using full-scale constant flow tunnels, proportional sampling mini-tunnels and constant dilution ratio mini-tunnels. The proportionally sampling mini-tunnel requires accurate measurement of exhaust gas flow (which is a difficult task) and knowledge of time alignment of signals. For System 1 to provide quantitative emissions data in units of g/mile, a proportional sampling mini-tunnel is recommended. For System 2 to provide a criterion level for gross emitters in units of g/gallon of fuel, a constant dilution ratio mini-tunnel is proposed. Both the gas analyzers and particulate matter (PM) measurement devices should draw from these tunnels. For the exhaust flow must be known. Methods for measuring exhaust flow include a variety of differential pressure devices, including the venturi, and vortex shedding devices and tracer gas methods. It was concluded that a system based on the Annubar device with differential pressure measurement was robust and most suitable.

Gas Analysis

A review of gas sensors and analyzers has revealed that light-duty I&M analyzers are unsuited for heavy-duty diesel application. In particular, these light-duty units fail to account for nitrogen dioxide in the exhaust, are typically formulated to record far higher levels of carbon monoxide (CO) than diesel vehicles produce, and examine a hydrocarbon spectrum that is not representative of species in diesel exhaust. It is recommended that research (laboratory) grade analyzers are used, with CO and carbon dioxide determined using non-dispersive infra-red analyzers, with oxides of nitrogen measured using a chemiluminescent analyzer and with hydrocarbons quantified using a flame ionization detector.

Particulate Mater Measurement

Certification procedures for diesel engines require the use of conditioned filters to determine PM mass gravimetrically, but this approach is too cumbersome and time-consuming for I&M application. A review of PM characterization instruments has revealed a wide variety of instruments that count particles or provide for size segregation, but only the Tapered Element Oscillating Microbalance (TEOM) provides for real-time PM measurement. The TEOM shows acceptable correlation with the conventional filter method when averaged over a cycle, and methods are being developed to improve TEOM signals to gain instantaneous PM data. Opacity meters were also examined. Opacity was found to be more suited as a screening tool than as a means to quantify PM mass.

Cost

Cost of the final system that could quantify emissions (System 1) was estimated by summing the cost of major components, and by considering integration and development costs spread over a minimum of 10 units. This cost was \$331,500. Cost for System 2, that could be used to detect high emitters, was \$241,000; with the primary difference being the lack of exhaust flow measurement and proportional mini-tunnel flow control. Itemized costs were determined in May 2001. Based upon experience with existing dynamometer systems, emissions measurement accuracy of 10% would be expected.

TABLE OF CONTENTS

EXECUTIVE SUMMARY.....	i
Table of Contents.....	iii
List of Figures.....	v
List of Tables.....	vi
1 INTRODUCTION AND OBJECTIVES.....	1
2 EXISTING INSPECTION AND MAINTENANCE PROGRAMS.....	2
3 BROAD REVIEW OF TECHNOLOGY OPTIONS.....	3
3.1 Methods Of Vehicle Loading.....	3
3.2 Measurement Of Gaseous Concentration.....	4
3.2.1 Polarographic Analyzers.....	5
3.2.2 Electrochemical Analyzers.....	6
3.2.3 Chemiluminescent Analyzers.....	7
3.2.4 Fluorescence Analyzers.....	8
3.2.5 Flame Photometric Analyzers.....	8
3.2.6 Heated Flame Ionization Detectors.....	8
3.2.7 Non-Dispersive Infrared Analyzers.....	9
3.2.8 Non-Dispersive Ultraviolet Photometers.....	10
3.2.9 General Commentary on Available Sensors.....	10
3.2.10 I&M Gas Concentration Instruments Overview.....	11
3.2.11 Fourier Transform Infrared Spectroscopy.....	13
3.2.12 Miniature Gas Chromatographs.....	13
3.2.13 Research-Grade Analyzers.....	13
3.2.14 Sample Conditioning Issues.....	13
3.3 Measurement of Particulate Matter.....	14
3.3.1 Scanning Mobility Particle Sizer.....	14
3.3.2 Electric Low Pressure Impactor.....	15
3.3.3 Quartz Crystal Microbalance.....	16
3.3.4 Sensors' METS 3200.....	16
3.3.5 Micro-Orifice Uniform Deposit Impactor.....	17
3.3.6 Cyclones.....	18
3.3.7 High Volume PM 10/2.5/1.0 Trichotomous Sampler.....	18
3.3.8 Photoelectric Aerosol Sensor.....	18
3.3.9 DustTrak TSI Model 8520.....	18
3.3.10 Tapered Element Oscillating Microbalance.....	19
3.3.11 Opacity Measurement.....	35
3.3.12 Description of Commercially Available Opacity Meters.....	36
CONFIGURATION EFFECTS ON COMPUTATIONS.....	47
3.4 Time Alignment.....	48
3.5 Diffusion In Measurement Systems.....	51
4 EXHAUST DILUTION.....	52

5	MEASUREMENT OF VEHICLE EXHAUST FLOW	55
5.1	Background	55
5.2	Flow Rate Range	56
5.3	General Discussion of Flow Sensors	56
5.4	Humidity Effects	57
5.5	Pressure Head Flow Sensors	57
5.6	Tracer Gas Method.....	58
5.7	Turbine Sensors	59
5.8	Ultrasonic Flow Sensors	59
5.9	Vortex Shedding Sensors	59
5.10	Hot Wire Anemometers	60
5.11	Estimation From Engine Parameters.....	60
5.12	Preferred Technology.....	60
6	ISSUES OF PORTABILITY	61
7	RECOMMENDATIONS	61
7.1	Reported Units	61
7.2	Comments on Test Cycle	62
7.3	Proposed Systems	63
8	Cost Estimation for I&M SYSTEMS	66
8.1	System Price Totals.....	66
8.1.1	System 1	67
8.1.2	System 2.....	68
	References.....	69
9	ACKNOWLEDGEMENTS	71

LIST OF FIGURES

Figure 3.4-1a. TEOM flow schematic.	20
Figure 3.4-1b. TEOM tapered element free end and filter.....	20
Figure 3.4-2. Real-time engine PM from a Navistar 7.3-l engine.....	21
Figure 3.4-3. Integrated TEOM PM as a function of filter-captured PM.	22
Figure 3.4-4. Temperature effects on TEOM data.....	27
Figure 3.4-5. Flow rate effects on TEOM data.	29
Figure 3.4-4. Static TEOM filter response to ambient relative humidity.	31
Figure 3.4-5. Dynamic TEOM filter response to transient relative humidity.	33
Figure 3.4-6. Original and moisture-corrected TEOM data.....	34
Figure 3.5-1. Electromagnetic wave interaction with a particle.	37
Figure 3.5-2. Bosch and Wager peak opacity values from a snap-acceleration test.	38
Figure 3.5-3. Wager peak opacity plotted as a function of Bosch peak opacity.	39
Figure 3.5-4. PM mass as a function of integrated opacity from snap-acceleration tests.	42
Figure 3.5-5. PM mass as a function of integrated opacity from loaded and non-loaded transient chassis tests	43
Figure 3.5-6. PM mass as a function of integrated opacity from a single vehicle exercised through different transient chassis tests.	44
Figure 3.5-7. PM mass as a function integrated opacity from the same vehicle and driving cycle at different simulated inertial loads.	45
Figure 3.5-8. PM mass as a function of integrated opacity for all tests.	46
Figure 4.1-1. Exhaust mass flow rate and raw NO _x concentration from the MEXA (NPIR) and electromechanical sensor.	49
Figure 4.1-2. Determination of time delay using cross-correlation	56
Figure 4.1-3. Figure 5.1-1 data after adjusting for time delay.	51
Figure 4.2-1. Dilution tunnel dispersive effects.....	51
Figure 4.2-2. Application of dispersion model.	52
Figure 8.2-1. System 1 exhaust flow schematic.....	65
Figure 8.2-2. System 2 exhaust flow schematic.....	65

LIST OF TABLES

Table 3.4-1. TEOM and PM results from a Navistar T444E engine.	26
Table 3.4-2. TEOM and PM results from a Cummins engine.	26
Table 3.4-3. Real-time PM/water collection evaluation for varying air temperature.	27
Table 3.4-4. Flow rate effects on the TEOM/PM mass ratio.	28
Table 3.4-5. Temperature effects on the TEOM PM/water ratio.	29
Table 3.4-6. Comparison of old and new TEOM filters 70 mm filter data.	34
Table 4.1-1. Time alignment effects on emissions mass measurement.	49
Table 8.1-1. Cost itemization of System 1 as of May 2001.	67
Table 8.1-2. Cost itemization of System 2 as of May 2001.	68

1 INTRODUCTION AND OBJECTIVES

This report specifically addresses the measurement of emissions relevant to an inspection and maintenance (I&M) program for heavy-duty vehicles in the State of California. The desire to establish a heavy-duty I&M program is to support the California State Implementation Plan, measure M-17, "Further Emissions Reductions from Heavy-duty Engines." The thrust is to identify gross emitters and hence reduce their contribution to the emissions inventory, leading ultimately to improvements in air quality.

The objectives of the report are:

1. To review vehicle loading techniques and emissions measurement techniques relevant to I&M.
2. To identify a suitable system for detection of gross emitters.
3. To identify a suitable system that can realistically quantify emissions from in-service vehicles and identify gross emitters.

Heavy-duty vehicles are not at present certified holistically for emissions, but rather their engines are certified to meet energy-specific emissions output levels. The engines must also meet these levels for a specified lifetime, through the establishment of maximum deterioration factors. A program which seeks to examine whether heavy-duty engines do meet emissions levels over their prescribed lifetime would be termed a compliance program and would, of necessity, be required to employ a certification test to evaluate the engines. It is not the objective of this report to identify systems for evaluation of compliance. It is true that screening tests may be developed to identify engines likely to fail certification, but these screening tests would need to be closely related to, or correlated with, the certification test if the program is to be successful. Such correlation is difficult to establish through either science or law.

Correlation between an I&M test and certification would require that the I&M procedure explore all engine behaviors seen during certification. Previously, for light duty I&M, the I/M 240 test was compared with the FTP-75 certification test. A similar process might be followed for heavy-duty I&M, but it is complicated by the fact that heavy-duty engines are certified independently. This is in contrast to an I&M procedure that specifically seeks to mimic in-use vehicle behaviors.

An I&M program seeks to establish a procedure whereby emissions from vehicles can be reduced by identifying high emitters and causing them to be repaired or improved. If the I&M program is to be successful in improving the environment, then the vehicles must be challenged in a manner that reasonably represents their use in real operation, or in a manner that elicits some engine behavior that is typical of high emission modes in real operation.

An I&M program may coincidentally provide emissions inventory information if it employs test schedules that mimic real use, or it may provide limited useful inventory information if only certain engine behaviors are examined to determine gross emitters.

In this report, the emissions of concern are particulate matter (PM), oxides of nitrogen (NO_x), hydrocarbons (HC) and carbon monoxide (CO). From both an inventory and I&M perspective, PM and NO_x are the species of major interest for heavy-duty diesel vehicles, but there is increasing interest in both gaseous and PM-bound HC due to concern over toxic air contaminants. NO_x is associated with smog formation, while PM is a named toxic air contaminant and is implicated in human health effects.

This report examines in detail the hardware needed to affect I&M programs, and considers choices of dynamometer systems, PM measurement systems, gaseous emissions measurement systems, and exhaust gas dilution apparatus.

2 EXISTING INSPECTION AND MAINTENANCE PROGRAMS

Light-duty vehicle I&M is more mature than heavy-duty I&M. In contrast to heavy-duty vehicles, light-duty vehicles are certified as a whole, using a chassis dynamometer, exhaust dilution system and laboratory grade analyzers to measure dilute exhaust either directly or from bags. During emissions certification, the vehicle is driven through a cycle (such as the FTP-75) designed to mimic real world driving conditions. Recently, more challenging cycles have been added to the certification repertoire that include high acceleration rates, high speeds and air conditioning load. Since the light-duty vehicles are certified using a chassis dynamometer, I&M processes may be more readily derived from certification processes than in the heavy-duty case.

In many regions of the US, I&M has been performed on light-duty vehicles by determining exhaust gas composition under idle or high idle conditions, without the aid of a dynamometer to load the vehicle, and this is certainly successful in identifying high CO emissions from rich idle conditions. More recently, some regions have replaced tailpipe idle measurement with loaded dynamometer tests, employing cycles such as the IM240, which is argued to represent an abbreviated certification FTP-75. The design and construction of dynamometers and emissions measuring equipment for these loaded tests is now well established, and a number of emissions measurement systems is approved for use by the Bureau of Automotive Repair in California.

The use of loaded vehicle I&M in light-duty applications has certainly been facilitated by the certification procedure, but this connection is lacking in heavy-duty applications. Although chassis dynamometer based emissions measurement has become established over the last decade, heavy-duty measurements have been geared to evaluations of technology and fuels, rather than inspection and maintenance. Laboratories used for this purpose have employed research grade equipment and measurement has been associated with high cost.

Previous I&M for heavy-duty vehicles has been limited to measurement of smoke opacity from the vehicle exhaust tailpipe or stack. Although some Asian programs and the States of Arizona (Pima County) and Colorado load the vehicle while evaluating smoke, generally opacity has been measured during a snap-acceleration or “snap-idle” test. In the snap-acceleration test, the engine experiences momentary load associated with acceleration of its internal components as the engine speed is rapidly increased. A rigorous snap-acceleration test protocol is presented in Society of Automotive Engineers (SAE) Surface Vehicle Recommended Practice J1667 (SAE, 1996). The

snap-acceleration operation does not mimic real world operation, although it can elicit PM “puff” that occurs during transient over fueling. It is widely acknowledged that opacity does not provide quantitative prediction of particulate matter mass, but that it can screen for high emitters. In addition, there is a well-established tradeoff between NOx and PM as injection timing of the diesel engine is changed. Snap-idle opacity testing is therefore unlikely to reduce NOx production from heavy-duty vehicles in a region.

3 BROAD REVIEW OF TECHNOLOGY OPTIONS

Section 3 presents the reviews of the technologies available to load the vehicle, measure the emissions concentrations and exhaust flow, and translate the data gathered into comparative values. All considered methods of loading the vehicle require the use of rollers, but there is a choice as to whether to use flywheels or not. There is also a choice for power absorber. AC, DC, eddy-current and water brake dynamometers are all employed by industry. A wide variety of instruments is available to determine gas concentrations. However, for diesel applications research grade analyzers are favored. PM characterization and opacity meters are reviewed, but only the TEOM offers real-time mass measurement suitable for diesel I&M application.

3.1 Methods Of Vehicle Loading

This report is based on the assumption that measurements of emissions will be made with the engine installed in the vehicle, using a chassis dynamometer system.

To elicit emissions which are sufficiently representative of real use, or that elicit engine behaviors that are typical of real use, the vehicle must be loaded using a chassis dynamometer to apply load to the rear wheels. An exception is the snap-acceleration test, where the inertia of the internal engine components is used to provide a fleeting load to the engine as engine speed is increased, but the snap-acceleration test is therefore limited in the engine behaviors that it can examine.

Conceivable dynamometer configurations include rollers to apply the load to the wheels, and these rollers might be connected to:

1. Flywheels alone
2. Motoring AC or DC dynamometers
3. Eddy-current dynamometers
4. Water brake dynamometers
5. Combinations of flywheels with any of the dynamometers presented above

Flywheels are able to provide a retarding force during vehicle acceleration if used alone, but provide no load during steady state operation. They would, therefore, be useful only in a loaded acceleration test. Such an acceleration test could examine vehicle acceleration, and include the changing of gears, or acceleration while a single gear is engaged, with the engine increasing in speed from idle to rated speed. This “loaded engine acceleration” test using a single gear cannot be conducted on automatic vehicles where the vehicle cannot be held in a single gear. Flywheels

offer the detraction that either all testing must be conducted at a single inertia, or that flywheel sets must be used, with elements that can be engaged or disengaged mechanically.

Motoring AC or DC dynamometers are the most versatile power absorbers. They are able both to absorb power and to act as a motor and are widely used for diesel engine emissions certification and testing. However, it is unlikely that motoring emissions are of interest in examining a diesel fleet, except perhaps in examining “white smoking” in old technology engines. The AC or DC dynamometer, if used over a vehicle speed-time cycle, may prove unable to mimic full load on the vehicle in low gear (at low road speeds) due to limits in torque available from the dynamometer. The AC or DC dynamometer could also be used to exercise the engine through a speed-torque cycle with a single gear engaged, with automatic transmission vehicles excluded for reasons discussed above. Disadvantages of these units are that they require both a power supply and a means to dissipate power. Dissipation can be achieved either by using resistor banks (air or water cooled) or by returning conditioned power to the grid. AC and DC dynamometers are expensive and require substantial control hardware for operation, but can perform highly transient tests. Dynamometers of this type have been used in state-of-the-art fixed base chassis dynamometer designs.

Eddy-current dynamometers may be used in a similar fashion to the AC or DC units described above but do not offer the option of motoring. They can dissipate their absorbed energy through either water cooling or air cooling, the latter being an attractive option. Modest currents are needed to produce the retarding load and the eddy-current absorbers can be used to implement reasonably transient tests. Several manufacturers, including Clayton Dynamometer and Mustang Dynamometer, already produce roller dynamometers with air-cooled eddy-current absorbers, for both light-duty and heavy-duty use. Eddy current dynamometers have high load adsorbing capability while cold, but reduced capacity when hot, so that units must be sized to cope with anticipated loads, test duration, and ambient conditions.

Water brake dynamometers operate essentially as zero efficiency fluid pumps. They are able to perform economical steady state testing but customarily have a fairly slow transient response. Provision to cool the water is needed, and the retarding force at low speeds can be insufficient to load the vehicle in low gears when they are incorporated into a chassis dynamometer. They have outstanding characteristics for long duration high load testing.

Combinations of flywheels with a dynamometer are attractive because the flywheels can be used to mimic the inertia effectively at all speeds, while the dynamometer can be dedicated solely to road load mimicry and hence can be small in size. The combination of flywheels with water brake or eddy-current dynamometers has been used widely in the light-duty arena for both certification and I&M applications. West Virginia University has employed two systems that incorporate flywheel sets and eddy-current power absorbers in transportable laboratories used for heavy-duty vehicle emissions characterization.

3.2 Measurement Of Gaseous Concentration

The emissions of a vehicle are usually characterized by measuring the concentration of emissions species in either raw or diluted exhaust gas, and by converting these concentrations into units of interest. Where distance-specific, energy-specific, or properly weighted fuel-specific emissions

are required, the mass flow of the raw or diluted exhaust must be measured or known for conversion of emissions concentration to a mass quantity.

Raw gas emissions measurement can present condensation difficulties due to high water vapor content if no provisions are made to dewater the flow or keep the flow at a high temperature. Exhaust gas dilution lessens the concerns over water condensation. In some cases, dilution may also be desirable to lessen the maximum concentration of constituents.

Emissions analyzers may be classified broadly into those that are considered “research grade” or “laboratory grade” and those which are customarily used in portable instruments, gasoline I&M programs, and for engine control purposes. In addition, there are analytic instruments that seek to identify non-regulated species or scan for a wide variety of components. Research grade analyzers are well established, and are used in both light and heavy-duty emissions measurement operations as described by the Environmental Protection Agency’s (EPA) Code of Federal Regulations (CFR), Title 40 (EPA, 1998). Most important of the analyzers, for diesel emissions evaluation, is the NO_x analyzer, which works on the principle of chemiluminescence. HC emissions are measured by a heated flame ionization detector, which essentially “counts” carbon atoms bound in the hydrocarbons. CO is measured using a non-dispersive infrared detector (NDIR). Carbon dioxide (CO₂) is not regulated, but is usually measured to confirm fuel consumption, and is also measured using the NDIR principle. I&M level analyzers are represented by the multi-gas microbench units that are typically designed for use in light-duty California Bureau of Automotive Repair (BAR)-97 Emissions Inspection. Detailed review of a wide variety of gas analyzers follows.

3.2.1 Polarographic Analyzers

Polarographic analyzers, also called voltametric or electrochemical analyzers, use chemical reactions and associated electron flow to deduce the concentrations of candidate gases in sample streams. These analyzers utilize an electrochemical transducer, which consists of a semipermeable membrane, a porous sensing electrode, an electrolytic solution, and a counter electrode. The sensing and counter electrodes are separated by a thin layer of electrolyte and are connected by a low resistance external circuit. Gas diffusing into the sensor is reacted at the surface of the sensing electrode by oxidation or reduction, causing a current to flow between the electrodes through the external circuit. The current is proportional to the concentration of the candidate gas species and can be measured across a load resistor in the external circuit. Selection of the counter electrode and sensing electrode is governed by their respective electric potentials, so that the oxidation-reduction reaction takes place at the sensing electrode. As the candidate gas concentration increases, so does the current flow, causing a change in the potential of the counter electrode, or polarization. If the candidate gas concentration is too high, the sensing electrode potential will move outside its designed range. In such a case, the sensor will become nonlinear. In order to overcome this effect, sensor manufacturers have implemented a third reference electrode. Such a design enables the sensing electrode to be held at a fixed potential relative to the reference electrode. Since no current is drawn from the reference electrode, both maintain a constant potential. If the candidate gas concentration causes the counter electrode to polarize, the sensing electrode is not affected and the sensor does not move into a nonlinear region of

operation. A potentiostatic operating circuit has also been used in order to provide greater selectivity and improved response.

Polarographic analyzers have been developed to measure a variety of gases, including sulfur dioxide (SO₂), nitrogen monoxide (NO), nitrogen dioxide (NO₂), NO_x, CO, CO₂, and O₂. They are inexpensive and portable, and thus may be suitable for I&M applications. However, the operation of the electrochemical cell is very sensitive to temperature variations so that the system should be designed to maintain cell temperature within certain limits. In addition, due to the delicate nature of the membrane, care must be taken to remove PM from the exhaust stream, else fouling would likely occur. The response times of electrochemical cells is quite long and has been a limiting factor in their usage for measuring the instantaneous emissions concentration levels in transient exhaust streams. Slow response causes difficulty in the calculation of mass emissions rates, a complication which is discussed later in this report. There have been some recent improvements in the response time of sensors used for the detection of some gas species. Currently, NO sensors are available with a response time to measure 90% concentration levels (T₉₀) of less than 4.5 seconds. However, sensors used for measuring other gases, such as NO₂ and CO, still have response times of more than 30-40 seconds. Another factor that may restrict the use of electrochemical cells is that their inlet temperatures are generally limited to 50°C. Such limitations require that the sample stream be cooled, which would likely result in the loss of some heavy-end HC compounds due to condensation. Lastly, like any chemical-based system, the cells will eventually be consumed, requiring either refurbishment or replacement.

3.2.2 *Electrocatalytic Analyzers*

Electrocatalytic analyzers utilize sensors that were developed as an outgrowth of fuel cell technology and are commonly used to detect O₂ concentrations in sample streams. These sensors use a solid catalytic electrolyte to aid the flow of electrons from a sample gas cell to a reference gas cell. In practice, catalyst-coated ceramic materials (such as ZrO₂) separate the reference cell (containing a high concentration of O₂) and the sample stream. When heated, the electrolyte allows transfer of ionic oxygen components from the reference cell to the sample cell. The surface of the electrolyte has a special electrocatalytic coating that catalyzes the transfer process and serves as an electrode surface in order to attract released electrons. The ions migrating from the reference side to the sample side release electrons on this surface, striving toward equilibrium. However, since the sample is continuously replenished, a continual flow of electrons is induced across the measurement load resistor, and the current flow is used to infer the concentration of oxygen in the gas sample stream.

Electrocatalytic analyzers have been developed to measure the concentrations of O₂. The electrocatalytic transducers are inexpensive, portable, and quite small. The presence of other species in the sample gas (such as CO and HC) may interfere with the response caused by oxidation reactions. This oxidation process would cause a decrease in the oxygen concentration of the sample cell, which in turn would yield erroneously low readings of O₂ concentration in the sample stream.

A variation of this concept is used to produce catalytic oxidation sensors for CO and HC, commonly referred to as pellistors. These sensors consist of a matched pair of elements – detector and compensator. Each of these elements is comprised of a coil of platinum wire

embedded within a catalytic bed. An electrical power source heats the elements to a point where the active detector is capable of oxidizing combustible gases. Due to oxidation, the detector element experiences a rise in temperature, which is associated with an increase in element resistance. In contrast, the compensator element is poisoned so that it is inert to the presence of the same gas. Thus, any temperature change of this element is an indication of sample stream temperature variations. The compensator arms correct the resistance changes of the detector elements due to sample stream conditions. The pairs are placed as opposite arms on a Wheatstone bridge circuit so that an out-of-balance voltage across the bridge can be used to detect a resistance change of one element with respect to the other. When no combustible gas is present the bridge is balanced and a zero gas signal is registered. However, the introduction of a combustible gas results in a resistance imbalance and triggers a response. For low concentrations, the signal response is linear. Therefore, by calibrating with a gas of known concentration, the magnitude of the imbalance can be used to infer candidate gas concentration.

Catalytic oxidation sensors have been developed to measure a variety of combustible gases, including CO and various HC species. One application where these devices are used is for sensors to indicate dangerous exposure limits of the candidate gas.

3.2.3 Chemiluminescent Analyzers

Chemiluminescent analyzers measure NO concentration by observing a narrow band of the infrared emission spectrum produced as NO reacts with ozone (O_3). NO components of the sample gas stream are quantitatively converted into NO_2 by gas-phase oxidation with molecular ozone. When this reaction takes place, approximately 10% of the NO_2 molecules are elevated to an electronically excited state, followed by immediate reversion to the non-excited state. This conversion process produces a photon emission. A photon detector (multiplier tube) is then used to produce an instrument response that is proportional to the NO present in the original sample. The operation for NO_x is identical to that of NO except that the gas sample stream is first passed through a converter which converts most of the NO_2 of NO_x into NO. In this case, the instrument response is proportional to the NO present in the original sample plus the NO produced by the dissociation of NO_2 .

NO_2 in conventional diesel engines typically represents a few percent of total NO_x over a test cycle, but may represent over 10% of the NO_x at light load and high engine speed. In addition, some emerging engine emissions reduction strategies may increase the NO_2/NO ratio, so that total measurement will be more desirable than NO measurement alone.

Chemiluminescent analyzers offer the benefits of a relatively fast response time and a linear response over 90% of the output range. They are currently considered the most accurate method for the determination of NO_x . The presence of ammonia or other oxides of nitrogen may bias analyzer response, however these components may be scrubbed from the sample line by utilization of molybdenum converters. Another associated problem involves the quenching/absorption of the released photons by other sample gas components while the sample stream is in the excited state. The effects can be minimized by operating the reaction at lower pressures and by flowing O_3 into the sample chamber to dilute the sample gas stream. Due to the necessary ozone supply, the packaging requirements of the reaction chamber, and the associated

need for the sample stream conditioning, chemiluminescent analyzers are usually associated with research grade equipment and are not associated with light-duty I&M systems.

3.2.4 Fluorescence Analyzers

Fluorescence analyzers are based upon a photoluminescent process and are currently used only for the measurement of SO₂. In principle, the operation of these analyzers involves irradiating a gas sample containing SO₂ with ultraviolet (UV) light. The impinging light initiates the fluorescence process in which SO₂ is elevated to an excited state. Accompanying this elevation in energy state is a release of longer-wavelength fluorescent radiation. This radiation is then measured via a photomultiplier tube and the collected details of the released energy spectrum are used to infer SO₂ concentrations in the gas sample stream. In order to prevent interference, commercially available units implement band pass filters to narrow the fluorescence emission spectrum. The released photons can be absorbed by other sample components, such as water, O₂, CO₂, nitrogen, and HC, which introduce error to the analyzer's measurement of SO₂. Commercially available systems have attempted to minimize the interfering component effects by using lower wavelength UV light (to reduce the time for fluorescence to occur), lowering the pressure of the sample cell, and diluting the cell with air.

3.2.5 Flame Photometric Analyzers

Using a principle similar to the chemiluminescence technique, these analyzers detect candidate gas concentrations by measuring the light energy released by excited gas molecules. A hydrogen flame is used to excite the sample gas molecules. As with other luminescent technologies, filters and scrubbers may be implemented in order to reduce interference effects generated by photon release from sample constituents other than the candidate gas. Flame photometric analyzers are currently used for the detection of sulfur compounds. For detecting SO₂, they offer improved response times over NDIR analyzers which are discussed below.

3.2.6 Heated Flame Ionization Detectors

Heated flame ionization detectors (HFID) are currently used for the detection of HC. Exhaust HC levels are measured by counting elemental carbon atoms detected in the sample gas stream. A regulated flow of sample gas is ionized by heating it with a hydrogen/helium fuel gas flame (FID fuel). The flame ionization process involves a release of electrons, which are collected by polarized electrodes. The ion absorption produces a current flow which is proportional to the rate at which carbon atoms enter the burner. Benefits of the HFID analyzer include the capability of measuring HC concentrations over the broad range (50 to 250,000 ppm) with an associated full-scale linear output. Although response is taken as a "per-carbon-atom" count, methane enjoys a slightly different response than heavier hydrocarbons and oxygenated species are not detected as regular hydrocarbons. HFID are usually calibrated using propane, but unlike NDIR analyzers discussed below, this does not substantially bias the correct quantification of other hydrocarbon species.

3.2.7 *Non-Dispersive Infrared Analyzers*

Non-dispersive infrared analyzers (NDIR) operate upon the principle of selective absorption. Loosely stated, the infrared energy of a particular band of wavelengths, specific to a certain gas, will be absorbed by that gas, whereas the gas will transmit infrared energy of other bands. The NDIR determines gas concentration by the amount of transmitted (or absorbed) energy in the selected band of wavelength. The transmission (or absorption) is directly proportional to the concentration of the component gas that is being measured. Detection of the transmission amount (or absorption) is accomplished by one of two methods. The first simply involves the direct measurement of the emerging light from a single sample cell. A reference level of measured infrared energy is obtained by flooding the measurement cell with zero gas. The zero gas is selected so as to transmit the infrared energy of the candidate gases' absorption band. This energy value can be compared to the attenuated value obtained from the detection of gas exiting the sample cell when the candidate gas is present. In portable units, a solid-state measurement device typically performs infrared energy detection. This detection scheme is robust and enables the NDIR instrument to be packaged for limited space applications. However, such a detection scheme may be susceptible to absorption interference by some other component that coexists in the sample stream with the candidate gas.

In order to minimize such interference effects, the second method employs three measurement cells: a sample cell, a reference cell, and a detection cell. The infrared source beam is alternated between two paths via a chopper-wheel assembly. The reference cell path is configured in parallel to the sample detection cell path and uses a quantity of zero gas in order to establish the reference amount of transmitted energy. The zero gas is chosen so as to transmit energy in the absorption band that is characteristic of the candidate gas. A detection cell is mounted downstream of the sample gas cell. The detection cell is subdivided into two unequal length chambers. Concentration levels of the candidate gas in the sample cell are inferred from the pressure imbalance that develops between the front and rear chambers of the detection cell. The front chamber is shorter than the rear chamber, and is used to absorb the light energy at the center of the absorption band. The infrared energy passed onto the rear chamber of the detection cell is primarily comprised of radiation with frequencies at the fringes of the absorption band. Since energy at fringe frequencies is not as efficiently absorbed, the rear chamber must be longer in order to achieve a balance of absorbed energy between the two cells. Detection of absorbed energy is accomplished via a microflow sensor that measures the pressure differential between the front and rear sections of the detection cell. If the candidate gas is present in the sample cell, infrared radiation of the band-center wavelength is absorbed. In such a case, the front chamber of the detection cell does not absorb as much energy as the rear chamber. The differential pressure is used to determine the concentration of candidate gas in the sample cell. If, however, interference gases were present in the sample cell, the interference will present itself as a broadband absorption of infrared energy. This will not produce a measurable pressure differential in the detection cell. Thus, the absorption effects of interference gases will be minimized. Such a detection scheme is employed in most laboratory-grade analyzers. Although very accurate and quite reliable, the instruments using this second method require considerable space and are therefore suited to current research applications.

NDIR analyzers are currently used to measure CO, CO₂, SO₂, and HC. Present day HC analyzers are oriented toward spark ignited engine exhaust applications and seek absorption lines for

propane or hexane, which are not predominant in diesel exhaust. Instrument size and accuracy have been improved with the implementation of solid-state detectors used to replace the photomultiplier tubes. NDIR analyzers not only require the removal of PM from the sample exhaust stream, but also require that the sample be conditioned in order to limit the effects of water interference due to condensation. Water interference may be minimized by heating the sample stream, condensing and removing the water vapor, or lowering the sample stream dew point. For the measurement of CO, CO₂, SO₂, and lighter-end HC, the water may be condensed out. However, unlike gasoline exhaust streams, diesel exhaust includes heavy-end HC that will condense along with the water vapor. Therefore, in order to reduce water interference, the use of heated lines or dilution air to lower the dew point must be implemented. Typical CO analyzers measure concentration ranges of 0-20,000 ppm and 0-100,000 ppm while the low CO analyzer ranges are 0-1000 ppm and 0-5000 ppm. Typical CO₂ analyzer concentration ranges are 0-50,000 ppm and 0-200,000 ppm.

3.2.8 Non-Dispersive Ultraviolet Photometers

Non-dispersive ultraviolet photometers (NDUV) are similar in operation to NDIR analyzers. An ultraviolet source is used to radiate the sample gas streams, then a photomultiplier tube is used to monitor the amount of light energy absorbed. More recent NDUV units have replaced the photomultiplier with solid-state detectors. Ultraviolet electromagnetic waves are characteristically shorter in wavelength and higher in energy than infrared electromagnetic waves. Therefore, the absorption of energy is much greater and the subsequent detection and correlation to candidate gas concentration is much easier. In contrast to NDIR methods, instead of comparing the transmitted energy of a reference gas cell and the candidate gas sample cell, a differential absorption technique is employed. This process involves the comparison of radiant energy transmitted by the candidate gas sample cell for two distinct narrow UV bands. Two band-pass filters are chosen, one that passes radiant energy of the absorption bandwidth of the candidate gas, and one that passes radiant energy of a wavelength that the candidate gas cannot absorb. Utilizing a chopper-wheel mechanism, the differential absorption is measured and correlated to the concentration of the candidate gas in the sample stream. Sample conditioning for NDUV analyzers require the removal of PM, but do not require the removal of water vapor. NDUV analyzers may operate on a hot-wet basis, since water vapor does not absorb electromagnetic waves appreciably in the UV spectrum used for analysis. Thus, heated lines may be employed in order to prevent water condensation interference.

3.2.9 General Commentary on Available Sensors

This section addresses sensors or analyzers other than research grade tools. A summary of available emissions measurement sensors available from various manufacturers is reviewed in the following paragraphs. The primary suppliers of component-level NDIR benches for the industry are Androse, Horiba Instruments, Inc., and Sensors, Inc. The primary source for electrochemical sensors is City Technology Limited. In addition to the measurement specifications for the various measurement systems, there are special features and unique requirements for these devices that deserve discussion.

Currently, there are no portable analyzers available for total hydrocarbon (THC) measurement. It is recognized that the CFR Title 40 (Protection of Environment) Sub-Part 89 (Control of Emissions From New and In-Use Nonroad Engines) permits estimation of non-methane hydrocarbon (NMHC) to be 98% of the THC. In the absence of a reliable portable sensor for THC, the approach found in CFR 40 Sub-Part 89 may be employed, however this approach does introduce errors. West Virginia University is currently developing a portable HFID for in-field applications.

3.2.10 I&M Gas Concentration Instruments Overview

Various instrument manufacturers have developed a number of emissions measurement sensors and analyzers for I&M of light-duty vehicles. Portability and minimal power consumption are characteristic of these devices. Typically, these units involve NDIR determination of CO, CO₂, and HC (hexane band), with NO being measured by electrochemical sensors. Many of the analyzers were developed to meet requirements set forth in the State of California's BAR-97 Emissions Inspection System Specifications. BAR-97 specifications set standards for instruments primarily designed to measure exhaust emissions from gasoline-fueled automobiles. These specifications do include opacity meter standards for measuring diesel smoke, but do not include standards for analyzers for measuring other diesel exhaust gaseous emissions. There are currently no commercially available portable emission analyzers that are specifically designed to sample diesel exhaust emissions.

For CO and CO₂ the I&M technology level is based upon the same basic measurement principles as laboratory-grade analyzers. The major difference between the portable units and their laboratory counterparts is the manner in which the absorption (transmission) of infrared energy is detected. At higher concentrations of CO, and most typical CO₂ concentrations, the portable NDIR based CO and CO₂ measurements are in good agreement with laboratory grade instruments. In addition, the use of solid-state detectors and the elimination of mechanical chopper-wheel assemblies make the mobile units very resistant to vibration. However, current I&M instruments were designed to measure CO and CO₂ concentrations typical of gasoline exhaust. For instance, the DGA 1000 developed by SUN Inc. was designed to measure CO concentrations up to 100,000 ppm (10%) by volume, which is necessary for rich operation of gasoline engines. Most diesel engines produce CO exhaust concentrations less than 100 ppm (0.01%) by volume, which would entail instrument operation in the lowest region of total response range. Obviously, such practice is not conducive to accurate reporting of exhaust samples and it should be noted that diesel CO levels have dropped considerably over the last decade.

Due to response delay, determination of exhaust CO and CO₂ concentrations by electrochemical means is not recommended. ECOM America Ltd. reports that its CO analyzer has a T₉₀ response time of approximately 38 seconds. Such a substantial lag in instrument response is not suitable for transient diesel emissions measurement.

The majority of commercially available I&M-level analyzers use an optical NDIR technique for HC measurement. However, since most of these units were designed under BAR-97 specifications, instrument response has been tailored to the HC spectrum produced by gasoline engines. Most of the NDIR bench-type instruments are limited to detection of HC in the hexane

band and may be calibrated with hexane or propane. Detection of heavy-ended HC is not guaranteed. The spectral sensitivity dictates the instrument measurement ability and generally, these instruments utilize narrow infrared bands in order to improve accuracy and minimize interference of other components that coexist in the diesel exhaust stream. Diesel HC emissions consist of a wide variety of species. The normal paraffins are most often encountered, but they also span a range of molecular weights. Unfortunately, for the instruments available from Horiba Inc., HC determination using NDIR will likely not include HC groups above the C8 or C9 level. Since diesel exhaust streams generally comprise a large percentage of heavy-ended HC, the measurement error associated with HC detection by an NDIR is expected to be unacceptably high unless the unit is re-engineered to identify larger molecules of HC.

City Technology markets a miniature catalytic oxidation sensor (or pellistor) that is used by ECOM in their SG Plus portable emission analyzer. These sensors were designed to measure the concentration levels of combustible gases present in an environment. The sensors are used to provide a warning of an explosive buildup. ECOM lists accuracy of 2% by volume, with associated resolution of 0.1% by volume. However, these sensors respond to any combustible gas, and do not directly determine HC content. No specialized electrochemical sensors currently exist for the detection of individual HC species or families. Also, the HC level produced by late model diesel engines is remarkably low and may be at or near background levels.

A prior experimental study was conducted by Stephens et al. (1996) to compare FID measurements with other instruments for HC measurement. Stephens et al. compared HC measurements performed by a number of different instruments: a gas chromatograph (GC), an FID, an FTIR, a commercially produced NDIR, and two remote sensors. General Motors NAO Research and Development Center conducted a study in collaboration with the US EPA, Research Triangle Park, comparing HC measurements made with a GC, an FID, an FTIR, a NDIR, and two remote sensors (NDIR-based). HC concentrations in a variety of samples (individual HC species; 12 different gasoline-vehicle exhaust samples; three different volatilized fuel samples) were measured. To quantify the degree to which the various instruments agreed with the FID, a parameter called the response factor was used. The response factor was defined as the HC/CO₂ ratio measured by each instrument divided by the HC/CO₂ ratio measured by the FID. Of the various instruments, only the GC yielded response factors that were consistently at or close to unity. Stephens et al. reported that the NDIR analyzers currently have poor accuracy for quantitative determinations of exhaust HC concentration. The NDIR techniques agree well with FID for alkane compounds and poorly for olefinic and aromatic compounds. The ability to measure complex mixtures accurately improves with the amount of alkane species present in the mixture. NDIRs measured between 0.23 and 0.68 of the values reported by the FID.

Most portable I&M instruments utilize an electrochemical cell for measuring NO. No provisions are required to measure NO₂ concentrations in gasoline exhaust on the assumption that NO₂ levels are very low. NO₂ concentrations in diesel exhaust are expected and the use of such devices would necessitate either the implementation of an external converter to convert NO₂ to NO or the addition of a separate NO₂ electrochemical sensor. ECOM reports NO sensor response times to be in the sub-4.5 second range. The NO₂ sensor used by the ECOM instrument has a T₉₀ greater than 40 seconds, which is too slow for many applications. Field tests conducted by a California state agency responsible for roadside audit programs found substantial sensor-to-

sensor variability in accuracy, sensor life, pressure sensitivity, drift, and response times for the electrochemical sensors currently used for NO measurement in BAR-97 certified devices (Butler et al., 1994). Water and CO interferences were also identified as substantial problems with these instruments. The results of these field surveys and subsequent manufacturer consultations recently led to tighter specifications and required improvements to such NO detection cells. However, the field tests also indicated that properly functioning electrochemical NO sensors did produce surprisingly accurate results. Horiba markets an improved NDIR instrument for the determination of NO. The device uses a Luft-type detector, where diaphragm capacitance is used to deduce the absorption of infrared energy. These units have been reported to exhibit improved response times, increased accuracy, and reduced unit-to-unit variability. However, their cost has prevented widespread implementation by the secondary analyzer market.

3.2.11 Fourier Transform Infrared Spectroscopy

Fourier transform infrared spectroscopy (FTIR) provides an advancement in emission measurement technology. A limitation is the high price of the commercially available models. Nicolet Instrument Corp. currently offers an FTIR priced in the \$45,000 range. FTIR devices have some published correlations to the industry-accepted HC measurements made by the HFID. The units tend to be rather large and quite susceptible to vibration.

3.2.12 Miniature Gas Chromatographs

Hewlett Packard currently markets the HP P Series Heated Micro Gas Chromatograph which was formerly offered by Microsensor Technology Incorporated. The unit is advertised as being a self-contained portable analysis unit capable of analyzing gas samples consisting of multiple compounds with boiling points up to 220°C (428°F). Carrier gases are housed in an internal rechargeable tank. The unit includes a rechargeable 12 V lead-acid battery which provides up to 4 hours of operation. Its size is 6"x14"x16", and weight is 10 kg (23 lbs) which makes it portable. Unfortunately, the response time of the instrument is approximately 180 seconds, making it unsuitable except for averaged or bag analysis.

3.2.13 Research-Grade Analyzers

Research-grade analyzers have well documented performance concerning the measurement of constituent gases found in diesel engine exhaust. They have proven reliability and reproducibility and are established and accepted by the heavy-duty diesel industry and the regulatory agencies worldwide. Research-grade analyzers are available from several manufacturers, including Rosemont, Horiba, California Analytical, and Pierburg. While these analyzers are clearly larger than BAR I&M units, they can be incorporated into a bench and have modest power demands.

3.2.14 Sample Conditioning Issues

Unlike gasoline exhaust, diesel exhaust samples must be conditioned before they are analyzed. The foremost reason for sample conditioning is to avoid condensation of water and heavy-end

HC in the sampling lines. Design and operating conditions of diesel emission gas analyzers will dictate the nature of sample conditioning.

Water condensation in diesel exhaust sampling lines will result in the loss of water-soluble NO₂. Additionally, diesel exhaust samples have to be maintained above 190°C (375°F) to prevent condensation of heavy HC. Heating the sampling lines will also prevent HC deposition in the measurement systems. In certification applications, driers are used for CO and CO₂ measurement and heated lines are used to prevent water and heavy HC condensation for NO_x and HC analyzers.

3.3 Measurement of Particulate Matter

PM is presently regulated on a mass basis by means of filter capture and gravimetric weighing as specified in the CFR Title 40. However, this section will review a broad range of instruments designed to measure PM parameters including opacity (smoke) meters, mass measurement systems, and instruments which characterize particle count and/or size distribution. Section 3.3 presents below a discussion of these instruments. The TEOM is considered separately in Section 3.4, and opacity is discussed separately in Section 3.5.

PM mass measurement systems may be classified as integrated or continuous. Particle separation by size can be obtained by use of an appropriate cyclone in the sampling probe (discussed in detail in Section 3.3.6). Coarse particles are defined as particles with a diameter of less than 10 μm (PM₁₀), and fine particles are defined as particles with a diameter of less than 2.5 μm (PM_{2.5}). The integrated PM measurement systems involve collection of PM on filter media that undergo gravimetric analyses. This method is handicapped not in its ability to yield accurate information, but rather by its need for cumbersome weighing capability and the associated time requirements that are needed to equilibrate the filters in a controlled environment. Continuous PM measurements would be ideal for in-field, on-board emissions measurements of exhaust from portable and stationary engines. The most common dynamic (continuous) instruments for PM mass monitoring have been the Beta Attenuation, and Tapered Element mass monitors such as the Tapered Element Oscillating Microbalance (TEOM). The WVU authors have considerable experience in using the TEOM for diesel exhaust PM measurements over steady state and transient cycles. The accuracy of TEOM results can vary from 10% to 30% when compared with filter-captured PM measured gravimetrically with the difference often attributed to differences in soluble organic fraction content. The TEOM is discussed in greater detail in section 3.4.

A number of particle counters exists in the marketplace, but these require assumptions of particle shape, density and confidence in the measured particle size distribution or effective mass mean size to permit their use to predict mass rates of emissions. They are reviewed below, but use of this technology must be subjected to careful comparison with mass measurements.

3.3.1 Scanning Mobility Particle Sizer

The Scanning Mobility Particle Sizer (SMPS) provides a full scan of diesel PM size distribution and serves as the primary tool for particle size distribution and concentration measurement. The SMPS (built by TSI Instruments Inc.) determines size distribution by utilizing the electrical mobility of aerosol (electrical mobility technique). During operation the sample aerosol passes

through a single stage inertial impactor which removes any large particles above 1.0 μm aerodynamic diameter, since they may carry more electrostatic charge than the data reduction procedure will permit (resulting in the propagation of large errors throughout the measured size distribution). The aerosol is then charged (according to the Boltzmann distribution) in a Kr-85 bipolar charge equilibrators, with most of the charged particles being charged with either one positive or one negative electronic charge. The particles then pass through an electrostatic classifier where they are separated according to their electrical mobility. An electrical field inside the classifier (generated by a cylindrical rod at potentials of 0 to 11,000 volts) influences the trajectory of the charged particles. Negatively charged particles are repelled into the chamber wall while positively charged particles are attracted to the central electrode. A narrow electrical mobility range of the positive ions passes through an open slit and exits the classifier as a mono-dispersed aerosol. This allows for size selection of the mono-dispersed aerosol by adjusting the mobility analyzer voltage and airflow rates. The aerosol then enters a Condensation Particle Counter (CPC) where each individual particle is counted.

The SMPS configuration incorporates the TSI Model 3025A CPC, which provides accurate measurements of the size distribution of aerosols in the size range from 0.005 to 1.0 μm and the concentration range from 20 particles/cm³ to 10⁷ particles/cm³ (TSI/SMPS manual, 1996). It should be noted that uncertainties become fairly large for PM less than 0.01 μm . Ideal scan time is at least 2 minutes, but a total scan time of 90 seconds has been found to be adequate. Scan times less than 30 seconds yield a fairly distorted distribution. SMPS accuracy and repeatability results from 14 measurements were; percent coefficient of variance (CV%) was 0.2, random error was 0.1 % and total uncertainty was -3.3 to +3 % (Bischof, 1998).

The SMPS provides excellent sensitivity and size resolution for steady state tests, but is limited to a single size for transient tests. It can be argued that the test-to-test variability in particle size or concentration can skew the distribution for the particular test. However, uncertainties associated with other means (such as bag sampling) during transient testing will yield only an “averaged” distribution due to the inherent dispersion in the sampling system.

An Electrospray particle generator should be used for calibration of the SMPS, and all flow rates are checked with a bubble flow meter. Particle losses in sampling streams should also be documented prior to each set-up and on a weekly basis once the study begins.

Computations of PM mass using a SPMS requires assumptions of particle volume as a function of SMPS reported size, and assumption of particle density. The weights of all particles detected can then be computed and summed.

3.3.2 *Electric Low Pressure Impactor*

The Electric Low Pressure Impactor (ELPI) was developed using the Berner type multi-jet low-pressure impactor stages. The difference between a conventional impactor and the ELPI is that the ELPI charges the particles prior to entering the stages. The PM size classification is based on aerodynamic diameter. Each stage is connected to an electrometer that measures the current produced by the particles in that stage. The measured current is an indication of the particle concentration in that stage.

When operated in mass mode, the ELPI acts as a low pressure impactor, measuring particle mass distributions on twelve stages from 0.032 to 1.0 μm . The collection substrate is made from tin foil, with the particle mass distribution determined by weighing each foil before and after each test. The ELPI in mass mode is equivalent to a cascade impactor and does not measure real-time PM data. It gives good size discrimination in the size range of interest, and with care can give good mass distribution data.

The biggest advantage of the ELPI is that it provides an excellent real-time record of the sub-micron sized PM with the sensitivity and size resolution (within its range of operation) comparable to the corresponding values of the SMPS. The instrument has a lower size cutoff of 0.03 μm . However, diesel and gasoline PM from modern low emissions engines has been measured down to 0.01 μm . It may be argued that the after-filter on the ELPI could be used to measure PM mass for particles below 0.03 μm , but the last few stages operate at such low pressures that evaporation of volatile matter (and particles) poses a problem. The ELPI also has diffusion problems in its upper stages. Calibrations with the SMPS have shown that the ELPI measures lower concentrations and yields a larger size distribution. However, the Ford Motor Company presented data that show the ELPI measured distributions and concentrations accurately.

3.3.3 *Quartz Crystal Microbalance*

The quartz crystal microbalance (QCM) measures particle mass distributions in 10 stages from 0.05 to 25 μm in near real-time. With diesel vehicle emissions it was found to under report total mass, by 90% compared to a filter sample (Kelly and Groblicki, 1993). The repeatability was worse than that for other available instruments. The size distributions were biased to smaller particles when compared with results from a SMPS and an ELPI. This resulted to high inter-stage losses, especially for small particles, and bad coupling between the particles and measurement stages; particles break free from stages after impaction, and either deposit between stages or reach the next stage down. QCM's were popular in the 1970's and 1980's, but because the sensor is easily overloaded with mass, the TEOM and Beta devices became dominant for ambient PM₁₀ monitoring. However, recent technological developments have yielded quartz sensors with greater sensitivity that can accurately measure very low PM mass emissions.

3.3.4 *Sensors' METS 3200*

Sensors' METS 3200 is a small, portable unit designed for continuous PM measurement from a diluted air sample. Measurements are reported as particle counts per liter in the various size distribution "buckets". The system employs a light scattering technique for single particle counts. A semiconductor laser serves as the light source and the particles passing through the laser beam scatters the signal, which is then collected at approximately 90° by a mirror and transferred to a recipient diode. The pulse height analyzer classifies the signal by channel for data display and/or storage. The unit uses a volume-controlled pump to sample the dilute exhaust at 1.2 liters per minute (lpm). A High Efficiency Particle Air (HEPA) filter removes nearly all particles from the exhaust stream except for a small sample that is drawn through a capillary. Dividing the flows (bypass and capillary) is caused by the pressure drop of the thin capillary in comparison to the HEPA filter flow resistance. A regulation valve behind the HEPA

filter adjusts the flow rate balance between the bypass and capillary sample streams. The defined dilution ratio is 100:1.

3.3.5 *Micro-Orifice Uniform Deposit Impactor*

The Micro-Orifice Uniform Deposit Impactor (MOUDI), MSP Model 110 is a cascade impactor that classifies particles by their aerodynamic diameter in the range of 0.056 to 18 μm . The model 110 has ten stages with nominal 50% efficiency curve aerodynamic diameters of 0.056, 0.100, 0.180, 0.320, 0.560, 1.0, 1.8, 3.2, 5.6, 10 and 18.0 μm . The MOUDI moderates the pressure drop needed to size sub-micron aerosols by using nozzles of very small diameter (2000 nozzles of 52 μm in diameter in the final stage). It operates at a rather high flow rate of 30 lpm. The flow rate is monitored by measuring the pressure drop between the first and the fifth stage with a differential gage. The differential pressure is adjusted by a needle valve to a pre-calibrated pressure drop corresponding to a flow rate of 30 lpm. The advantage that the MOUDI has over other cascade type impactors is its ability to collect ultra-fine particles with a moderate pressure drop and a uniform deposit.

By rotating the impaction plates, a uniform deposit can be obtained upon the MOUDI substrates. The nozzles are placed at calculated distances from the center of rotation to allow a concentric deposit. This reduces the chance for particle stacking and caking, which could lead to greater bounce and uneven surface impaction. The stages are rotated relative to those above and below. While the impaction plate is rotated in conjunction with the upper nozzle plate, the nozzle plate is rotated in relation to the lower impaction plate. This concept creates a system where each nozzle plate rotates relative to its corresponding impaction plate.

With the features presented above, the MOUDI is well suited to measure diluted engine exhaust PM. It should be noted that most users of the MOUDI and its derivative (the Nano-MOUDI) have failed to follow correct operating procedures. Problems encountered by other MOUDI users can be traced back to improper operation and/or lack of sufficient care in balancing the pressures, and the consequent flow rates through the upper and lower stages of the MOUDI.

Samples from the MOUDI should be collected on greased substrates to prevent bounce problems. The after-filter may be a 37 mm Gelman Sciences Teflo™ filter with a pore size of 2.0 μm . This thin, Teflon-membrane filter with a polyolefin ring collects particles with aerodynamic diameters less than 0.052 μm . These filters have a collection efficiency of 99.98% for particles greater than 0.035 μm at a filter-face velocity of 23 cm/s, or an equivalent sample flow rate of 15 lpm.

Substrate greasing procedures established by the U. S. Bureau of Mines, MN have been found to be very effective. According to the majority of researchers, particle bounce is not an important issue in diesel PM sampling. However, the principal investigators of an NREL-funded study (Gautam, 1999) found this claim to be in error. Upon impact, some of the particles may bounce off the substrates and get re-entrained in the sample stream where they will pass to successive stages. This will distort the size distribution toward the smaller diameter regions, with no definitive method to predict or correct for this phenomenon.

3.3.6 Cyclones

Cyclones do not measure PM mass, but are auxiliary units used to exclude large particles from PM mass measurements. Size-selective cyclone samplers (URG Model 2000-30 EA, 28.3 lpm, $_{50}d_{ae}=10 \text{ }\mu\text{m}$; URG Model 2000-30 EH, 16.7 lpm, $_{50}d_{ae}=2.5 \text{ }\mu\text{m}$; and URG Model 2000-30 EHB, 16.7 lpm, $_{50}d_{ae}=1.0 \text{ }\mu\text{m}$) are used to collect PM₁₀, PM_{2.5} and PM₁ respectively. PM₁₀, PM_{2.5} and PM₁ cyclones are inertial particle separators that use centrifugal forces to remove heavier particles from a gas stream ($>10 \text{ }\mu\text{m}$ and $>2.5 \text{ }\mu\text{m}$, $>1.0 \text{ }\mu\text{m}$ respectively). The diluted exhaust sample enters the cyclone tangentially and is drawn through the cyclone body and an in-line filter by a vacuum pump. Maintenance of this exact flow can be difficult if the conditions at which the sample is being collected are not near standard. Cyclone use in a dilution tunnel requires a feedback control system to adjust the flow to account for temperature and pressure variations. This signal is used to control a mass flow rate controller which is responsible for maintaining the required constant flow.

3.3.7 High Volume PM 10/2.5/1.0 Trichotomous Sampler

The trichotomous sampler consists of a high volume (40 cfm) sampler with a $10 \text{ }\mu\text{m}$ cut, omnidirectional inlet to remove all particles larger than $10 \text{ }\mu\text{m}$. Two high-volume virtual impactors (HVVI) are mounted in series downstream of the inlet. The first HVVI has a cut-size of $2.5 \text{ }\mu\text{m}$, and the second has a cut-size of $1.0 \text{ }\mu\text{m}$. The sampler collects PM₁₀, PM_{2.5}, and PM_{1.0} particulate mass fractions. In addition, PM₁₀ to PM_{2.5} and PM_{2.5} to PM_{1.0} can be determined. The sampler has seven, 47 mm filter holders: one to collect particles greater than PM₁₀, two for particles between PM₁₀ and PM_{2.5}, one for PM_{2.5}, two for particles between PM_{2.5} and PM_{1.0}, and two for PM_{1.0}. In addition, an 8"x10" after-filter is used to collect PM_{1.0}. Filters of different media can be placed in the 47 mm filter holders, allowing for different types of analysis.

3.3.8 Photoelectric Aerosol Sensor

The Photoelectric Aerosol Sensor (PAS) can, in principal, measure concentration of sub-micron particles in real-time. The time resolution of a few seconds allows for the monitoring of diesel PM during transient driving cycles. The instrument is sensitive to the surface of aerosol particles and their surface chemistry. Soot particles can be ionized with UV light. This charge, for many aerosols, is proportional to the concentration of particle bound PAH. At the beginning of each test, the instrument initiates a self-test, which lasts approximately 30 seconds. The PC-based software collects data every 6 seconds. The results are displayed and stored to a file with a time stamp for each data point. Burtscher and Siegmann (1994) have observed a correlation between diesel PM and the charge and concentration of elemental carbon (EC). The PAS is not recommended for PM analysis at this point since the PI's believe the instrument is still in the experimental stages and the quality of the data is suspect.

3.3.9 DustTrak TSI Model 8520

The DustTrak TSI Model 8520 is a laser photometer that has traditionally been used for dust sampling but more recently has gained favor among certain sectors of the diesel PM sampling community. The DustTrak sensing element consists of a laser diode (780 nm) directed at the sampled aerosol stream. A lens at 90° to both the aerosol stream and laser beam collects a

portion of the scattered light and focuses it onto a photodetector. The intensity of the scattered light is a function of the particle mass concentration, and light scattering follows the Mie light-scattering theory. The intensity of scattered light is a function of particle size, index of refraction, and light absorbing characteristics. It is well known that light scattering monitors have a linear response to aerosol mass distribution, but this is only true for monodisperse aerosols. The laser diode (with a wavelength of 780 nm) allows measurement of particles in the range of 390 nm to 3900 nm, however the DustTrak literature claims that the device may be recalibrated for specific aerosols types and can measure accurately down to 100 nm. It is well established that diesel PM has a mass median aerodynamic diameter of approximately 100-200 nm and can range from 10 to 1000 nm. These numbers will vary from engine to engine and will also vary as a function of fuel types, engine operating conditions, fuel control strategies, ambient and driving conditions, and aftertreatment devices. Given this and the fact that the DustTrak responds best to monodispersed particles, the authors believe that the DustTrak is not well suited to quantify diesel PM mass.

3.3.10 Tapered Element Oscillating Microbalance

The Tapered Element Oscillating Microbalance (TEOM) is a PM mass measuring device manufactured by Rupprecht & Patashnick Co., Inc. The TEOM unit measures PM mass, mass rate, and mass concentration from diluted engine emissions. The key component of the TEOM is a hollow, tapered, cantilever element, which is forced to oscillate at its natural frequency via a feedback system. The TEOM filter is mounted onto the free end of the cantilevered tapered element which is part of the mass transducer shown in the TEOM flow schematic in Figure 3.4-1a. Figure 3.4-1b shows the free end of the tapered element and filter in greater detail. An internal volumetric flow controller maintains a constant sample flow rate of diluted exhaust gas across the TEOM filter. Simplistically, the tapered element and filter can be represented by a spring-mass system, where a change in mass correlates to a change in the system's natural frequency. As the filter weight changes due to PM accumulation, the oscillation frequency of the element changes.

The TEOM measures the frequency of the tapered element oscillation and calculates a change in filter mass approximately five times per second. The TEOM is controlled by a personal computer via counter timer and analog/digital input/output boards. These boards are managed through TEOMPLUS software (supplied by Rupprecht & Patashnick) which provides an interface for instrument set-up and data acquisition. User-defined operation parameters are sample flow rate and sample line temperature. User-defined data acquisition variables include data acquisition rate and time window averaging. Proper precautions must be taken when selecting a location for the TEOM to isolate the unit from possible external mechanical excitations. It is also generally believed that moisture from combustion adsorbs and desorbs onto/from the filter material causing errors in mass rate magnitude readings but not integrated mass values. Moisture desorption is most evident as negative mass rate data and is discussed in section 3.4.3 below.

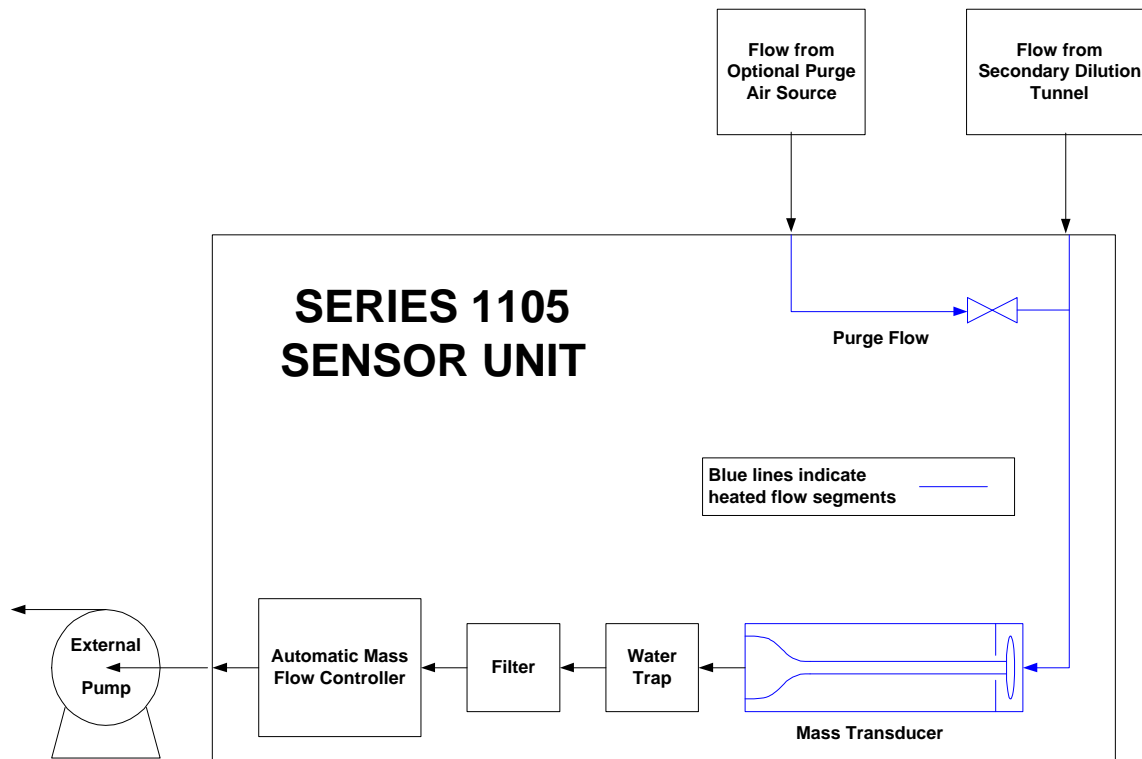


Figure 3.4-1a. This diagram shows the flow schematic of the R&P Series 1105 Tapered Element Oscillating Microbalance (TEOM). The TEOM filter is mounted at the head of the tapered element, which is part of the mass transducer. A change in mass on the filter is determined by measuring a change in the natural frequency of the tapered element.

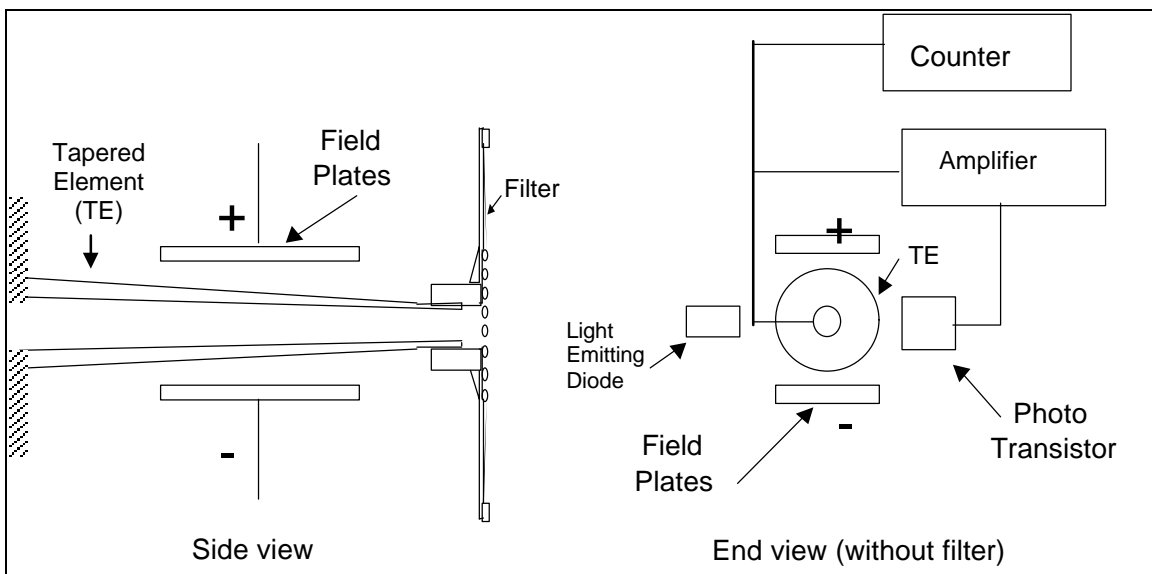


Figure 3.4-1b. This figure shows the filter and free end of the tapered element in greater detail.

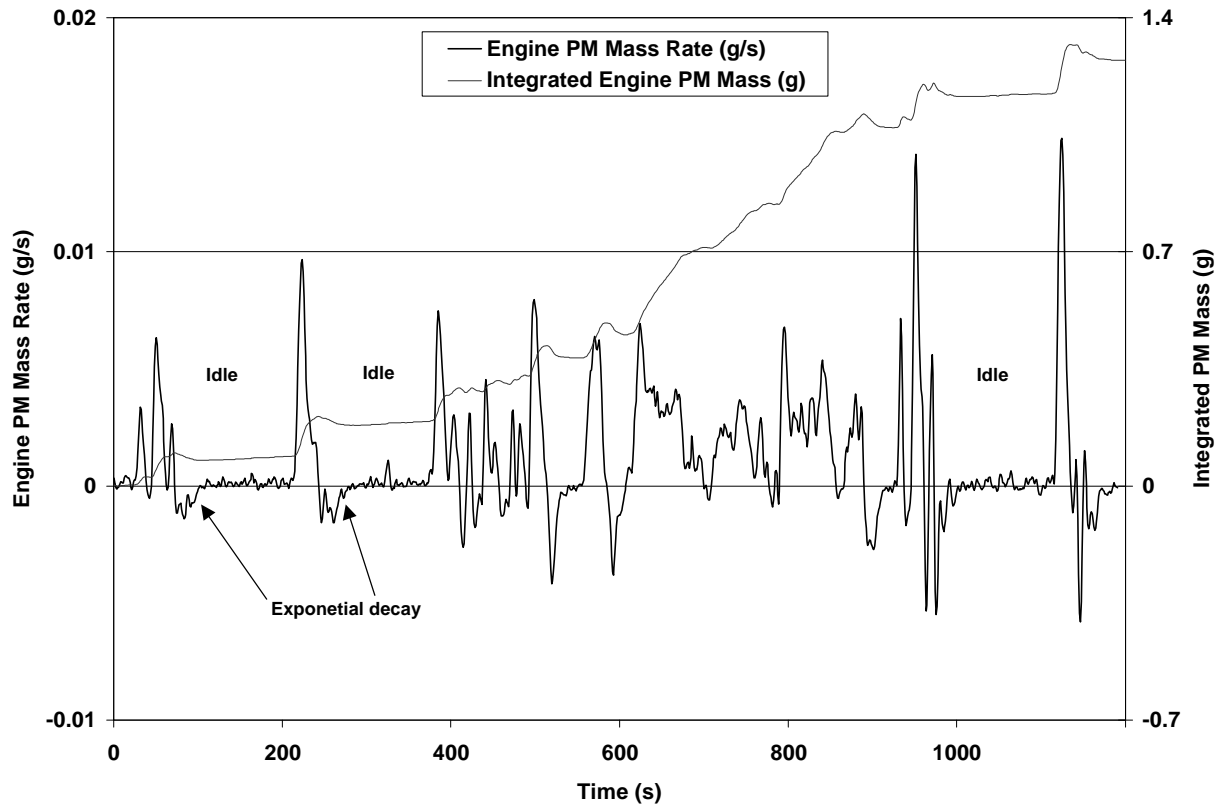


Figure 3.4-2. Real time engine particulate data from a Navistar 7.3-liter diesel engine exercised through an FTP transient engine test. The data shown represent tail-pipe values of PM mass and mass rate extrapolated from TEOM data.

TEOM Operating Parameters

As exhaust gases cool during dilution with ambient air, some gas-phase hydrocarbons condense onto carbon particles generated from incomplete combustion. Thus, PM mass is a partial function of temperature. For this reason, the CFR Title 40, which provides criteria governing PM sampling from engines, specifies that filter face temperatures not exceed 52°C (125°F). The CFR Title 40 also specifies the filter face volumetric flux to be from 0.792 to 2.638 liters per cm²-minute which would correspond to a TEOM flow rate of 0.94 to 3.13 lpm based on a filter diameter of 1.23 cm. However, these regulations do not cover TEOM filters and researchers are still evaluating the temperature and flow rate effects on TEOM sampling.

Determining optimum flow rate and sample line temperature settings are based on correlation of integrated TEOM data with 70 mm filter data and elimination of negative continuous TEOM data. Sample flow rate and sample line temperature affects PM deposition rate, PM composition on the filter medium, filter face temperature, change in pressure across the filter medium, and air density inside the tapered element. Variation in these parameters during operation are undesirable due to changes in air density within the hollow tapered element which in turn causes a change in the mass transducer's natural frequency giving a false change in mass reading.

The TEOM unit sample flow rate ranges from 0.5 to 5.0 lpm. External and internal sample line temperature settings and mass transducer temperature settings range from ambient (i.e. no heating) to 80°C with a default setting of 50°C. Shore and Cuthbertson (1985) found a near-direct proportion of filter retention to flow rate for flows within 0.8 to 3.0 lpm, and further concluded that a flow rate chosen within this range was not critical. Okrent (1998) found integrated TEOM data correlated better with EPA gravimetric results for flow rates in the range of 5 lpm and that total particulate retention did not change significantly when filter face temperatures ranged from 35 to 55°C. Gilbert (2001 [in review]) found that a flow rate of 1.0 lpm yielded the best correlation with 70 mm filter data and that particulate collection was not significantly affected at 30 and 40°C, but decreased at 50°C. Figure 3.4-3 shows a plot of total PM mass determined from integrated TEOM data as a function of total PM mass from 70 mm gravimetric filter capture. This plot shows a strong correlation between integrated TEOM data and gravimetric filter data with the TEOM unit indicating less total mass than the filter-captured method.

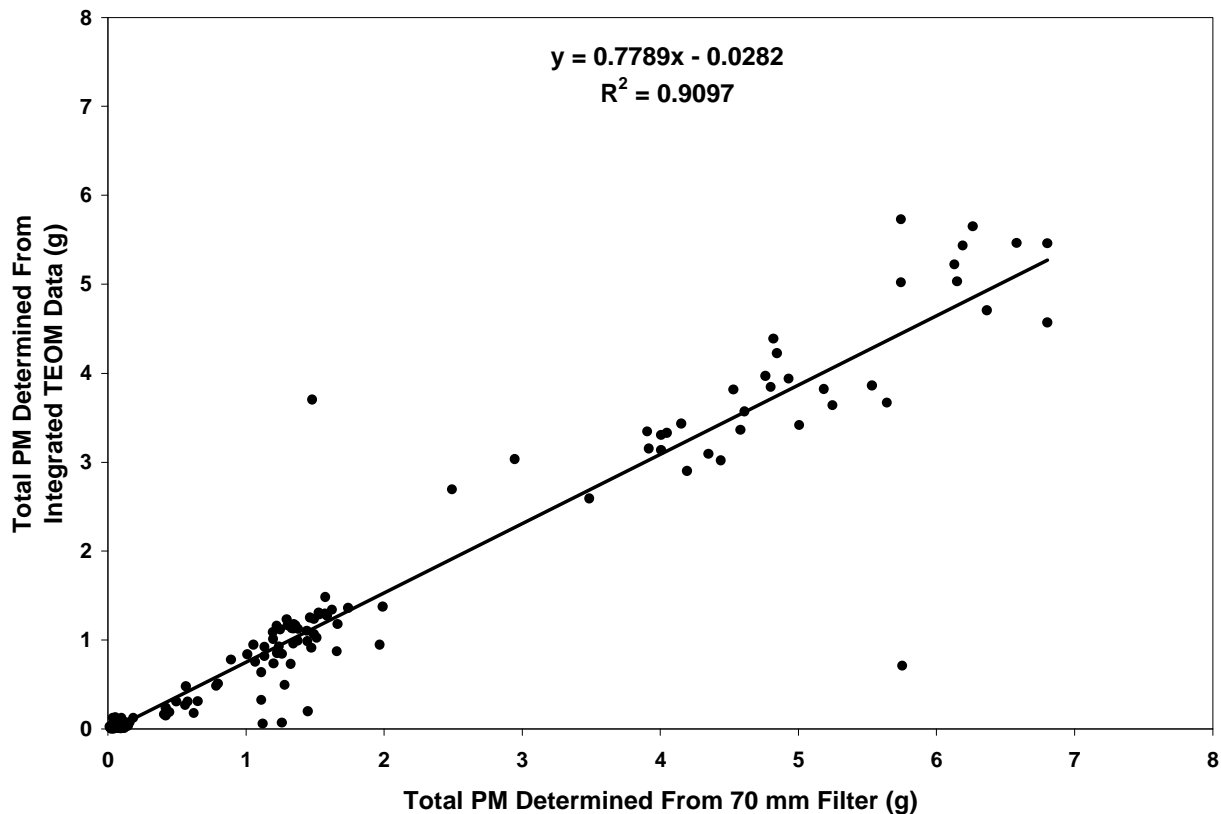


Figure 3.4-3. Comparison of total PM determined from integrated TEOM data and total PM measured gravimetrically from 70 mm filters. Data were collected by WVU from buses exercised through different transient chassis tests (WVU 5-Mile Route and the CSHVR).

Effects of Temperature and Pressure on TEOM Data

Parameters that influence TEOM data are the sample path temperatures (including the tapered element and filter), dilution tunnel pressure variations, filter face sample velocity (flow rate), and pressure drop across the TEOM filter (Whitby, 1982.). Temperature changes in the tapered element affect the natural resonance frequency of the tapered element unit, so that a constant element temperature must be self-maintained, to eliminate this variable. During heavy engine loading in a transient test, PM, moisture, and volatile organic compounds (VOCs) will deposit on the TEOM filter. This results in TEOM data magnitudes higher than “true” PM mass rates because of water accumulation from the high humidity flow. During lighter loading conditions, moisture and some VOCs will evaporate from the TEOM filter. This mass departure from the filter is revealed in the data as a negative mass rate. The negative TEOM mass rate data also exhibit an exponential decay in time towards zero, which suggests a reduction in potential as a function of time. The difference in moisture concentration between the gas sample flow and the TEOM filter is the primary source of this potential.

Higher filter temperatures tend to reduce the moisture and VOCs deposition rate, thus reducing the amount of build up that will evaporate during lighter loading conditions. This helps to reduce the negative trends in the TEOM data (Okrent, 1998). As the particulate travels through formation, dilution, and filtration, it becomes an adsorption site for gas-phase hydrocarbons. Thus, Whitby (1982) claims the temperature limit for filtration should not exceed 52°C (125.6°F). It has been found that the total TEOM particulate retention does not change significantly with temperatures ranging from 35 to 55°C (95 to 131°F) (Okrent, 1998). That is, the total mass accumulated onto the filter, not including moisture and VOCs, does not change significantly within this temperature range. Pressure changes directly affect the oscillating element’s frequency by changing the density of air in the element. Pressure variations should be avoided, and are generally small in most dilution tunnels (Okrent, 1998). Shore and Cuthbertson (1985) found that there was a near-direct proportion of filter retention to flow rate for flows within 0.8 to 3.0 lpm, and furthermore concluded that the flow rate chosen within this range was not critical. Okrent (1998) claims that a better correlation between TEOM and EPA gravimetric results was found from higher flow rates in the range of 5.0 lpm. Although a high sample rate decreases filter life, Okrent had found sample rates in the range of 3.0 to 5.0 lpm helped reduce the negative mass trends in the data. These trends can never be totally eliminated by instrument configurations due to the real phenomena of moisture and VOC adsorption and desorption on the TEOM filter during transient testing. This will be discussed further in Section 3.4.3 of this report.

Recently, at West Virginia University, researchers gathered TEOM data in a study that has not yet been published. A General Electric DC dynamometer system was used to control the transient speed of the diesel test engines in the study. The engine speed and load points came from the Federal Test Procedure (FTP) cycle. Two engines were used in the study, a Cummins ISM 370 ESP and a Navistar T444E. Exhaust gases were ducted from the engine to a primary dilution tunnel. The primary dilution tunnel was 46 cm in diameter, and included a mixing orifice to promote mixing of the engine emission with the temperature conditioned test cell air. The TEOM sampling probe was placed 457 cm downstream of the tunnel opening.

To collect PM in accordance with the EPA regulations, a sample of diluted exhaust gas was pulled from the sampling plane in the primary dilution tunnel into a secondary dilution tunnel. The sample was drawn through two 70 mm diameter micro-fiber filters in series at a set volumetric flow rate via a mass flow controller and vacuum pump. The filters used were Pall-Gelman Science “Pallflex Fiberfilm” T60A20 heat resistant borosilicate glass fiber coated with TFE. No secondary dilution was necessary in this experimental effort, as the sample filter face temperature remained below 52°C (125°F). The set volumetric sample rate was five scfm (141 lpm). The filters were conditioned in an environmentally controlled chamber where the temperature remained at 21°C ± 6°C (70°F ± 10°F) and the relative humidity was constrained to 50% ± 10%. The filters were conditioned and weighed before and after each test with a Cahn C-32 microbalance to calculate the collected PM mass.

The TEOM allows the user to change its sample path temperature and sample flow rate. These two variables were changed individually to evaluate the effects of each on TEOM response. The researchers chose to vary the temperature settings of the TEOM while keeping flow at a chosen value, after which the flow was varied using the best temperature identified. This temperature was a compromise between conventional PM agreement and PM/water collection ratio. The PM/water ratio is the integrated positive TEOM mass rate divided by the integrated negative rate. This ratio was used to describe the transitional water content on the filter. This ratio is reported since it is argued that the negative rates are indicative of water being removed from the filter during lower engine load conditions. There was no specific attempt to match the sample temperatures of the TEOM directly to the sample temperatures of the conventional PM filters. From the previous research discussed above, an initial flow rate of 3 lpm was chosen.

The first tests were conducted on the Navistar engine. The engine was run through an FTP speed-load cycle to bring the engine and tunnel to operating temperature before data were collected. Twelve FTP speed-load cycles were run back to back with a nominal heat soak time of 10 minutes between tests. Three FTP speed-load cycles were used for each TEOM sample tube temperature set point. The TEOM tapered element housing, external and internal sample tube temperature set points were 35°C, 40°C, 50°C, and 60°C (95°F, 104°F, 122°F, and 140°F). To remain consistent and identify new filter collection efficiency, a new TEOM filter was used at the start of every test set. It is conceded that new filters may pass some PM species before deposition increases capture efficiency. Only on this set of experiments was the initial test reported and included in calculations.

The second set of tests was conducted on the Cummins 10.8-liter DI diesel engine. The engine was run through an FTP cycle to bring the engine and tunnel to operating temperature before data were collected. Nine FTP speed-load cycles were run back to back with a nominal heat soak time of 10 minutes between tests. When the TEOM filter was changed, an FTP was run to condition the filter in an attempt to minimize the filter capture efficiency variability. These conditioning FTP tests were not included in the analysis of the data. Three FTP speed load cycles were run for each TEOM temperature. These set points were 30°C, 40°C, and 50°C (86°C, 104°C, and 122°C).

Flow was varied from one to four lpm in one lpm increments. The EPA limits for filter face volumetric flux are 0.792 to 2.638 liters per cm²-minute (EPA, 1998). The TEOM effective filter face was approximately 1.23 cm in diameter, giving an EPA allowable TEOM sample rate of 0.97 lpm to 3.24 lpm. The conventional 7 cm PM filter system had an effective filter face of 6.2 cm². All conventional PM samples were taken at approximately five scfm, or 141 lpm, yielding 4.69 liters per cm²-minute. This flux is higher than the EPA upper limit and may therefore yield reduced SOF fraction, but higher total PM mass than the limit would suggest. The tests were conducted on the Cummins 10.8 liter DI diesel engine. The engine was run through one FTP cycle to bring the engine and tunnel to operating temperature before data were taken. Eight FTP cycles were run back to back with a nominal heat soak time of 10 minutes between tests. When the TEOM filter was changed, an FTP was run to condition the filter in an attempt to eliminate the variable of filter efficiency. These conditioning FTPs were not included in the analysis of the data.

For the Navistar, CV% of the conventional PM flow normalized data was 2.6%, proving data consistency. The CV% for the average air temperature for the conventional PM sampling system was 3.3%, proving the consistency of the sample temperatures. The 35°C set point resulted in a sample air temperature of 34°C (93°F). The first test with a new TEOM filter displayed poor collection efficiency relative to the conventional PM filters. The 40°C (104°F) resulted in a sample air temperature of 39°C (102°F). Again, the relative initial inefficiency of the new TEOM filter was apparent in the first test of this set. The rise in TEOM sampling temperature caused an increase in the average TEOM to conventional PM ratio to rise from 0.89 to 0.78. This ratio decrease could possibly be due to the lack of moisture and VOC collecting on the TEOM filter as a result of the increase in temperature. A 50°C (122°F) setting resulted in a sample air temperature of 48°C (118°F). The rise in TEOM sampling temperature caused an increase in the average difference between TEOM and conventional PM values from 0.78 to 0.72. A 60°C (140°F) setting resulted in a sample air temperature of 56°C (133°F). The average difference continued to increase with temperature, from the previous test value of 0.72 to 0.50. A trend in initial collection efficiency became apparent. As the temperature increased, the difference associated with the initial collection increased rapidly, looking as if it were following an exponential trend. Results from the Navistar testing are tabulated in Table 3.4-1.

For the Cummins, the TEOM filter was conditioned with a dummy test to reduce filter efficiency variability. However, even the second test on a new TEOM filter will show effects of efficiency changes. This is evident in Table 3.4-1 when comparing the TEOM mass concentration of tests two, five, and eleven with the previous new filter concentrations. The CV% of the conventional PM flow normalized data was 1.3%, proving data viability. The CV% for the average air temperature for the conventional PM sampling system was 4.1%, proving the consistency of the sample temperatures. The average relative humidity of the ambient air for the duration of the test series was 25%. Results from the Cummins testing are tabulated in Table 3.4-2.

Test	TEOM Temp. Set-point	Average TEOM Filter-Face Temp.	Average PM Filter-Face Temp.	PM Mass Concentration	TEOM Mass Concentration	TEOM/PM Mass Ratio
	(°C)	(°C)	(°C)	(mg/m ³)	(mg/m ³)	
1(New Filter)	35	34.04	36	1.16	0.9	0.78
2	35	33.97	38	1.16	1.06	0.91
3	35	33.76	39	1.19	1.16	0.97
4 (New Filter)	40	38.85	38	1.21	0.83	0.68
5	40	38.85	39	1.2	0.95	0.79
6	40	38.79	40	1.21	1.03	0.86
7 (New Filter)	50	47.39	37	1.27	0.69	0.54
8	50	47.65	39	1.2	0.98	0.82
9	50	47.82	38	1.21	0.98	0.81
10 (New Filter)	60	56.17	36	1.24	0.11	0.09
11	60	56.1	38	1.23	0.77	0.63
12	60	56.16	39	1.22	0.96	0.79

Table 3.4-1. TEOM and PM results from FTP speed-load cycle testing on a Navistar T444E engine while changing TEOM sample tube temperature. TEOM sample flow was 3 lpm. Average values are time averaged over the entire cycle.

Test	TEOM Temp. Set-point	Average TEOM Filter-Face Temp.	Average PM Filter-Face Temp.	PM Mass Concentration	TEOM Mass Concentration	TEOM/PM Mass Ratio
	(°C)	(°C)	(°C)	(mg/m ³)	(mg/m ³)	
1(New Filter)	30	29.93	38	1.24	1.11	0.89
2	30	30.06	39	1.24	1.14	0.92
3	30	30.11	39	1.26	1.14	0.91
4 (New Filter)	40	39.28	39	1.22	1.11	0.92
5	40	39.44	35	1.2	1.1	0.91
6	40	39.51	36	1.24	1.13	0.92
7 (New Filter)	50	48.4	36	1.25	0.94	0.75
8	50	48.45	39	1.24	1.01	0.82
9	50	48.47	39	1.24	1.02	0.82

Table 3.4-2. TEOM and PM results from FTP speed-load cycle testing on a Cummins engine while changing TEOM sample tube temperature. No new filter data were analyzed. TEOM data were sampled at 3 liter per minute.

For the Navistar, the best measured TEOM to conventional PM agreement was at a sampling temperature of 35°C. This was also the closest applied TEOM temperature to the conventional PM temperature averaged of the cycle. This trend continued in the Cummins data. For the best agreement with conventional PM results, the TEOM temperature set point was close to the conventional PM filter temperature, approximately 40°C. Temperature also affects real-time TEOM data. The Cummins data were chosen to evaluate real-time results due to the consistent

trend of the data. Tests two, six and nine were chosen to represent 30°C, 40°C and 50°C set points on the lowest TEOM/PM mass ratio criterion. FTP data showed that as TEOM temperature increased, both the positive and negative amplitude of the response decreased. However, as TEOM temperature increased, the ratio of the total positive mass collected to mass lost increased. This observation can best be displayed as a ratio, referred to in Table 3.4-3 as the PM/water ratio. The 50°C set point yielded the largest PM/water ratio, as well as a 11% lower total collection. The 30°C and 40°C set points yielded total collection mass less than 1% from each other. Figure 3.4-4 shows a sample of TEOM real-time data and illustrates the temperature effects on TEOM mass rate data. Table 3.4-3 illustrates the difference in the positive to negative ratio on integrated data.

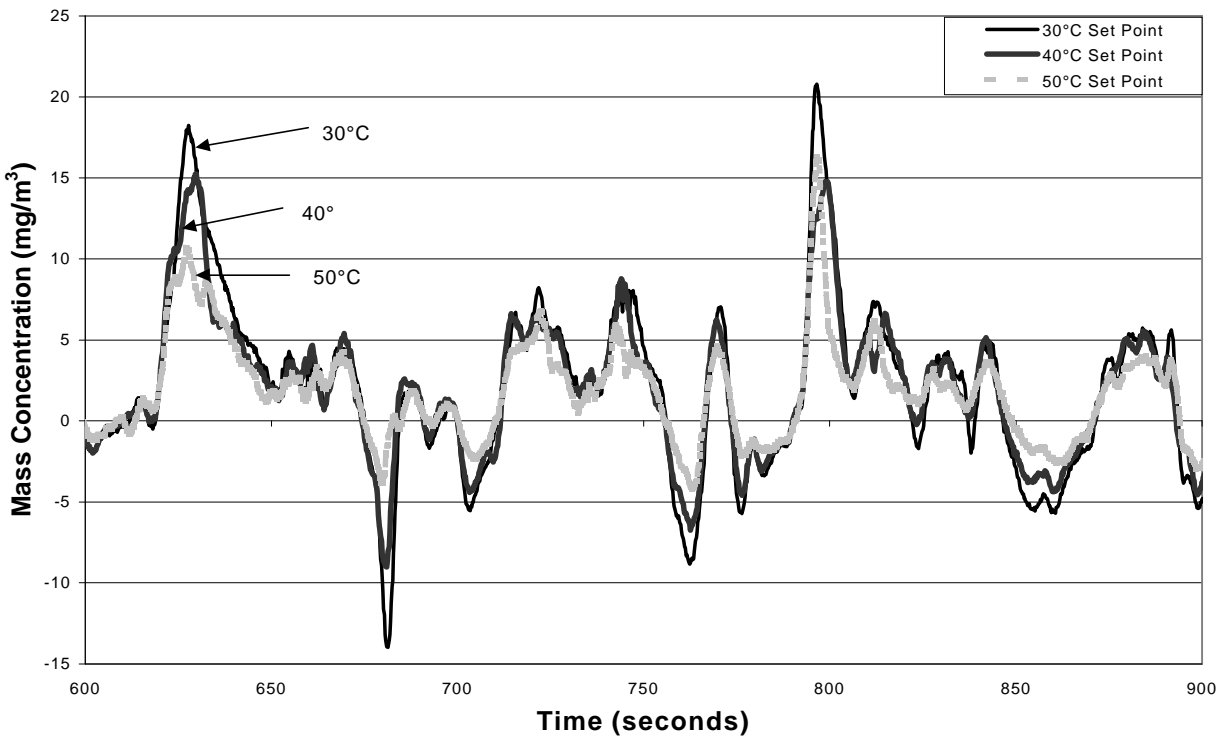


Figure 3.4-4. A section of the FTP illustrating that increased temperature decreased TEOM real-time amplitude of both negative and positive peaks.

TEOM Temperature Set-Point	30°C	40°C	50°C
Positive Collected Mass, or PM (micrograms)	120.83	107.96	85.43
Negative Collected Mass, or water (micrograms)	-49.61	-38.47	-23.48
PM/water Ratio	2.44	2.81	3.64

Table 3.4-3. Real-time PM/water collection evaluation for varying air temperature.

Due to the better conventional PM agreement and moderate PM/water collection ratio, the compromise of a 40°C set point was chosen to perform the flow effects investigation on the Cummins engine. The TEOM filter was subjected to a conditioning FTP test cycle to reduce variability seen with the Navistar tests. The results of these conditioning tests were discarded. However, sampling at 4 lpm caused a filter loading high enough to restrict multiple tests per TEOM filter, so a new filter was used for each test. The CV% for the eight tests of conventional PM flow normalized data was 3.2%, proving data viability. The average relative humidity of the ambient air for the duration of the test series was 25%. Results from the Cummins testing are tabulated in Table 3.4-4

Test #	TEOM Sample Flow Rate	Conventional PM Concentration	TEOM Concentration	TEOM/ PM Ratio
	(l/min.)	(mg/m ³)	(mg/m ³)	
1	1	1.2	1.09	0.9
2	1	1.25	1.13	0.9
3	2	1.29	1.15	0.89
4	2	1.25	1.12	0.9
5	3	1.17	1.01	0.86
6	3	1.25	1.1	0.88
7	4	1.29	1.05	0.82
8	4	1.27	0.97	0.77

Table 3.4-4. As TEOM sample flow rate was increased, TEOM/PM mass ratio decreased. Samples were measured with a path temperature of 40°C.

It was noted that tests five and six in Table 3.4-4 had the same TEOM settings as tests four, five, and six shown in Table 3.4-2, 40°C sample path temperature and 3 lpm sample flow rate. However, the tests in the temperature effects section resulted in a lower error value. This was due to a cooler conventional PM air temperature during the flow effect test series. The cooler conventional PM temperature was a result of cooler ambient conditions in the test cell. As TEOM sample flow rate increases, TEOM values increasingly deviate from conventional PM results. Results from tests seven and eight may have been closer to conventional PM values if new filters had not been required for each test. As with temperature, flow also affected real-time data. Tests one, four, six, and seven were chosen to represent 1, 2, 3, and 4 lpm set points on least error criteria.

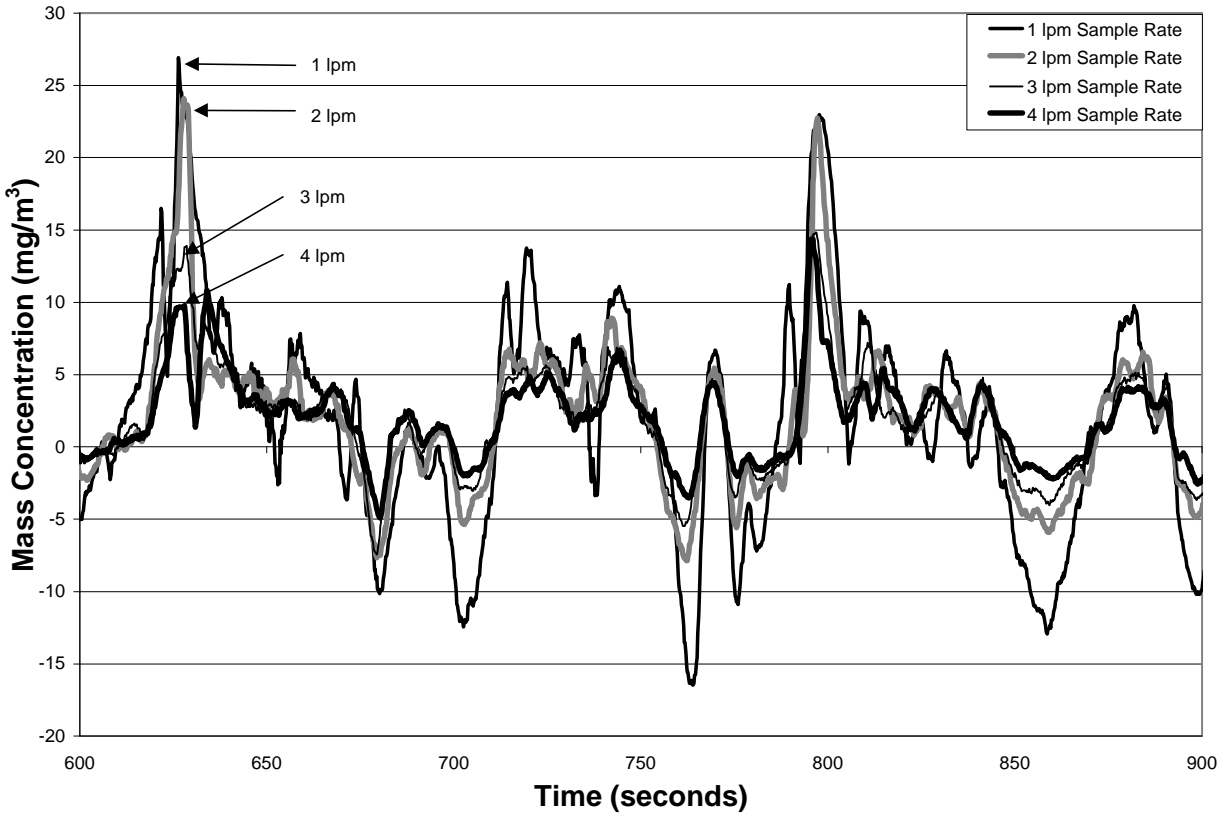


Figure 3.4-5. A section of the FTP illustrating increased flow decreased TEOM real-time data amplitude.

TEOM Sample Flow Rate (lpm)	1	2	3	4
Positive Collected Mass, or PM (micrograms)	55.62	77.15	99.04	111.24
Negative Collected Mass, or water (micrograms)	-33.1	-31.49	-32.05	-25.57
PM/water Ratio	1.68	2.45	3.09	4.35

Table 3.4-5. Real-time PM/water collection evaluation for varying air temperature.

FTP data show that as TEOM sample rate increased, amplitude of the response decreased for both positive and negative. However, as TEOM sample rate increased, the ratio of the total positive mass collected to negative mass collected increased. The 4 lpm set point yielded the least collection of negative mass per positive mass collection. The flow set point chosen by the authors is 2 lpm. This flow rate displayed both good collection efficiency and water ratio results. Okrent states that flow rate does not have a significant affect on real time collection. However, Table 3.4-5 shows that flow does have an effect on water and VOC retention.

The study concludes that good agreement between integrated TEOM and PM filter data called for low TEOM temperature (30°C) and flow rate (1.0 lpm). However, these values elicited high negative mass rates due to transient discharge of water loading on the filter. Compromised values of 40°C and 2 lpm were chosen as recommended TEOM operating conditions for future research. If these values are used, data from the present study suggest that the TEOM will capture 90% of the conventional filter PM while keeping the positive to negative collection ratio at a value of 2.45 g/g.

TEOM Moisture Absorption and Desorption

In addition to comparing integrated TEOM data with gravimetric filter data, researchers are interested in evaluating the accuracy of the continuous TEOM data. Continuous data may prove important if proportional exhaust sampling is not used, as discussed later in this report. The primary indicator of inaccuracies is the negative segments of the continuous mass rate curve. During heavy engine loading in a transient test, PM, moisture, and some VOC deposit and adsorb onto the TEOM filter. This results in the TEOM unit reporting mass rates higher than actual PM mass rates. During lighter loading conditions, moisture and VOC desorb from the TEOM filter, resulting in lower reported mass rates than actual PM mass rates. In some cases the reported mass rate from the TEOM unit is negative. The negative TEOM data often exhibit an exponential decay towards zero as labeled in Figure 3.4-2. Okrent found that higher filter temperatures tended to reduce the moisture and VOC adsorption rate, thus reducing the amount of build-up that desorbed during lighter loading conditions. Gilbert (2001 [in review]) found that a higher flow rate reduced the negative values in the continuous TEOM data. Jarrett et al. (2001 [in press]) sought to numerically correct continuous TEOM data by predicting change in moisture on the TEOM filter. Moisture mass rates from combustion were deduced by assuming a direct correlation with continuous CO₂ emission data. Good results were obtained from this technique.

Correction for Combustion Moisture Effects on TEOM Data

This section provides information on improving the value of continuous TEOM data by predicting and subtracting water adsorption and desorption effects. These effects do not need to be considered if only the total (cumulative) TEOM mass from a cycle is sought. However, if there is a desire to capture continuous PM data, or data by short duration mode, then correction will prove necessary.

Evaluation of continuous TEOM data from transient engine tests show mass leaving the filter during engine idle periods immediately after heavy engine loading, and is evident during the idle period of an FTP test as shown in Figure 3.4-2. Furthermore, the exponential decay of the negative data suggests a time-based decay in potential to shed mass. With the assumption that no particulate matter is leaving the filter, the authors assume the loss of mass to be moisture and possibly volatile and semi-volatile HC from combustion. HC levels are typically low for diesel-powered engines (average of 0.002 g/s for one typical modern heavy-duty engine) and are believed to be minimal at best when compared to moisture effects (average of 2.25 g/s). Thus, with the assumption that TEOM mass rate data represent legitimate PM deposition and moisture adsorption and desorption, development of an accurate model to predict change in moisture mass rate on the TEOM filter and subtracting these results from original TEOM data would yield a

more accurate representation of PM mass rate during transient operation. To determine the TEOM moisture relation, static and dynamic tests were conducted recently by the investigators, and some conclusions are presented below.

To evaluate the static relation, gravimetric mass readings were collected from new and used TEOM filters at 5 different relative humidity (RH) set-points (ranging from 40% RH to 85% RH) after 12 hour soak times in an environmental chamber. Humidity ratios were determined for each filter (w_f) and for the ambient environmental chamber air (w_a) with results plotted in Figure 3.4-4. The near-zero intercept of the linear best fit yields the relation;

$$w_f = mw_a \tag{Equation 3.4-1}$$

which suggests moisture mass on the TEOM filter is directly proportional the moisture mass concentration in the surrounding air.

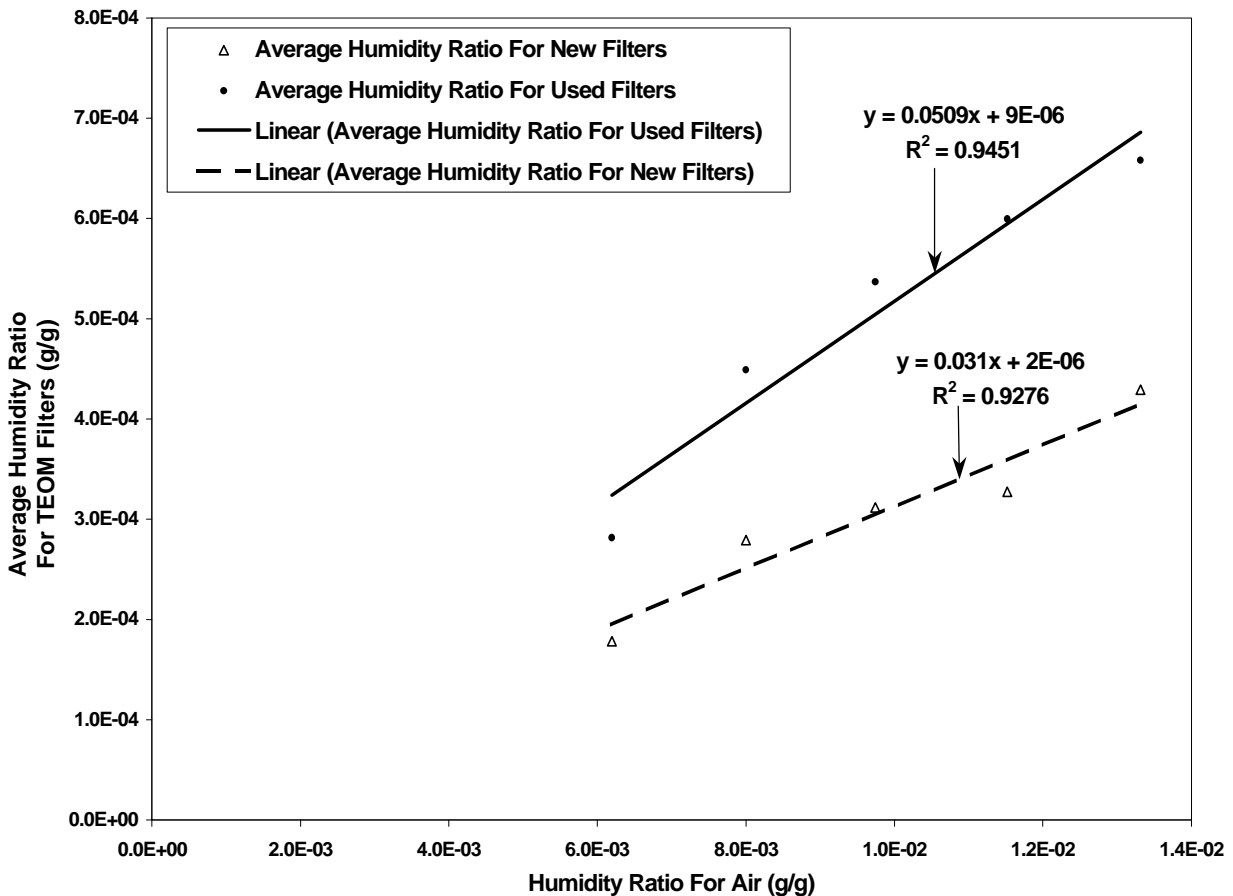


Figure 3.4-4. Results from new and used TEOM filter gravimetric readings at different relative humidity settings in an environmental chamber. These results show the linear relation between TEOM filter humidity ratio (w_f) and the humidity ratio of ambient air (w_a). The ordinate or “y” intercept for both new and used filters is near zero, agreeing with the logic that zero moisture in the air would result in near zero moisture on the filter. It is also noted that the moisture retention of used filters is greater than that of new filters.

To evaluate the dynamic TEOM response to moisture from combustion, TEOM data were collected during a series of steam injection tests. For these tests, a Navistar T444E, 7.3-liter, turbocharged, after-cooled V8 diesel engine was operated at steady state (1600 rpm with a 678 N-m [500 ft.-lbs.] torque load supplied by the DC dynamometer). The steady state engine operation allowed for typical dilution tunnel temperature and humidity conditions, and for the assumption that engine PM and combustion moisture mass rates were constant. Thus, any change in TEOM mass rate could be attributed to steam injection, which was at a known mass rate. Representative TEOM data from steam injection is shown in Figure 3.4-5.

The model developed to predict change in moisture mass on the TEOM filter is based on the relation shown in Equation 3.4-2, which represents mass transfer on a molecular level with the absence of bulk flow (Coulson and Richardson, 1977).

$$N_A = k'(C_{Ai} - C_{Ao}) \quad \text{Equation 3.4-2}$$

where,

N_A is the molar rate of diffusion per unit area and has units of (kmol/m²s).

k' is the mass transfer coefficient and has units of (m/s).

$(C_{Ai} - C_{Ao})$ is the mass transfer driving force created by the molar concentration gradient and has units of (kmol/m³). The subscript 'A' represents any substance, 'i' represents the system in evaluation, and 'o' represents the system's surrounding.

For this research, the authors assumed that the volume of the TEOM filter was constant, the surface area from which mass transfer occurs was constant, and that the volumetric flow rate of the dilute exhaust sample across the TEOM filter was constant. Now the concentration gradient from Equation 3.4-2 can be represented as a moisture mass gradient between the TEOM filter and the dilute exhaust sample so that,

$$\dot{H}_2O_f = C_1(C_2 \cdot H_2O_a - H_2O_f) \quad \text{Equation 3.4-3}$$

where,

$(C_2 \cdot H_2O_a - H_2O_f)$ is the mass transfer driving force created by the mass concentration gradient between the TEOM sample gases and TEOM filter and has units of (g). H_2O_a is the moisture mass in TEOM sample during a time period Dt and has units of (g). H_2O_f is the moisture mass in the TEOM filter during a time period Dt and has units of (g). C_1 is a constant describing mass transfer, is dependent on flow through the filter and has units of (s⁻¹). C_2 is a unitless constant relating the equilibrium concentration of moisture in the air and in the filter, and is related to the slope in Equation 3.4-1.

An iterative Newtonian solver was used to determine values of C_1 and C_2 by minimizing the least mean square between collected TEOM data and the results of applying Equation 3.4-3 to the known moisture mass rate from steam injection. This yielded values of 0.00706 and 0.00061 for C_1 and C_2 respectively. A plot of the predicted TEOM response to the steam in injection is shown in Figure 3.4-5.

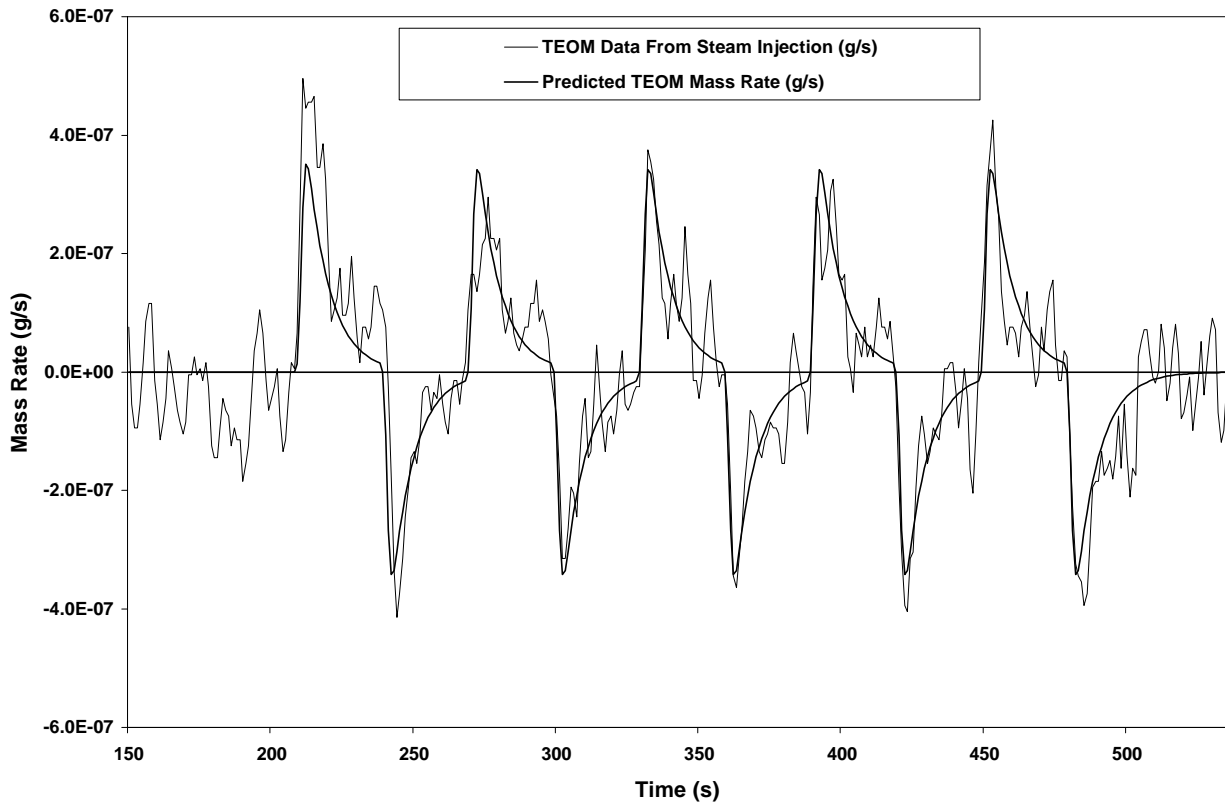


Figure 3.4-5. TEOM mass rate data and the resulting model to predict TEOM filter moisture adsorption and desorption. The TEOM data were collected while steam was injected at a known mass rate into the exhaust in an on/off step-wise function in a 60 second cycle (30 seconds on and 30 seconds off).

To apply this model to TEOM data from transient emission tests, continuous CO_2 data were used to predict combustion moisture based on a mole-to-mass conversion and the coefficients from the stoichiometric combustion equation. Results from applying Equation 3.4-3 to predicted combustion moisture and subtracting this from original TEOM data are shown in Figure 3.4-6. Given that there are still some negative values in the corrected TEOM data, it is possible that there is some mass loss due to VOC desorption; possibly from airborne VOC that were deposited on the TEOM filter, but more likely from VOC components of PM which evaporated once the PM was deposited on the TEOM filter.

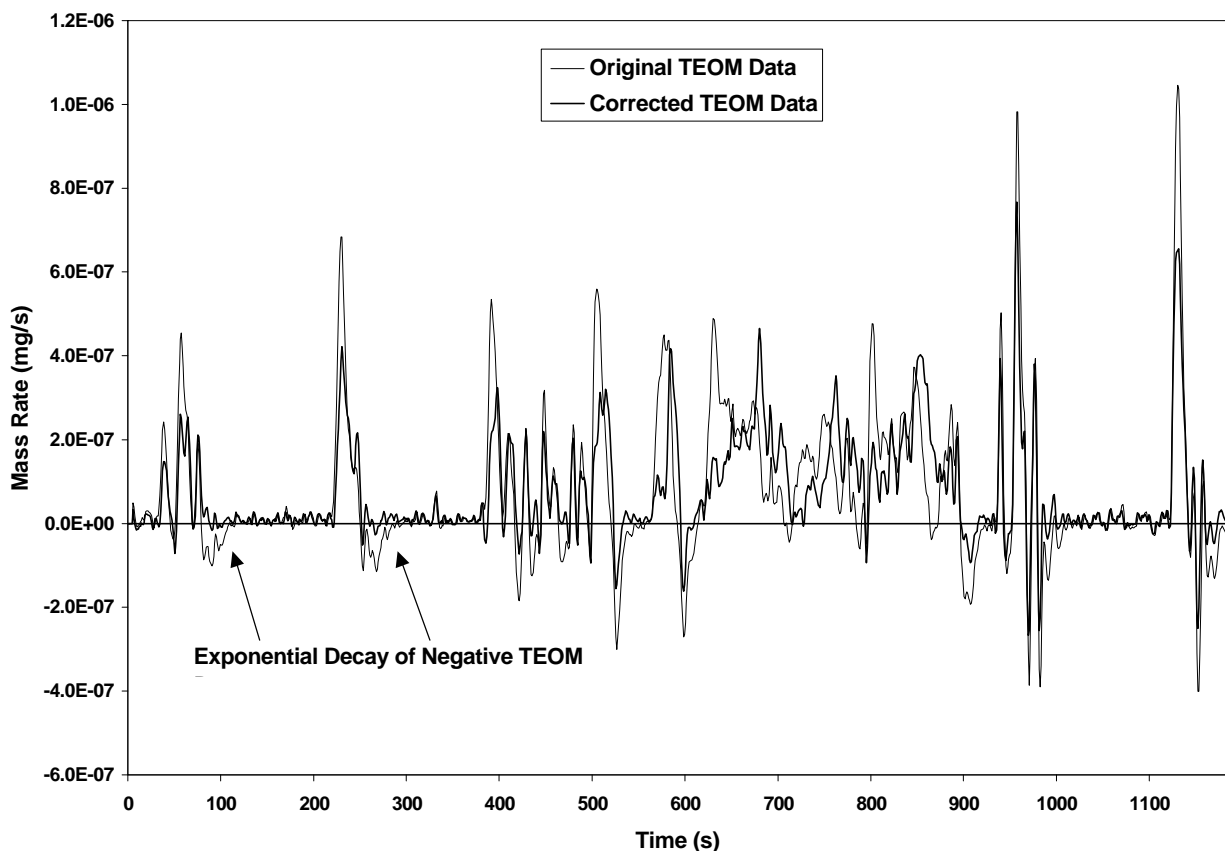


Figure 3.4-6. Original and corrected continuous TEOM mass rate data from a Navistar 7.3-liter diesel engine exercised through an FTP transient test cycle. These results suggest that moisture adsorption and desorption cause TEOM results to over-predict and under-predict PM mass rates during various portions of the transient test.

It should be noted that Rupprecht & Patashnick have recently made improvements to the TEOM filter resulting in better repeatability, better collection efficiency, and improved filter-face velocity as a function of change in pressure across the filter. This has been observed by recent testing at WVU and shown in Table 3.4-6. However, all TEOM data and results in this report are from earlier TEOM filters.

Old TEOM Filter	70mm (g)	TEOM (g)	% Dif.	New TEOM Filter	70mm (g)	TEOM (g)	% Dif.
FTP 01	1.694	1.11	34.47	FTP 06	3.107	2.72	12.46
FTP 02	3.043	2.23	26.72	FTP 07	3.178	2.77	12.84
FTP 03R	3.076	2.45	20.35	FTP 08	3.217	2.80	12.96
FTP 04	3.076	2.42	21.33	FTP 09	3.160	2.72	13.92
FTP 05	3.143	2.50	20.52	FTP 10	3.066	2.67	12.92
Average	3.085	2.40	24.68	Average	3.146	2.74	13.02
Std. Dev.	0.042	0.117	6.070	Std. Dev.	0.060	0.050	0.544
CV%	1.36	4.90	24.60	CV%	1.89	1.84	4.18

Table 3.4-6. Comparison of old and new TEOM filter total PM results with 70 mm filter data.

3.3.11 Opacity Measurement

Optical analysis of PM emissions by continuous opacity monitoring appears promising in that opacity meters are easily transportable, relatively inexpensive, installation requires little to no modifications to the vehicle, and operation is simple and requires little technical knowledge. Opacity meter smoke testing is attractive to states that want to check and regulate vehicles in the field since present energy-specific PM emissions regulations can only be enforced at the manufacturing stage of an engine.

A snap-acceleration test is commonly used for roadside opacity inspection. In general, the test is a series of rapid engine accelerations from idle to governed speed while the transmission is in neutral. This test simulates transient engine operation associated with PM production, but does not provide continuous engine loading, which also contributes to PM production. In an effort to provide state-to-state consistency, the EPA has established recommended peak opacity limits for HD vehicles tested using the snap-acceleration test as specified by the SAE J1667 (SAE, 1997). The guidelines recommend a threshold of 55% peak opacity for 1990 model years and earlier, and 40% for 1991 model years and newer. These values represent opacity data which have been corrected for ambient atmospheric conditions. Detailed correction methods are found in the SAE J1667 publication. SAE J1243 and ISO 3173 provide minimum specifications for opacity meter performance. All opacity meters presented in this report meet or exceed SAE and ISO standards.

When considering the use of opacity measurement in an I&M program, it is important to identify whether the opacity readings are intended to quantify PM production or simply identify a gross PM emitter since research has shown the lack of correlation between opacity and diesel PM mass during transient operation (Clark et al., 1999). In addition, there is concern over an opacity meter's ability to "see" the particulate matter since much of the PM mean diameter is smaller than the wavelength of the light source used (Jarrett, 2000). If there is little correlation between continuous opacity data and total PM, then it could be argued that opacity data obtained from snap-acceleration tests is of questionable worth in meeting ambient air quality standards.

Opacity is the preferred form of smoke measurement in the United States. The absorption coefficient (k) is a quantification of the light absorbing abilities of the exhaust plume when measured across a one-meter optical path, has units of (m^{-1}), and is the preferred form of smoke measurement in Europe.

Opacity meters (or smoke meters) can be classified as either full flow or partial flow meters. A full flow meter measures opacity from the entire exhaust plume whereas a partial flow meter draws a sample from the plume for analysis. When opacity readings are taken from a snap-acceleration test for certification purposes, readings must be adjusted for ambient conditions such as relative humidity, temperature, and barometric pressure. Some partial flow meters condition the exhaust sample before opacity analysis which eliminates the need for ambient condition correction. For the partial flow meters that do not condition the sample and for full flow meters, peak opacity readings must be corrected for ambient conditions as specified in the SAE J1667 special report.

3.3.12 Description of Commercially Available Opacity Meters

Described below are eleven commercially available opacity meters from five different manufacturers ranging in price from \$4000 to \$10,000. Some meters are designed specifically for use with the snap-acceleration test and provide only peak opacity readings and print-outs for certification purposes, while other units provide continuous opacity readings which can be collected continuously through a personal computer (PC) and are more suitable for research applications.

Telonic Berkeley Inc. offers two models, the Celesco 107 and the Celesco 300. Both are full flow meters and capable of providing continuous opacity data. The 107 is designed specifically for research use.

CalTest Instruments Inc. offers four models, the CalTest 1000, CalTest 1000 TR, the CalTest 2001 WIN, and the CalTest 2001 WIN TR. The 1000 series are full flow meters and the 2001 series are partial flow. The 2001 series have ambient RH, temperature, and barometric sensors for automatic ambient condition correction. The "TR" indicates units with engine speed sensors, oil temperature probes, and a BAR code reader. All four units are specifically designed for snap-acceleration testing.

Red Mountain Engineering Inc. offers the Smoke Check 1667 which is a partial flow meter that provides automatic ambient condition correction. The unit is designed specifically for snap-acceleration testing and has optional engine speed and oil temperature sensors.

Robert H. Wager Inc. offers three models, the 6500, 6700, and 7500. All three are designed primarily for snap-acceleration testing. The 6500 and 7500 models have full flow and partial flow options depending on the sensor head ordered. Continuous opacity data can be collected with a PC. The 6700 model is only a partial flow unit which provides peak opacity readings and print-out (with the optional printer). Engine speed and oil temperature sensors are available options.

Robert Bosch Corp. offers the RTT 100 opacity meter which is a partial flow meter. The exhaust sample is drawn through a flexible sample line and conditioned in a heated chamber before analysis. The unit has several different modes of operation which includes snap-acceleration testing. The RTT 100 is capable of measuring exhaust smoke in terms of opacity, absorption coefficient (or smoke density), and mass concentration. Mass concentration is calculated from the absorption coefficient and is presented in milligrams of PM per cubic meter (mg/m^3). The range is 10 to 1966 mg/m^3 with a resolution of 1 mg/m^3 . The RTT 100 manual states that this calculation is only accurate under steady state engine operating conditions.

Electromagnetic Wave and Particle Interaction

When an electromagnetic wave comes in contact with a field of particles (or particle cloud) the wave intensity can be diminished by either absorption and/or scattering. Scattering is caused by diffraction, reflection, and/or refraction as shown in Figure 3.5-1. Particle cloud absorption and scattering effects on a light wave are a function of the particle size and/or size distribution, the clearance between particles, material composition of the particles, and relative size of the

particles in relation to the electromagnetic wavelength. Dalzell and Sarofim (1969), Hunt et al. (1998), and Modest (1993) have reported varying results of particle material properties on scattering and absorption effects.

The size parameter (x) (which is a unitless ratio between a particle's size and the electromagnetic wavelength) is one of the primary variables effecting the relation between opacity light and diesel exhaust particles. The Mie scattering theory states that the relation is a function of x^4 (Modest, 1993). Rickeard et al. reported particle effective diameters to range from approximately 16 to 400 nm, with peak size concentration at 100 nm. Hunt et al. found particle diameters to range from 2 to 500 nm under no-load operating conditions and 10 to 1000 nm under full-load operating conditions. The ISO 3173 standard governs opacity light-source wavelength to range from 550 to 570 nm. The resulting size parameter, x , between opacity light source and reported diesel PM size ranges from 0.011 to 5.51. This suggests that the standard size range of diesel PM has a broad ranging optical effect on opacity response, and that many particles may be undetectable by an opacity meter. This observation is supported by research results shown in Sections 3.5.3 through 3.5.7. As manufacturers strive for better fuel atomization through increased injection pressures and better injector design, PM size range is likely to reduce.

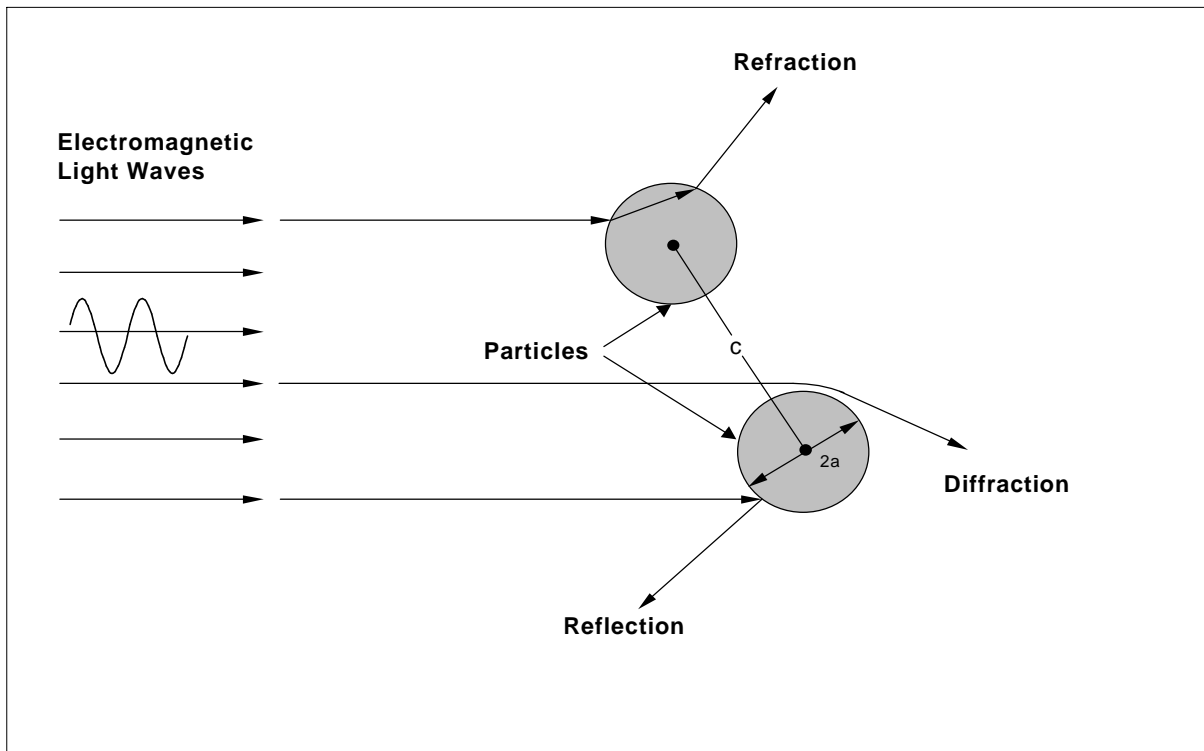


Figure 3.5-1. Diagram of the scattering effects of a particle on electromagnetic waves.

Comparison of Opacity Meters

Some opacity meter comparisons have been conducted at West Virginia University, using the Bosch RT 100 and a Wager 650CP. The Wager 650CP opacity meter is basically an earlier model of the 6500 mentioned above. It uses a light emitting diode (LED) green gallium phosphide light source (570 nm) and a Si photo diode with an infrared filter. It has a 0 to 1 volt analog output with a linearity of 1% from 0 to 100% opacity, and a response time of 0.45 seconds from 0 to 95% opacity. The Wager is readily configured to read continuous opacity.

Test results are shown in Figures 3.5-2 and 3.5-3. Figure 3.5-2 shows magnitude comparison as well as filter-captured PM mass averaged on a per snap basis (in the upper region of the bar graph). Figure 3.5-3 shows the scatter of the data readings. The Bosch readings were consistently higher than the Wager by a factor of almost two. This relation is quantified by the slope of the linear best fit between the data when Wager values are plotted as a function of Bosch values as shown in Figure 3.5-3. It is evident that overall the data scatter is high and that the two meters do not agree in value.

Without the reference of readings from other opacity meters, it is difficult to determine which meter is more accurate. The large difference between opacity raises some concern. Both meters use a light source of similar wavelength (approximately 570 nm), so it would first appear that the size parameter, x , would not be the source of difference. However, particle size may be a factor due to differences in sampling methods between the two meters.

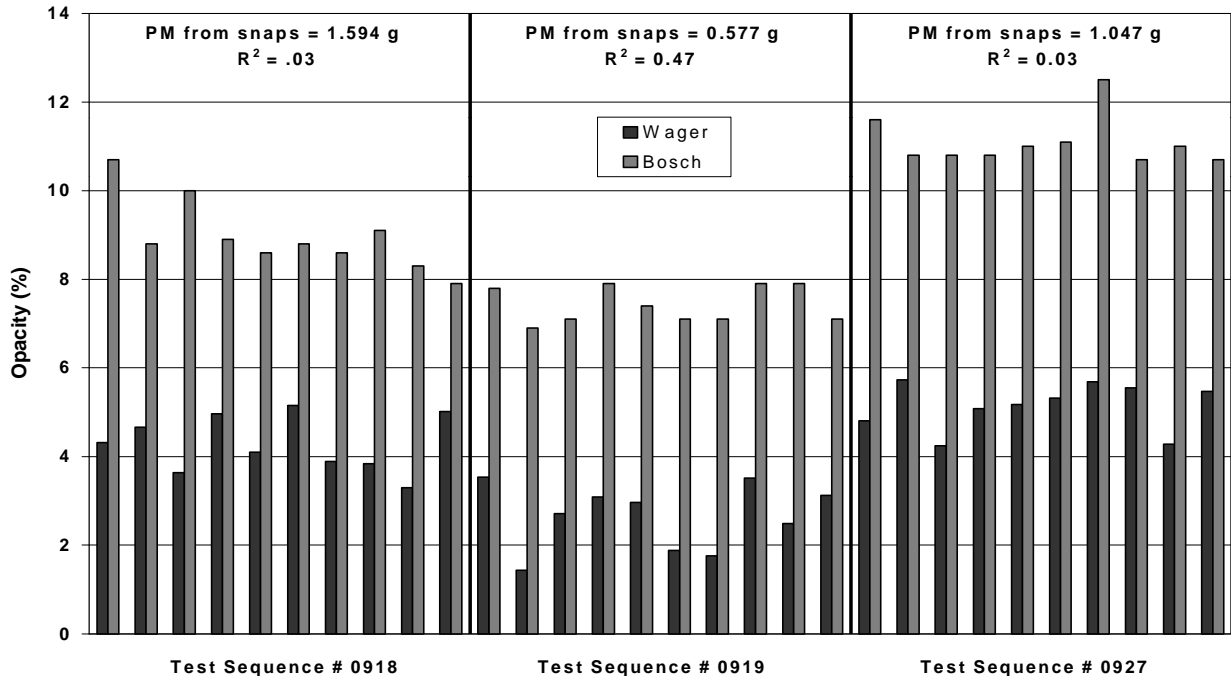


Figure 3.5-2. Bosch and Wager peak opacity values obtained from three transit buses powered by similar 1996 DDC Series 50 engines exercised through snap-acceleration tests. The R² values are from plotting Wager data as a function of Bosch data for each test.

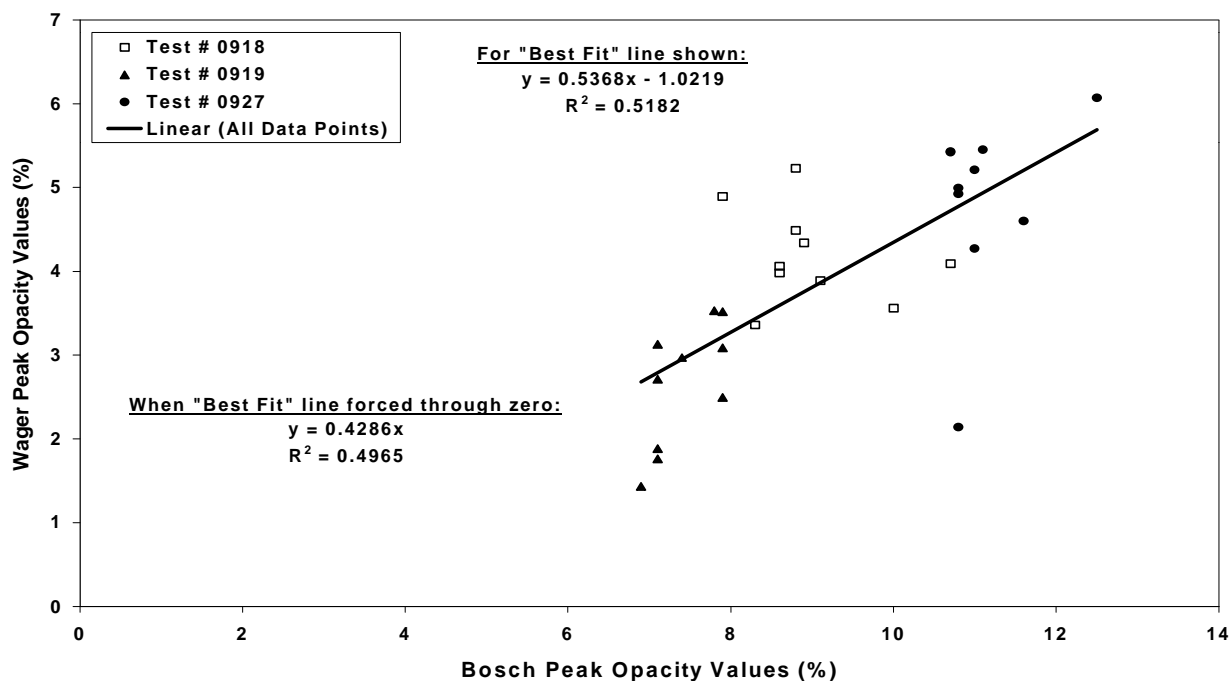


Figure 3.5-3. Wager peak opacity plotted as a function of Bosch peak opacity. The R^2 values are for a linear best fit to data from all three tests.

The Wager opacity meter was mounted at the end of the exhaust transfer pipe just prior to the dilution tunnel. The exhaust transfer pipe was insulated to minimize exhaust gas cooling and thus minimizing condensation of exhaust moisture in the pipe's inner wall. PM formation is a partial function of exhaust gas cooling, which is one of the primary purposes of the dilution tunnel. Thus, the Wager opacity meter was examining the PM before exhaust gas cooling and thus before complete particulate formation. In contrast, the Bosch opacity meter exhaust sample travels through a 5.2 m (17 ft.) silicone line before opacity is measured. Based on the silicone sample line dimensions and a flow rate of 1.2 l/s, the travel time of the exhaust sample in the silicone hose was approximately 0.31 seconds. Although this is a rather brief time period, there would be some cooling of the exhaust gas while traveling through the Bosch sample line and more time allowed for particle nucleation, adsorption, and conglomeration. Abdul-Khalek et al. (1998) evaluated particle size distribution and concentration from a diesel engine and found that the particle count increased by a factor of more than ten between residence times of 40 ms and 400 ms in the diluted sample. Another cause of the difference in opacity magnitude may be differences in data sampling rates. The Bosch RTT 100 sampled at a frequency of 100 Hz, whereas the Wager 650CP put out a continuous voltage signal which was sampled at a 10 Hz frequency through the laboratory's ADC data acquisition board. Jones et al. (1997) reported a 16% increase in smoke density (k) (12% when converted to opacity) when the data acquisition frequency was raised from 10 Hz to 20 Hz. Thus, data acquisition of the Wager opacity meter signal may have missed peak opacity values that the Bosch RT 100 was able to capture. It is noted that the Bosch opacimeter also examines the PM before adequate exhaust gas cooling occurs.

The lack of correlation between gravimetric PM and opacity data from both meters was probably due to geometric differences, improper sample conditioning at the point of optical analysis, and optical effects such as the size parameter and complex index of refraction. The geometric difference is based on the fact that opacity is a partial function of a particle's cross-sectional area whereas PM mass is a partial function of a particle's volume. If it is assumed for the moment that PM is spherical then the cross-sectional area is πr^2 and the volume is $4/3\pi r^3$. Assuming no change in density as the particulate conglomerates, it is evident that the ratio of opacity to PM is a partial function of radius. The opacity data were obtained just prior to the dilution tunnel. PM formation in diesel exhaust is strongly affected by the rapid cooling associated with mixing of ambient air. It is apparent that PM would not be fully formed at the point of optical analysis and thus the exhaust particulate would have a lower opacity signature prior to dilution. The absorption and scattering effects of the particle cloud are dependent on the particle's complex index of refraction (which is a function of shape and composition) and size parameter between each particle and the opacity meter light wavelength. Since PM size, shape, and composition vary throughout different operating conditions, the optical effects of the particle cloud will vary as well.

Opacity and Particulate Matter

The PM mass collected by filter during a transient test cycle is a function of the total exhaust volume sampled, the number concentration of particles, the particle size distribution, and the particle density, as well as filtering conditions such as filter face velocity, filter medium, and sampling temperature. In contrast, opacity is a function of the number concentration of the particles, the projected area of the particle, and the light extinction (absorption and scattering) properties of the particles. Thus, the ratio between PM and opacity is a function of particle size, as well as the light extinction effects of the particles. Even with the assumption that the particles are spherical, monodispersed, and of the same bulk density, it is evident that particle size and nature will affect the relationship between opacity and PM mass. However, it should be noted that these assumptions could create considerable error. The particle density is a partial a function of the amount of hydrocarbons deposited on the particle. Hydrocarbon deposition and particle effective radius are a function of fuel, engine design and type, nature of the exhaust gas dilution, and possibly speed and load within the same engine family. Furthermore, the light extinction effects of a particle are a function of the particle's complex index of refraction (m) and the size parameter (λ). Given that most diesel particles are in the sub-micron range, the particle diameter is of the same size order as the wavelength of the opacity meter light source. This results in Mie scattering for the larger particles and Rayleigh scattering for the smaller particles. Most diesel particles fall into the Rayleigh scattering classification which is a function of x^4 (Modest, 1993). Thus, a small change in particle size has a much larger effect on light extinction. As a result, prediction of instantaneous and total PM with present forms of optical exhaust measurement (light extinction) is elusive at best.

This report presents below data from the thesis of Jarrett (2000). The relationship between opacity and PM was evaluated from three perspectives. The first compares integrated PM and integrated opacity from twelve different vehicles (three different engine types) which were exercised through snap-acceleration tests. The second perspective compares integrated opacity

and integrated PM data from three different vehicles exercised through loaded (CBD cycle) and non-loaded (snap-acceleration) tests. The third perspective evaluates integrated PM plotted as a function of integrated opacity for one engine exercised through different simulated driving patterns, the same engine type exercised through the same transient test cycle, and different engine types exercised through different simulated driving patterns.

Snap-acceleration Tests

The first perspective was determined in part because the snap-acceleration test is intended to identify PM production and because most of the filter-captured PM can be attributed to the transient periods of a snap-acceleration test. The PM mass due to transient operation during snap-acceleration testing was isolated by the relation,

$$PM_{snaps} = PM_{test} - \dot{PM}_{idle} * t_{test} \quad \text{Equation 3.5-1}$$

where,

PM_{snaps} is the PM mass due solely to the transient operation during a snap-acceleration test (g).

PM_{test} is the total PM mass from a snap-acceleration test (g).

\dot{PM}_{idle} is the PM mass rate determined from an idle test (g/s).

t_{test} is the time length of a snap-acceleration test (s).

The average PM mass per snap was determined simply by dividing PM_{snaps} by the total number of full-throttle accelerations (or snaps) in the snap-acceleration test, which was ten for each of the three tests. Average opacity per snap was determined by summing the peak opacity data and dividing by the total number of snaps. The average integrated opacity per snap was determined by the relation,

$$OP_{aver / snap} = \frac{\sum OP - OP_{aver, idle} \cdot t_{test}}{n_{snap}} \quad \text{Equation 3.5-2}$$

where,

$\dot{a}OP$ is the integrated opacity for the entire test (%s).

$OP_{aver, idle}$ is the average opacity during idle (%).

The results of this analysis applied to three different engine types are shown in Figure 3.5-3. Best-fit lines are displayed for two of the three sets of data, the third being omitted due to only two data points (lower left corner of Figure 3.5-3). A best-fit line was also applied to all twelve of the data points. All three curves show a weak positive correlation between opacity and PM and also indicate that integrated opacity data cannot accurately predict the total integrated PM emitted by a HD diesel vehicle operated in a snap-acceleration test. From this one may also conclude that integrated opacity cannot predict total integrated PM for other transient driving conditions, and that instantaneous opacity cannot predict instantaneous PM in a general fashion.

The positive ordinate intercept of all three best-fit linear equations also suggests the existence of PM when instantaneous opacity is zero. In other words, PM may exist in the exhaust while eluding optical detection and/or additional PM formation had occurred in the dilution tunnel after optical analysis.

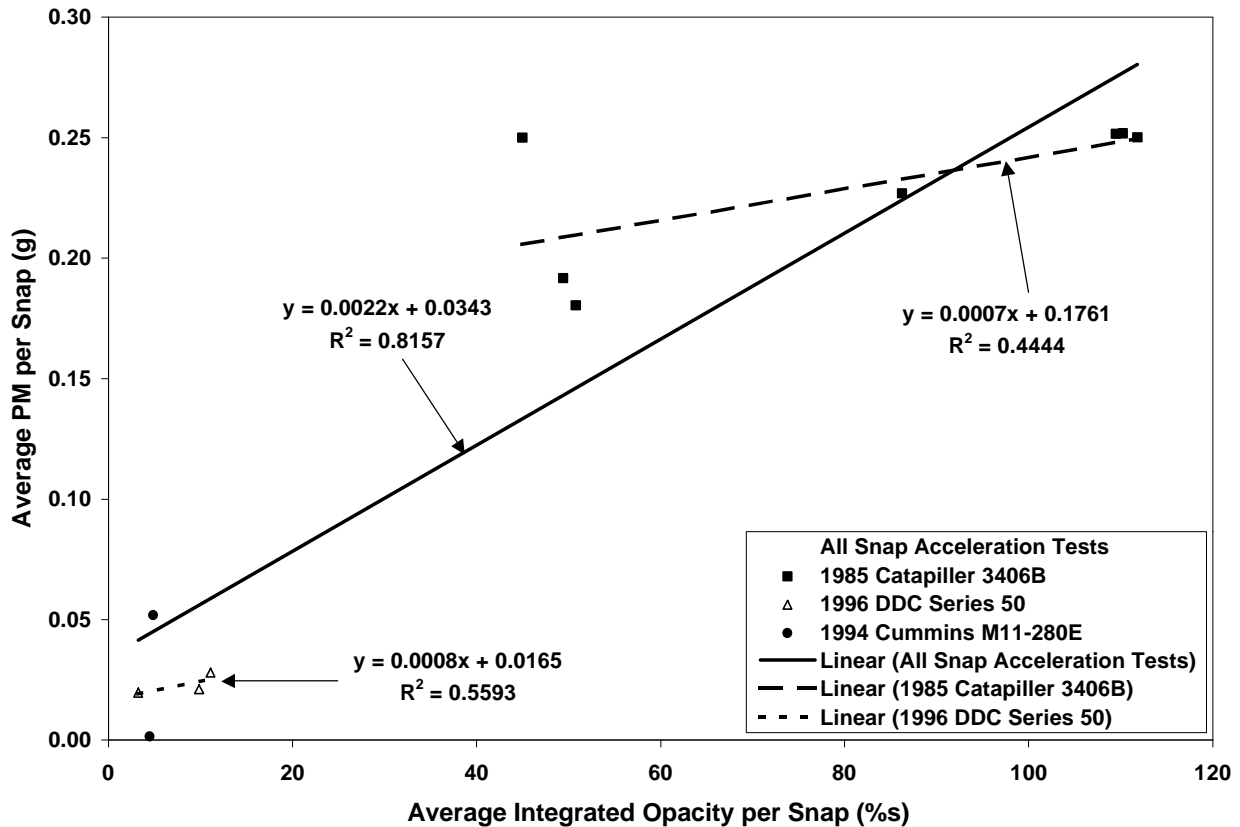


Figure 3.5-4. Average PM data as a function of average opacity data from three different vehicles exercised through snap-acceleration tests. Both PM and opacity were averaged on a “per snap” basis.

Engine Loading Effects

The next approach employed evaluated integrated PM and integrated opacity data from an engine exercised through a loaded transient test and a snap-acceleration test. The loaded transient test in this analysis was the CBD cycle. Since integrated PM cannot be attributed to any specific portions of the test, values used for this analysis are integrated PM and integrated opacity over the course of both tests. Results from two transit buses powered by different engines of the same model are shown in Figure 3.5-4. These plots further support the argument that the snap-acceleration tests fail to identify PM due to engine loading. The PM output from the CBD cycle for the same integrated opacity value is much higher than that of the snap-acceleration test for both engines. This is due to the difference in engine loading between the two tests. Furthermore, the R^2 values for the linear best fits from the CBD tests show little to no correlation between the integrated opacity and integrated PM. It is noted that the scaling of the figure to include data points from the snap-acceleration tests cause the CBD data points to appear closer in

proximity to the best fit line than they actually are. It is also noted that the ordinate intercept suggests PM production at zero opacity as observed in Figure 3.5-3.

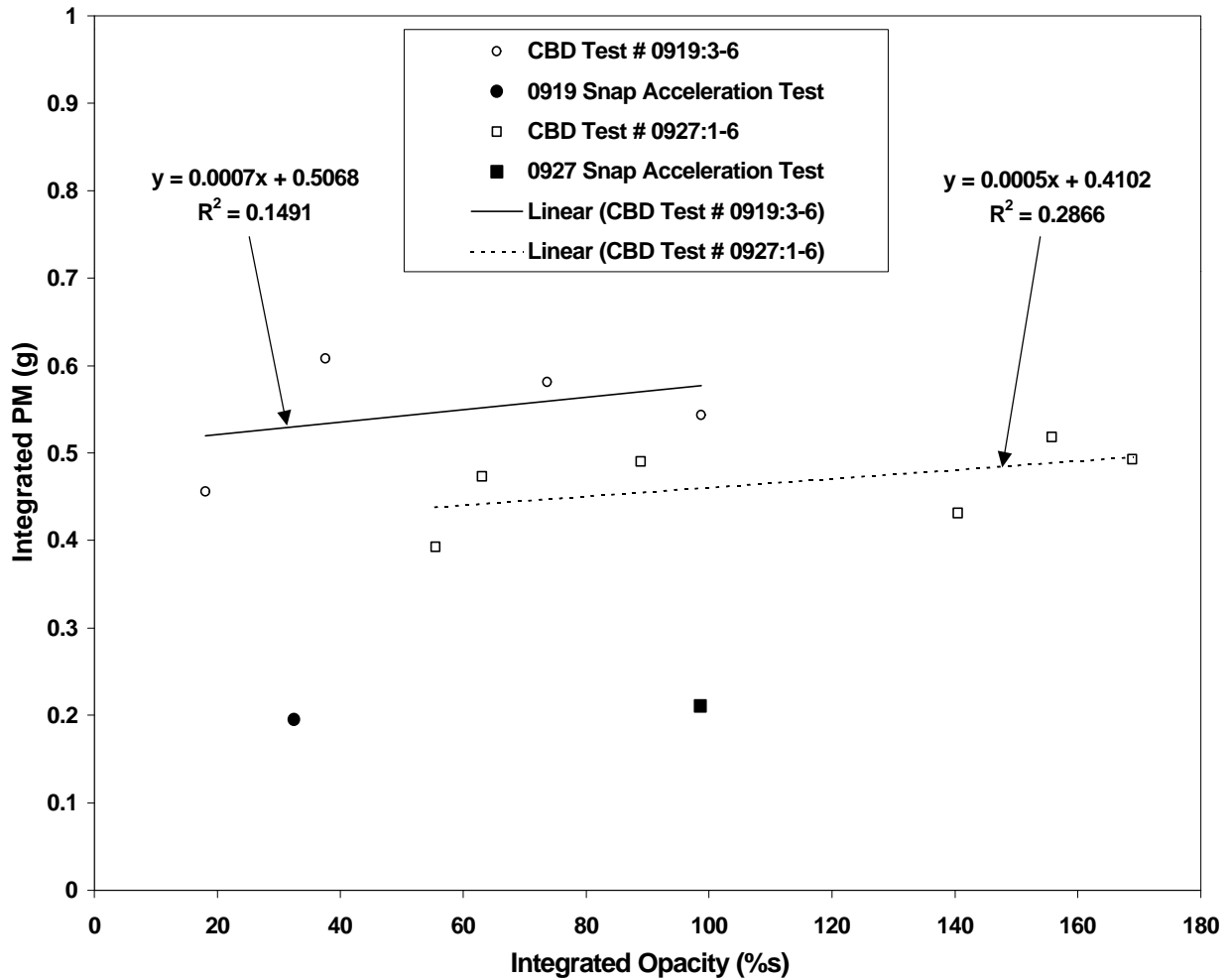


Figure 3.5-5. Comparison of integrated PM a as a function of integrated opacity from two 1996 transit buses powered by similar DDC Series 50 engines exercised through loaded and non-loading transient tests (CBD cycle and snap-acceleration). These plots show higher integrated PM for loaded operating conditions than for non-loaded operation for respective integrated opacity values.

Driving Cycle Effects

Since it is known that transient operation and loading affect PM production, then it would be logical that different driving conditions would affect PM production. For this evaluation PM and opacity data were collected from a single engine exercised through different driving cycles. Figure 3.5-5 shows integrated PM plotted as a function of integrated opacity on a per mile basis from a 1996 transit bus powered by a 1996 DDC Series 50 engine exercised through four different transient tests; 5-Mile route, NYCB cycle, Test D, and the CDB cycle.

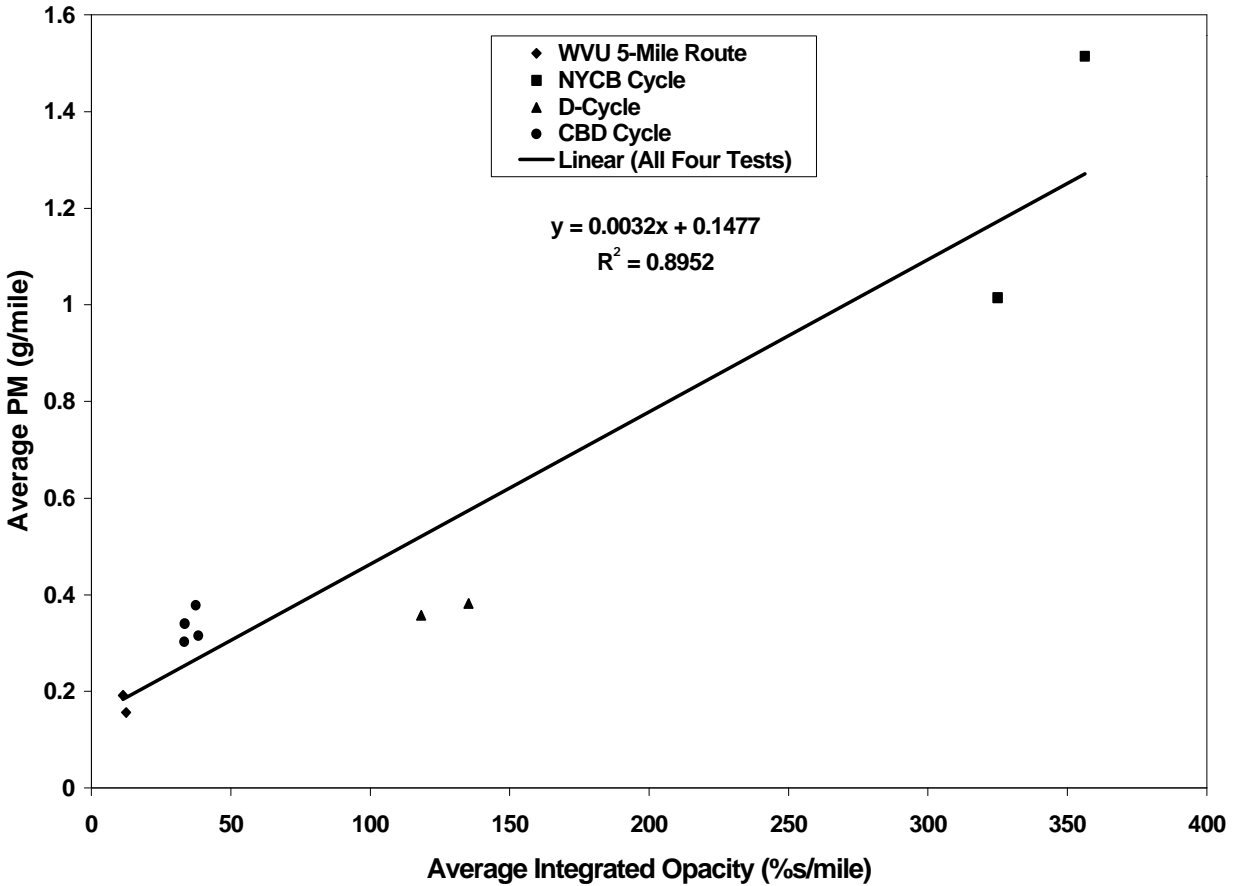


Figure 3.5-6. Integrated particulate matter as a function of integrated opacity from a DDC Series 50 engine exercised through four different transient tests. This plot shows the strongest correlation between integrated PM and integrated opacity which may suggest some correlation between PM and opacity for a specific engine.

This plot shows the highest linear correlation between PM and opacity within this research, suggesting that the PM/opacity relation may be engine specific. This would be supported by the fact that particle size, the ratio between soluble organic fraction and elemental carbon, and lubrication oil contribution to PM are all engine specific.

In addition to exercising the same vehicle through different driving cycles, a series of tests was completed where the same vehicle was exercised through the same driving cycle (CBD) for three different simulated inertial weights. Test 0920 was tested at 85% of the gross vehicle weight (GVW), or 14,897 kg (32,843 lb.); test 0921 was tested at the vehicle curb weight plus 113 kg (250 lb.); and test 0922 was tested at 100% of GVW 17,269 kg (38,072 lb.). Average PM plotted as a function of average integrated opacity from these tests is shown in Figure 3.5-6. The results show no correlation between PM and opacity when vehicle loading is varied. These results agree with results shown in Figure 3.5-4.

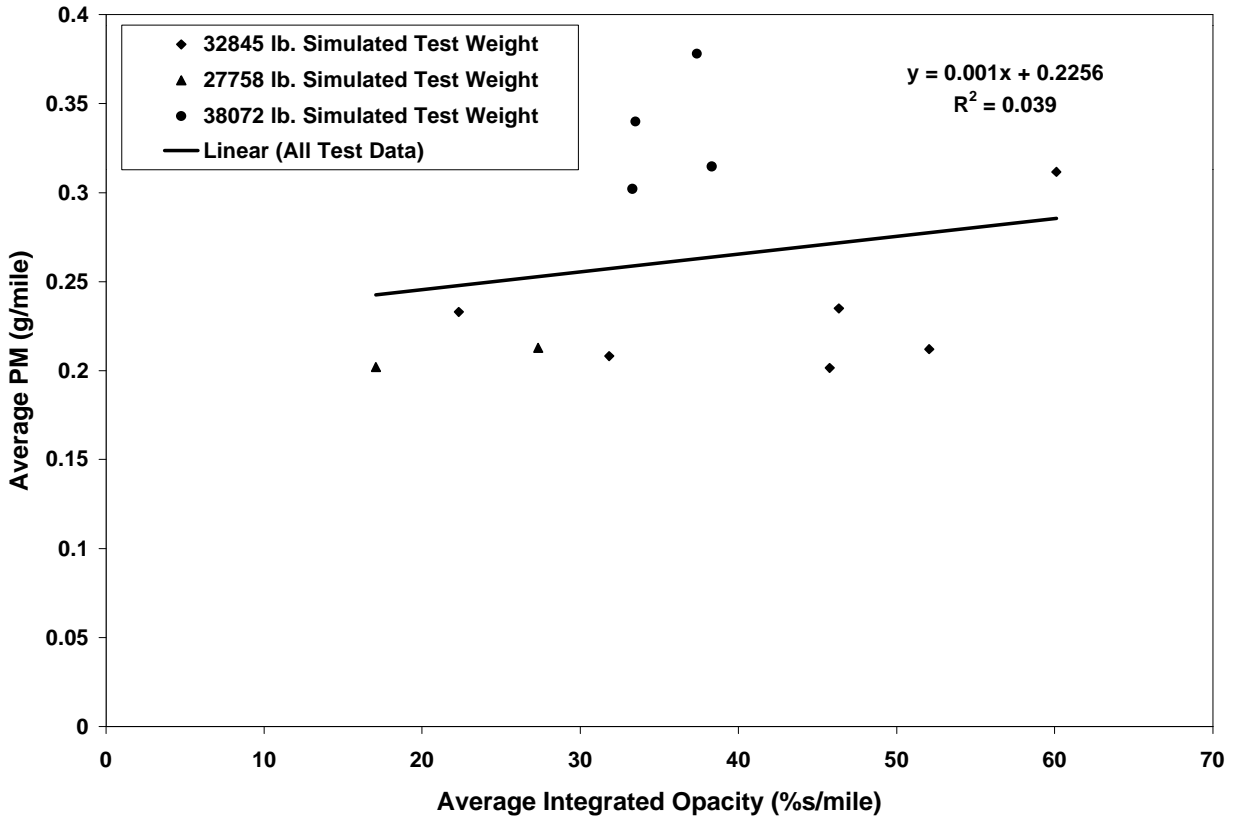


Figure 3.5-7. Average PM plotted as a function of average integrated opacity from a single vehicle exercised through similar driving conditions for three different simulated inertial weights. The vehicle was a 1996 transit bus powered by a 1996 DDC Series 50 engine exercised through a CBD cycle.

Figure 3.5-7 plots average PM as a function of average integrated opacity for all Flint, MI CBD tests with the same simulated inertial weight. This plot shows considerable scatter in the data, suggesting little to no correlation between average PM and average integrated opacity for the same engine type (i.e. different engines of the same model) exercised through similar driving and loading conditions. This could be due to several reasons including engine wear, maintenance history, fuel quality, driving habits, and ambient weather conditions. However, for the tests represented in Figure 3.5-7, vehicle odometer readings ranged from 43,000 to 66,000 km (27,000 to 41,000 miles), so engine wear and maintenance were probably not a factor. All buses were driven on the same fuel, driven by the same driver, and weather conditions varied little. Also noted is the positive ordinate intercept of the linear fit.

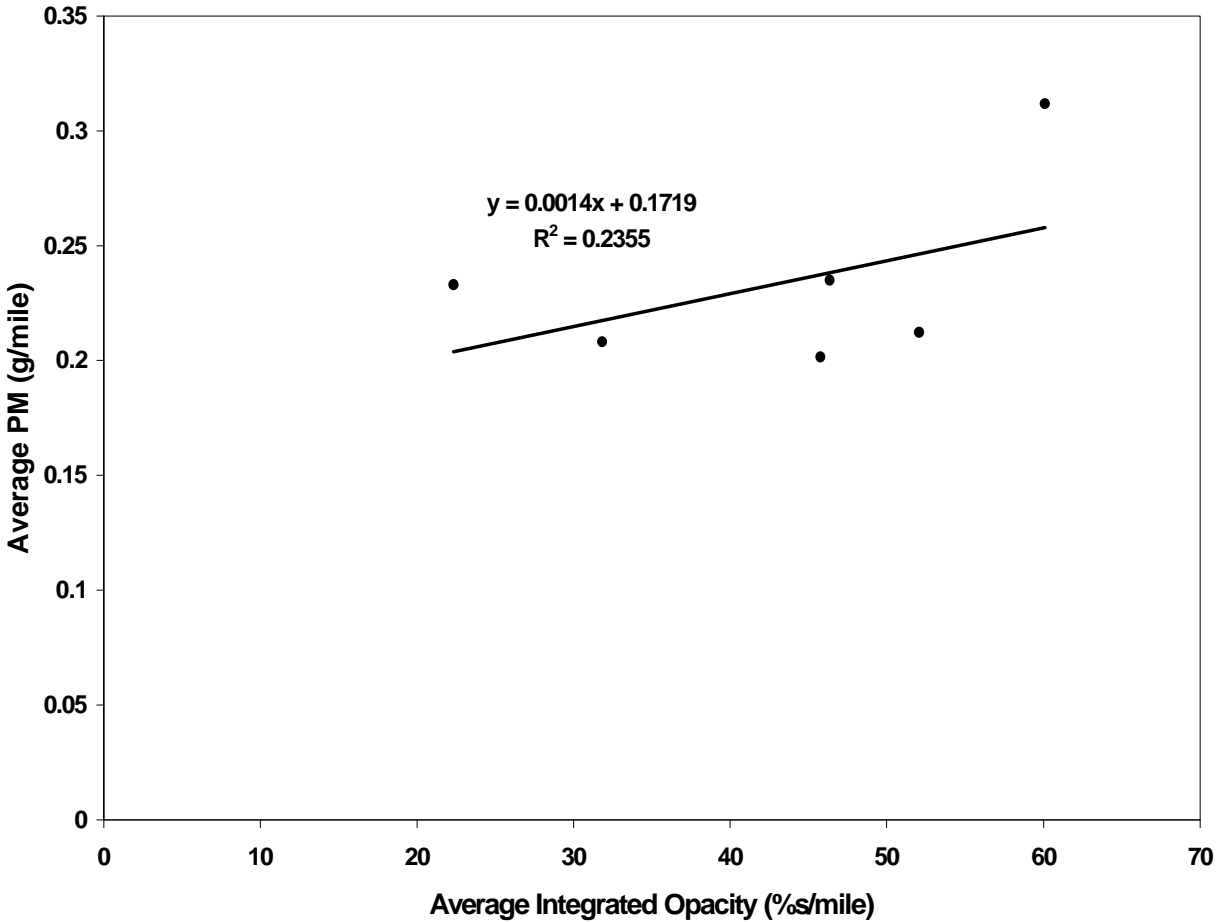


Figure 3.5-8. Integrated PM as a function of integrated opacity from six different 1996 transit buses powered by similar 1996 DDC Series 50 engines exercised through a total of twenty-three CBD transient tests.

The lack of universal relation between PM and opacity is confirmed by Figure 3.5-8. All transient chassis tests with valid PM and opacity data taken for Jarrett’s research are shown in Figure 3.5-8. The data in this plot represent twenty-one vehicles powered by five different engine types which were exercised through six different transient emission tests for a total of sixty-three data points. The plot shows a very weak correlation between PM and opacity, as well as a positive ordinate intercept as in all the other plots of PM as a function of opacity. These results are similar to those obtained by Byrd (1996) where he stated “no adequate correlation could be found between the snap acceleration test and the chassis dynamometer transient test when comparing smoke opacity and particulate matter emissions.”

The overall conclusion is that, although PM and opacity may be related for a specific vehicle, opacity is not a reliable metric for the quantification of PM mass from a wide variety of vehicles. It is acknowledged that opacity readings collected during snap-acceleration tests have proven to be quite valuable in identifying vehicles with high PM output, possibly due to poor maintenance and/or engine tampering, but one question raised in a study by Gautam et al. (2000) is whether high opacity values during the snap-acceleration were in part due to higher total PM emissions.

CONFIGURATION EFFECTS ON COMPUTATIONS

This section describes the difficulties associated with obtaining reliable mass emissions of each species. Mass emissions must be computed in cases where the data are required to be expressed in units such as g/mile, g/bhp-hr, or g/cycle.

When a full-scale tunnel is used, the flow through the tunnel remains fairly constant. Therefore, if gas species concentrations are measured during a transient test, one may take the product of flow and concentration, integrate the product over the cycle, and compute the total mass of each species reliably. Efforts to align flow and concentration data, as discussed in the section below, provide only marginal improvement in mass measurement with a full-scale tunnel.

Similarly, if a mini-dilution tunnel is configured to take a slipstream of the vehicle exhaust, and is configured to sample proportionally from that exhaust, only the product of the diluted gas concentrations and exit flow from the mini-tunnel are required for computation of mass emissions. In this case, though, the art lies in being able to maintain the proportionality of sampling by the mini-dilution tunnel, particularly during transient operation.

In contrast, if raw exhaust gas is sampled, it is critical that one must measure the flow and concentration in the exhaust at exactly the same time, or else perform a time shift in one of the data sets, as described immediately below.

Similarly, if a mini-dilution tunnel is configured merely to hold a constant dilution ratio, it draws a sample at a constant mass flow rate from the exhaust, and it is critical that the resulting concentration signals are time shifted to align with the mass flow measurement, as described below.

The nuisance encountered in acquiring accurate mass emissions data can therefore be summarized as follows. Either one must keep the exhaust sampling proportional to the whole exhaust flow (case i), or one must be prepared to align data in time (case ii). The choices for proportional sampling (case i) either involve consuming the whole exhaust (full-scale tunnel option) or controlling a proportional sampling mini-dilution tunnel. Controlling the proportionality is made difficult by the need to measure the exhaust flow rate accurately, and by the need to execute the control of mini-dilution flows rapidly, accurately and at the appropriate time. High dilution ratios render accurate proportional sampling more difficult. When the sampling is at a fixed rate (case ii), either raw gas may be sampled, or it may be diluted at a fixed dilution rate. In these choices, the mass flow data and emissions concentration data must be carefully aligned, which requires additional coding, and which may warrant occasional quality assurance verifications to insure that the time delays have not changed. In summary, only the full-scale tunnel offers ease of both operation and data manipulation, but these tunnels are large and costly.

3.4 Time Alignment

This section presents the difficulties that arise in computing mass emissions data when regulated species concentrations are measured either from raw gas or from gas that has been diluted by a mini-dilution tunnel with a fixed dilution ratio. If a fixed dilution ratio is used, then the concentrations in the raw gas are readily computed. In both of these cases it is possible to measure the actual vehicle exhaust flow at any moment in time, using methods described elsewhere in this report. A facile consideration would then suggest that the product of concentration and exhaust flow at any moment could yield instantaneous mass emissions, and that these values could be integrated over the test cycle to yield a total cycle mass for each species. This is not so. The multiplication of concentrations and exhaust mass flow rates is confounded by both the time lag between measurements and the diffusion of measurements of gas species due to travel through the sampling system and due to analyzer responses.

Time delays are discussed first. Consider a set of data gathered from a truck following an in-use driving schedule. The data consist of a measurement of exhaust gas mass flow rate and measurements of NO_x concentrations in the exhaust using two different raw gas analyzers. The mass flow was found using an Annubar differential pressure device, a differential pressure transducer, and pressure and temperature measurements. The two NO_x analyzers used the NDIR and electrochemical principles respectively. The reader should note that these data are sufficiently similar to data that would be acquired with a constant dilution ratio mini-dilution tunnel and research grade chemiluminescent analyzer to cover discussion of that system as well. Figure 4.1-1 shows the raw data. It is likely, from knowledge of engine performance, that in reality there is strong correlation between NO_x concentration and exhaust gas flow rate, since both NO_x concentration and flow rate will be linked to air/fuel ratio for a turbocharged engine. From this consideration it is evident that there is substantial time misalignment between the flow and NO_x data.

A correction can be effected by aligning the NO_x peaks with the flow peaks, and cross-correlation techniques may be used to find the best fit delay correction. Figure 4.1-2 shows the value of the product of NO_x concentration (electrochemical) and mass flow rate versus the chosen time shift to match the two signals. It is evident that on average over the test, a delay of 6.6 seconds existed between the NO_x data and flow measurement. Figure 4.1-3 shows the NO_x and flow signals when they are best aligned.

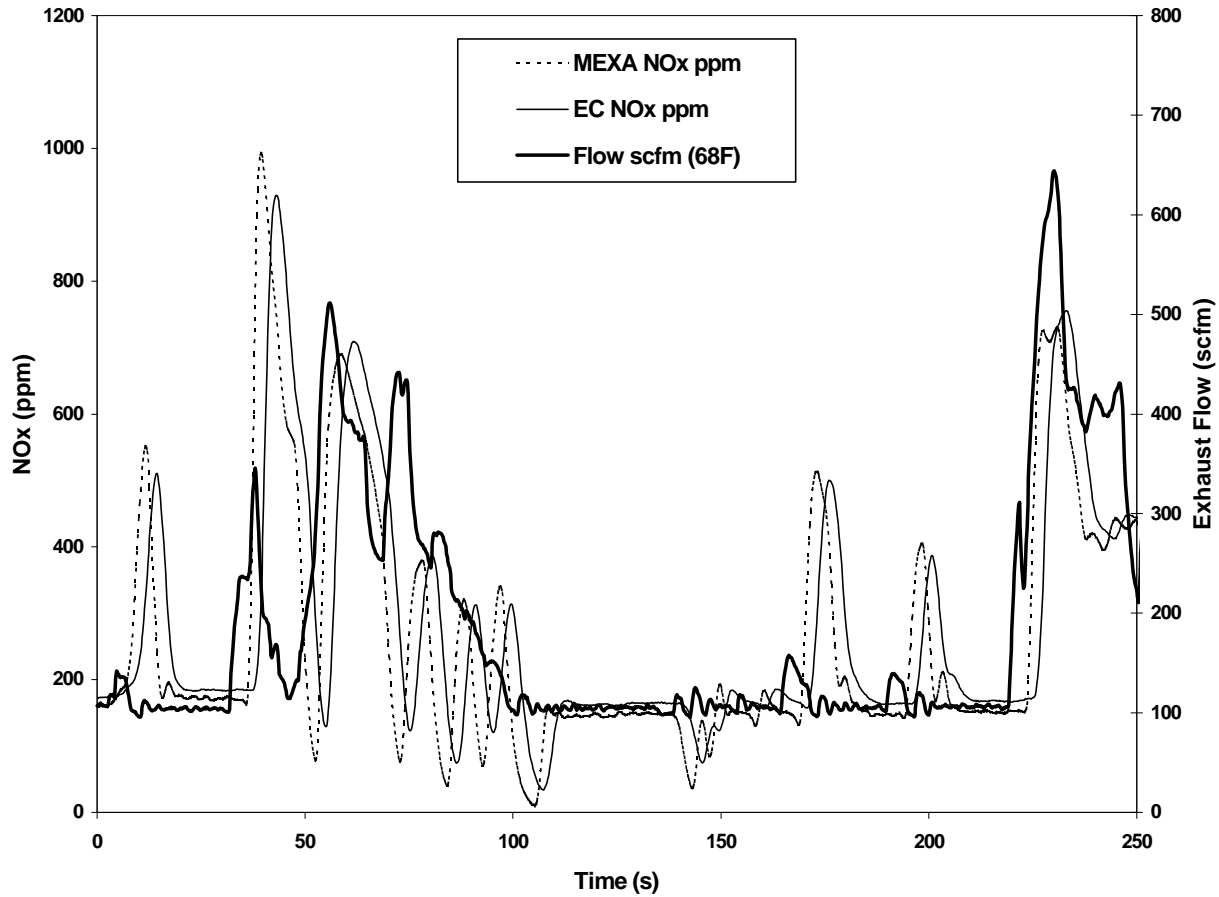


Figure 4.1-1. Data acquired for exhaust mass flow rate and raw NOx concentration from the MEXA (NPIR) and electromechanical sensor. Misalignment in time of the signal is evident.

Table 4.1-1 presents the products of flow and concentration, integrated over the cycle, for time aligned and unaligned data. These products are instantaneous values representing instantaneous mass flow of emissions species, and the integral over the cycle represents computed total mass of each species emitted. It is evident that failure to align data for transient cycles will cause underestimation of total mass emissions. In this case failure to align exhaust flow and NOx concentration would underestimate emissions by about 3 to 6%. The underestimation would depend on the transient nature of the cycle, analyzer response delay and turbocharger characteristics of the subject vehicle.

	Unaligned	Time Aligned	% Difference
NOx NDIR (MEXA)	5.84E+08	6.03E+08	3.15%
NOx (EC)	5.96E+08	6.33E+08	5.85%

Table 4.1-1. Improper time alignment typically causes underestimation of emissions.

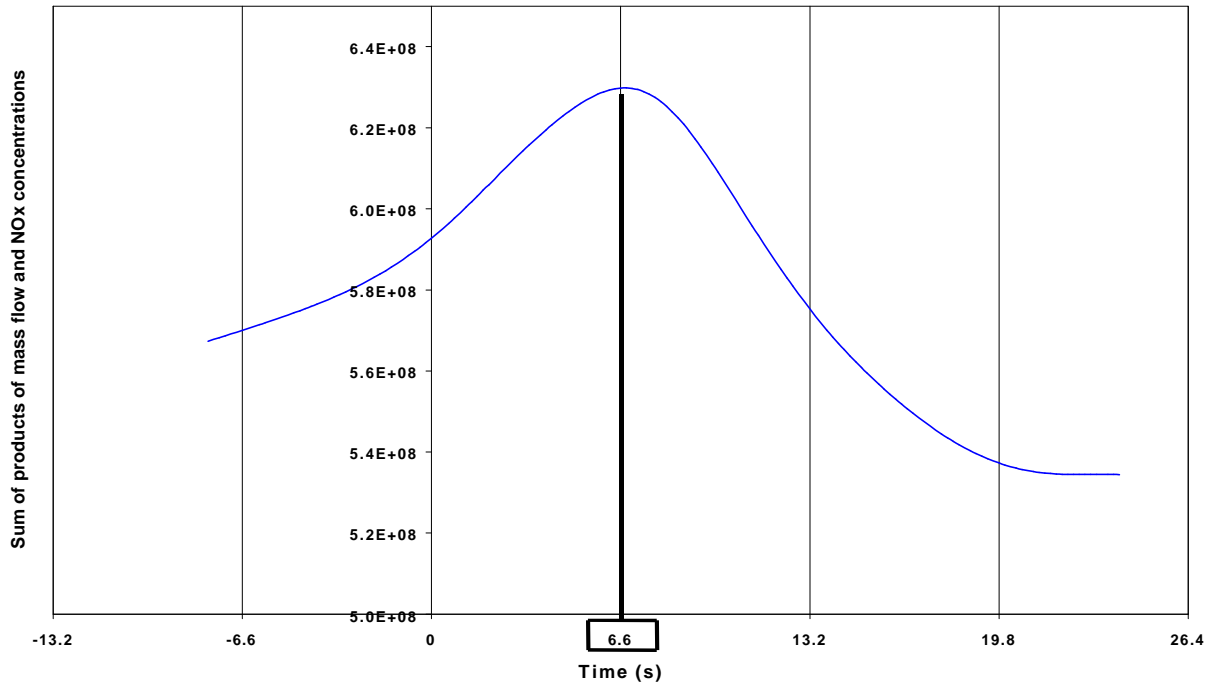


Figure 4.1-2. Determination of the time shift needed to provide best-fit alignment of NOx (electromechanical) and exhaust mass flow data.

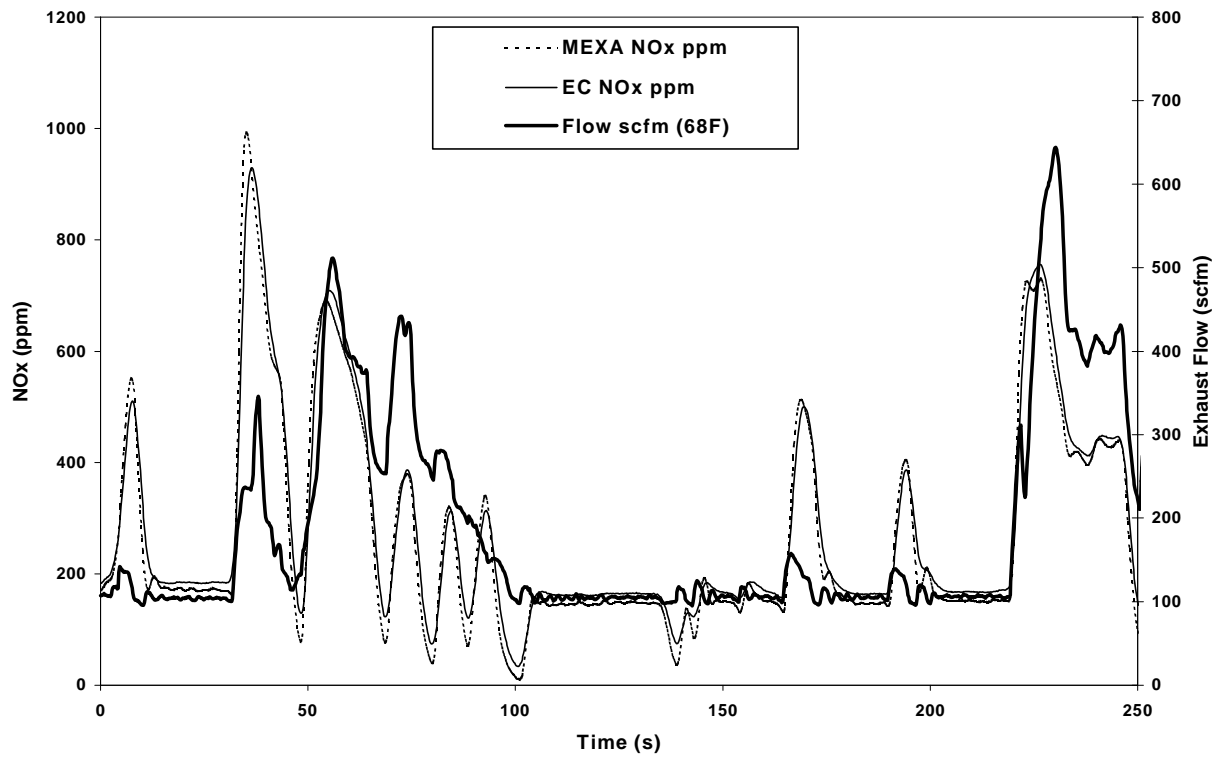


Figure 4.1-3. The same data as shown in Figure 4.1-1 after data has been shifted to adjust for proper time alignment.

3.5 Diffusion In Measurement Systems

The previous section has addressed the issue of time delay. Regrettably, there are also concerns over the diffusion of actual concentrations by the measuring device. To illustrate this point, consider the response of a conventional research grade NDIR CO₂ analyzer drawing from a full-scale dilution tunnel when a 4 second burst of CO₂ is introduced into the tunnel mouth. Figure 4.2-1 shows that not only delay, but diffusion of the sample also occurs. Much of the diffusion in this case is due to the nature of filling the measurement cells in the analyzer, but all analyzers will exhibit diffusion. The diffusion can be mimicked by a gamma distribution, as shown in Figure 4.2-1, and Ramamurthy & Clark (1999) previously used a more complex equation, due to Levenspiel, to model the shape. In highly transient test cycles, this diffusion may be of concern. Figure 4.2-2 shows that through modeling, the diffusion effect over transient cycles may be simulated, so that it is well understood. It introduces an error that is smaller than that due to failure to align signals in time. The reader will observe that the distribution appearing in Figure 4.2-1 is not symmetrical in time, so that alignment in time by peak and by mode would differ.

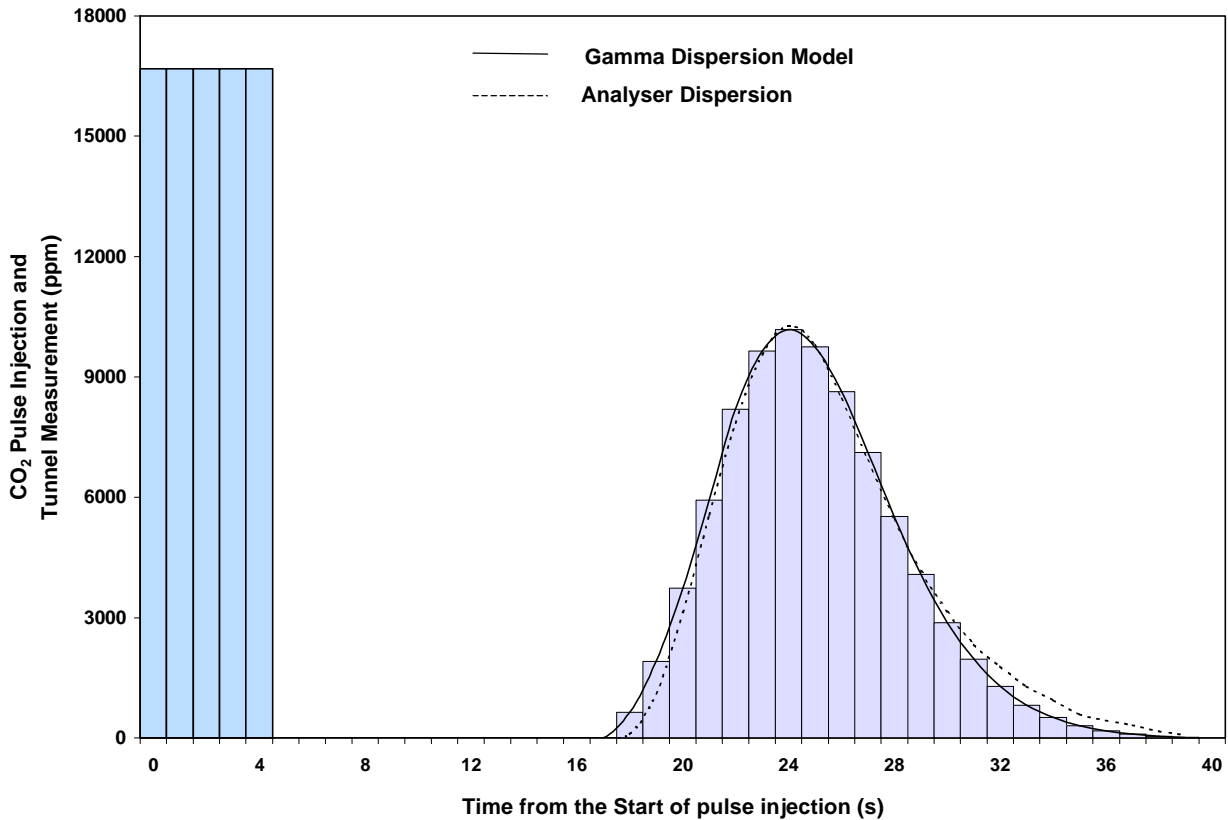


Figure 4.2-1. CO₂ emissions measured by a Rosemount infrared CO₂ analyzer (right) in response to a four second pulse injection of raw CO₂ (left).

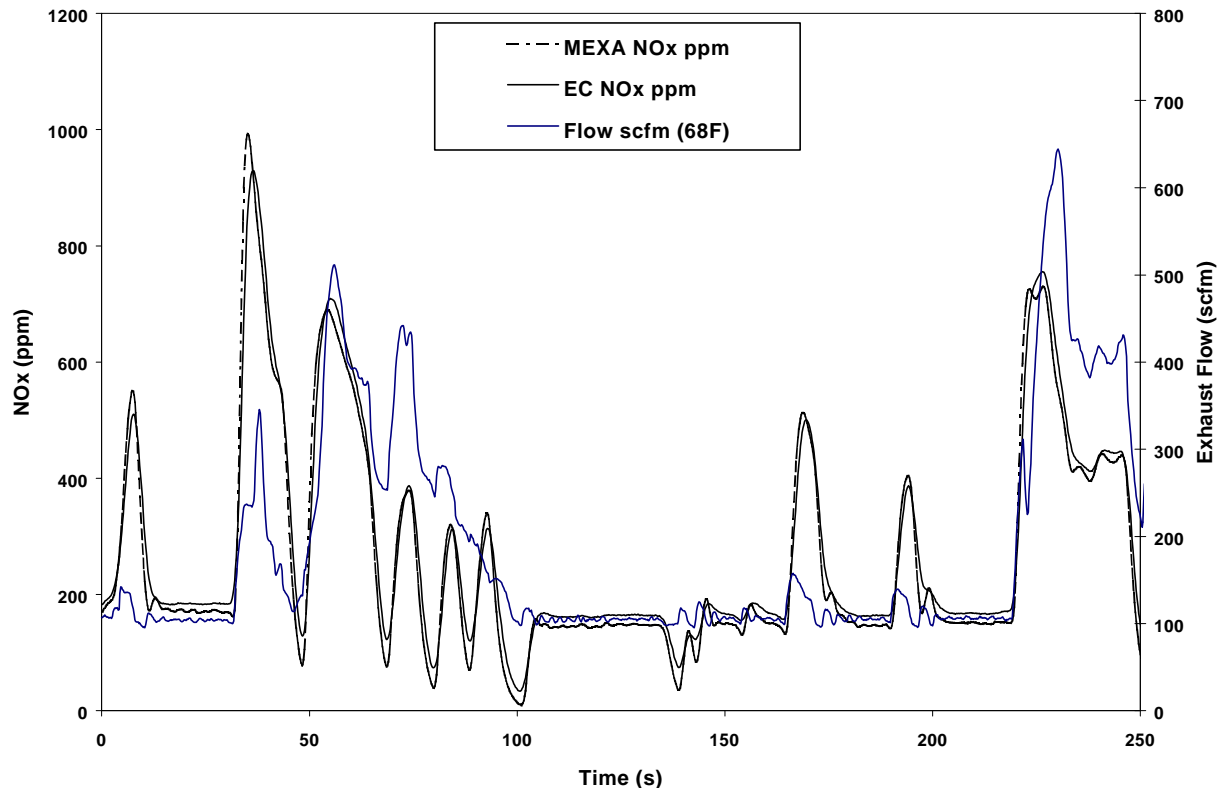


Figure 4.2-2. It is possible to model the response of the sampling system and analyzer by applying a diffusion model to the simulated instantaneous emissions at the engine manifold.

4 EXHAUST DILUTION

Commonly in research and certification of engine emissions characterization, the whole engine exhaust is ducted to a full flow dilution tunnel. For heavy-duty diesel emission analysis such a tunnel may have a diameter of 18 inches and a length of 220 inches. Analyzers and filters draw a diluted exhaust sample near the end of the dilution tunnel at a downstream distance ten times that of the tunnel diameter. Mass flow through the tunnel is held constant (or nearly constant) and is greater than the maximum flow from the engine, so that all exhaust must pass through the tunnel and excess tunnel flow is made up by dilution flow. Typically the minimum dilution ratio (dilution flow/exhaust flow), which occurs near the point of maximum engine power, would be a factor of two or more, and would increase to a dilution ratio greater than ten at light engine loads. The dilution flow (often ambient air) may be filtered or unfiltered, and cleaned or uncleaned. When dilution flow is unfiltered and uncleaned, the measured emissions must be corrected for dilution air (background) concentrations.

The flow through full flow dilution tunnels is maintained using either:

1. A positive displacement pump preceded by a heat exchanger to maintain the pumped gas at near constant density, or
2. A blower or fan which draws air through a critical flow venturi. Flow through the venturi varies as the square root of the absolute temperature, and so variations are small with respect to engine load and no heat exchanger is needed.

Gas density in the dilution tunnel varies little as a result of varying dilution ratio because the combination of CO₂ and H₂O as products of combustion has a net density very similar to that of air. In addition, these two combustion products account for more than 99% of the total exhaust gases.

The flow rate through the full flow tunnel, as a function of tunnel temperature and pressure, is accurately determined using coefficients gained during a primary calibration, and the system integrity is controlled using mass recovery from propane injection tests before use. Thorough mixing is achieved by the highly turbulent flow within the dilution tunnel, where Reynolds a number of greater than 100,000 is typical (Jarrett, 2000). Additional mixing can be encouraged by use of an orifice near the tunnel entrance.

Disadvantages of full flow tunnels are their bulk, cost and power demand in operation. Also, to maintain analyzers in suitable range, and to capture filter PM from such tunnels, the total mass flow rate in the tunnel must be changed to suit engines of substantially different size.

Advantages of full flow tunnels are that they provide a venue for good contact between exhaust and dilution air, with low wall effects due to their size, and that the instantaneous flow rate and total cumulative mass flow over a test are both known accurately. In this way, the product of gas concentration and tunnel flow rate, when time aligned, can yield actual mass flow rate of an emissions species in g/sec, as discussed above. These values can be summed over a test cycle to yield the total species mass for that cycle.

Where it is impractical to employ a full flow dilution tunnel, or where large dilution ratios are required, dilution of a slipstream of raw exhaust is favored. This is termed partial dilution. Although dilution may be achieved simply at a tee junction, a partial flow dilution tunnel (or mini-dilution tunnel) can provide good contact between the dilution air and raw exhaust. Their advantages over full flow dilution tunnels are that they have no engine size limit (large or small), the dilution ratio can be held constant and predetermined to account for various fuels, inert gas or filtered and dried air can be practically used as the diluent (due to the low volumetric flow demand), and, with the advent of more responsive flow controllers and feedback control, mini-dilution tunnels are able to respond to varying exhaust flow rates and temperature during transient operation. Mini-dilution tunnels are readily constructed but require comprehensive flow management in application. Two are commercially available from Horiba Instruments Inc. & Sierra Instruments Inc.

Horiba Instruments Inc. offers the MDLT-1300T mini-dilution tunnel which can operate in proportional sampling mode or constant dilution ratio mode. Diluted and diluent flow is controlled by venturi flow meters and rapid response piezo-electric valves. The piezo-electric valve operation is adjusted through the feedback control system to maintain proportional sampling or constant dilution ratio mixing. Flow control is also adjusted based on a moisture vapor sensor since exhaust and diluted volume flow rates are affected by changes in relative humidity. When operated in the proportional mode, the manufacture claims good correlation with full flow dilution tunnel results for transient engine operation.

Sierra Instruments Inc. offers the BG-2 mini-dilution tunnel which was co-developed by Sierra and Caterpillar. The dilution chamber is patented by Caterpillar and flow control is provided by two Sierra Series 860 Digital Mass Flow Controllers with sample flow accuracies of $< \pm 1\%$ and repeatability of $< \pm 1\%$. Flow rate or dilution ratio are initially determined by the operator and the mass flow controllers are continually adjusted by a microcomputer. Test results showed good correlation when the BG-2 results were compared with full flow dilution results (Graze, 1993).

The first level of concern in operating a mini-dilution tunnel is that the dilution ratio (say, as [dilute exhaust mass flow]/ [raw exhaust mass flow]) is known or properly maintained. Flow of raw exhaust is difficult to control, because the temperature of the gas varies widely and may be high. It is not desirable to cool the raw exhaust prior to dilution. The dilute exhaust mass flow and the dilution air flow are more readily controlled, but for a high dilution ratio any inaccuracies in these two flow rates are amplified substantially, since the raw exhaust flow is determined by the difference of the two. This issue, and the issue of increased wall effects, are two drawbacks of mini-dilution tunnels.

When a slipstream is drawn from the raw exhaust, it may be drawn at a fixed mass flow rate, or at a flow rate proportional to the total exhaust flow. If the flow rate is to be proportional, the measurement of exhaust mass flow rate is essential for control purposes, and the mini-dilution tunnel must be managed to permit time-varying ingestion of raw exhaust. The time-varying control of raw exhaust flow is accomplished usually by holding the dilute exhaust flow out of the mini-dilution tunnel at a fixed rate, using a mass flow controller and pump, and varying the amount of dilution air fed to the mini-dilution tunnel with a control valve. This means that the dilution ratio in the mini-tunnel must vary as the exhaust flow varies. Great skill is required to design a system that provides for proportional sampling by varying the dilution because accuracy of flow control is crucial at high dilution rates and because the control valve must respond very rapidly during engine transients.

If a fixed raw exhaust flow, and hence a fixed dilution ratio, are employed with the mini-dilution tunnel, then an issue of biasing in measuring total emissions over a cycle arises. This is best illustrated by considering a test cycle that exercises a vehicle at low power for two minutes (low exhaust mass flow) and then at high power for two minutes (high exhaust mass flow). Throughout the four minute period the mini-dilution tunnel would sample exhaust at a fixed flow rate, so that there would be no proportionality between total raw exhaust and the raw exhaust slipstream. If the concentration of a species in the dilute exhaust, averaged or integrated over the whole four minutes, were corrected for dilution and multiplied by the total vehicle raw exhaust

mass flow, the result would not reflect reality. Contribution of the low power segment would be overestimated and contribution of the high power segment would be underestimated. Perhaps, in a simple I&M procedure, such biasing could be neglected, but it can be substantial and would harm the defensibility of a procedure that failed to consider its effects in computing quantitative emissions values.

Instantaneous data gathered from a dilution tunnel with fixed dilution ratio may, however, be treated to yield a correct assessment of the emissions if the instantaneous data are used in combination with the instantaneous total exhaust mass flow rate. In real application, this would require a careful examination of both the time delays and diffusion that cause the analyzer signal and the exhaust mass flow rate signal to be misaligned. This is a difficult task that can at best receive an approximate solution.

If a TEOM were used to sample dilute exhaust from a mini-tunnel, either instantaneous TEOM data would need to be used to correct for varying exhaust gas flow, or the biasing discussed above would need to be endured if total TEOM mass captured over the cycle were used. Instantaneous TEOM data are substantially less reliable than an integral mass captured over a whole cycle.

In summary, mini-dilution tunnels are desirable where a full-scale tunnel is impractical. The tunnels may sample proportionally, in which case they are intensive in control hardware and costly. The tunnels may sample at a fixed rate, in which case data are biased for all but a steady-state test, unless software is developed to compensate reliably for varying exhaust gas flow. Also, such compensation is unlikely to be successful for TEOM measurement.

5 MEASUREMENT OF VEHICLE EXHAUST FLOW

5.1 Background

In cases where a full-scale tunnel is not used, in order to acquire mass emissions data, the vehicle raw exhaust mass flow rate may be measured. In the case of a proportionally sampling mini-dilution tunnel, the vehicle exhaust flow must be known to control the proportionality. In the case of raw gas measurement, the exhaust flow must be known directly to calculate mass emissions rates. If mass emissions data need not be known, for example where instantaneous emissions are expressed in g/gallon fuel or g/g(CO₂), the flow need not be measured.

Mass flow rate can be measured directly using momentum devices, or inferentially through volumetric flow meters and separate density measurements or computations. This section presents various methods for measuring gas flow rate through a heavy-duty diesel engine including the wide range of measurements necessary, contrast advantages and disadvantages of intake measurement versus exhaust flow rate measurement, discuss various instruments for their applicability, and make recommendations for both sensor placement and sensor choice.

Exhaust gas flow for heavy-duty diesel vehicles is well represented by the intake air mass flow, because air/fuel ratios for diesel engines are high and because some of the fuel mass is also lost

through leakage past the piston rings. This section therefore discusses mass measurement of either stream.

The mass flow rate could be measured in one of three general areas on the vehicle:

1. The intake, prior to any compressor (along with knowledge of the fuel flow rate)
2. After the compressor and inter-cooler but before the engine
3. In the exhaust stream

Each location has advantages and disadvantages. The exhaust is an obvious choice since it is the flow of this section that will contain the emissions to be monitored, and it is usually accessible. Installation of a sampling and measurement system to the exhaust is usually simple except in the case of twin stack trucks or low discharge transit buses. However, the types of instruments that can be employed in this section are limited due to the elevated temperature (~420°C) and presence of PM in the exhaust. The intake location is a cleaner, cooler environment, but for accurate exhaust flow rate prediction, care must be taken to estimate blow-by effects and mass of fuel added through the injectors. It is usual to employ engine intake flow measurement for the proportional control of mini-dilution tunnels in a laboratory setting. In addition, measurement at the intake would require the coupling of two separate systems to the vehicle: one for mass flow measurement, and one for measurement of exhaust species concentration. Also, intake mass measurement is limited by permitted in-line pressure drop. Typically, the intake can tolerate a total loss of about 18 inches of water while the exhaust may have about 40 inches of water pressure loss without dramatically affecting engine performance. The location between the intercooler and engine is the least likely to be favored for I&M because it represents intrusion into the vehicle and would slow the test throughput. The time delay during transient mass flow variations between a change in intake flow and the corresponding change in exhaust flow is of little concern, being at worst approximately 0.1 seconds.

5.2 Flow Rate Range

In measuring exhaust or intake flow, it is essential to realize that the variation of flow rates that will be encountered is substantial, both over the operating range of a single truck and between trucks of different sizes. The mass air flow may vary by almost an order of magnitude between idle and rated conditions, and the exhaust velocity will vary by a greater amount due to the effect of load on temperature. In the exhaust, absolute temperatures can vary by a factor of over 2 between idle and rated conditions. In this case, exhaust velocities can vary by a factor of up to 20. These values for flow ratios presented above are typical, rather than conservative. Smaller displacement heavy-duty engines have higher ratios of rated to idle speed, and boost pressures of Class 8 tractor engines have been steadily increasing by the year. It is conceivable that some future engines may have an exhaust velocity ratio exceeding 30, which challenges accurate exhaust flow measurement. The I&M program will also measure emissions from a wide variety of trucks. The ratio of exhaust mass throughput of a lightly powered medium heavy-duty vehicle to a Class 8 over the road highly powered truck may approach a ratio of four. It is evident that with most flow measurement technologies, an I&M program would need to have several differently sized flow meters (based on 4, 5, and 6 inch nominal exhaust sizes) on hand to cope with wide variation.

5.3 General Discussion of Flow Sensors

Repeatability and range are the most important attributes of a sensor. However, pressure loss in the fluid stream resulting from the addition of instrumentation should be minimized and rate of response to transient conditions should be maximized. Temperature and PM sensitivity and to some extent the measurement range will determine if the instrument may be used in the exhaust or if it is restricted to intake usage. Many of the sensor technologies discussed below require accompanying pressure and temperature measurements to compensate for varying density effects. Most flow sensors require a consistent velocity profile free from swirl effects. Ordinarily, this is achieved through a long section of pipe to permit fully developed flow. Many flow sensors employ a differential pressure measurement to sense the flow rate. During transient operation, systems that employ differential pressure transducers fed via probes and lines may fail to respond accurately to changing flow. Firstly, if the "dead volume" of the transducer, probe, and connecting tubing is too large, the response times of these systems will be slow. Secondly, if the two halves of the probe, tubing and dead volume associated with differential pressure measurement are mismatched, then the resulting signal will not faithfully represent differential pressure, but instead will be a corruption of absolute pressure and differential pressure during transients. If instantaneous flow rate is to be calculated using three sensors to measure simultaneously differential pressure, absolute pressure, and temperature, the three sensor systems must be matched in frequency response, or their differing responses must be considered in calculating the flow. A first order approximate correction may be considered using time lags, but the true behavior is more complex. This issue is compounded further when instantaneous emissions levels are required, because there will be lag times and residence time distributions for the gas analyzers that must be correlated in time with the mass flow rate and torque measurements.

Although it is desirable to consider the composition of the exhaust gas in computing thermodynamic gas properties, these properties do not vary substantially from those of air in the exhaust of a diesel engine. This statement assumes that no substantial condensation of water occurs in the exhaust, which may prove false under cold operating conditions. The most significant variation is in specific heat, which would be of interest only in addressing compressibility effects. Density and viscosity variations are dominated by temperature rather than by composition.

5.4 Humidity Effects

Gas composition, and hence density and compressibility relationships for the intake air will change due to relative humidity changes but this may be neglected in I&M applications since it will contribute less than 0.5% error.

5.5 Pressure Head Flow Sensors

Pressure head flow sensors include orifices, flow nozzles, and venturies. The principle behind these pressure differential devices is that the conservation of mass will hold true even when the geometry of the flow passage is changed. Of these types of devices, the venturi has the advantage of the lowest total in-line pressure drop while providing a high measurement pressure drop which improves instrument sensitivity. The permanent pressure loss of a "Herschel type" venturi can be 10-15% of the pressure differential for discharge cone angles of between 5 and 7

degrees or as much as 10-30% for a large discharge cone angle of 15 degrees. The pressure sample points for the venturi are in the sidewalls, upstream of the venturi and in the narrow throat, making for a robust, self-cleaning instrument. The typical industry venturi/pressure transducer system has a rangeability of about 3:1. The insufficient range favors intake placement and probably requires multiple pressure sensors with different operating ranges but similar overpressure limits to achieve the necessary full range.

The principle of the pitot tube is that the difference between the impact pressure in a flow-stream and the static pressure in the flow stream is proportional to the velocity squared and the gas density. From the measured velocity, the mass flow rates can be computed using cross-sectional area, fluid density and a velocity profile correction factor. Compressibility may be ignored below 60 m/s (200 ft/s). The very low differential pressure drop for gases at low velocities may require dual pressure transducers to span the range with accurate measurement. Rather than base the measurement on a single point sample in the flow stream which is sensitive to a uniform velocity profile, commercially available instruments favor an averaging multi-port sensor such as those produced by Annubar, Omega, and Kurz. The FPT 6000 series by Omega reports a repeatability of 0.1% of flow rate with a pressure drop of only 2.75 inches of water. The 93°C (200°F) maximum specification limits the use of this probe to the intake. The low sensitivity in the flow rate regime is a limiting factor. It is unknown at this time if a dual set of pressure transducers, each to cover part of the range, can satisfactorily address this concern. The transient time response due to the dead air volume between the ports and the sensors is of additional concern. Placement of pitot tubes in the exhaust has the further concern of PM blockage of the pressure ports. Since port-to-port flow is possible in these devices, blockage could be a significant source of measurement error.

5.6 Tracer Gas Method

One way in which to measure exhaust flow is by employing tracer gas methods. This method involves the use of a highly sensitive tracer gas and a sensor or flow meter. The tracer gas is injected into the exhaust flow, the mixed gas is sampled, and the concentration is analyzed and a flow rate can be determined. This is typically performed using a sector field mass spectrometer for the continuous analysis of the tracer gas in the exhaust gas and a mass flow controller that can inject the tracer gas at a constant rate. Adachi et al. (1997) completed a study in which helium was used as a tracer gas and injected using a mass flow controller at the intake manifold. An advantage of this tracer gas method is that a mass emission rate can be determined by multiplying the dry based gas concentration by the dry based flow rate.

There are several different gases that can be used as a tracer gas. A common tracer gas is helium. Horiba Instruments Inc. makes a Helium Trace Exhaust Gas Flow meter which can provide accurate, real-time measurements of exhaust flow in both transient and steady state modes of operation (Horiba, 2000). Helium has chemical stability in high temperature conditions and has no cross sensitivity between other gaseous constituents in the exhaust when measured by a mass spectrometer (Adachi et al., 1997). Another gas that can be used as a tracer is sulfur hexafluoride (SF₆). However, there is societal concern over SF₆ as a “greenhouse gas.” Sulfur hexafluoride is a chemically stable, non-toxic gas that can be detected to a very high sensitivity (Roetzer et al., 1996) and is also relatively inexpensive to purchase and ship. Hydrocarbons may also be used as

a tracer gas. However, injecting hydrocarbons into a diesel exhaust stream could yield inaccurate measurements of the hydrocarbons produced by the engine, thus making it a less desirable tracer gas to use.

Tracer gas methods can be used to measure accurately exhaust flow rate from an engine. The principles for determining flow rate using tracer gases are similar, mainly varying in the components of the tracer gas itself and the mass spectrometer or sensor used downstream.

5.7 Turbine Sensors

The turbine is a multi-vaned device occupying either the full pipe cross section or a small sampled location within it. The rate of spin is determined through a magnetic type pickup. Turbines are fairly linear with respect to fluid flow rate. Though their rangeability is about 100:1 for gas streams at high pressure, it is only 10:1 near atmospheric pressure. They are limited to intake air flow measurements due to elevated temperature and particulate sensitivities. Larger sensors will not have transient response and could cause pressure loss while smaller sensors may not be as accurate. Since the turbine is not a low insertion pressure drop device it could cause intake pressure drop for engines on the order of 18 inches of water.

5.8 Ultrasonic Flow Sensors

There are two types of ultrasonic flow sensors, one is a Doppler device relying on reflections from PM in the flow stream and the second is a time-of-flight type device which requires a transmitting and receiving transducer on opposite ends of a path at an acute angle to the moving fluid. The time of the propagating acoustic wave is proportional to the speed of the medium. Though literature indicates that this technique can be employed for gas streams, there are no commercially available instruments for high temperature exhaust gas streams. Ultrasonic meters enjoy the advantages of no pressure loss, a 25:1 range and 0.5% repeatability. Though the precision of ultrasonic meters may ultimately make it a good calibration tool, elevated temperature near the Curie point of the exhaust gases excludes it from exhaust usage. It should be noted that Flow Technology, Inc. has introduced an exhaust mass flow measurement system, Vertical E-Flow that reflects the efforts of American Industry/Government Emissions Research (AIGER) group. However, the vertical E-Flow system is limited to gasoline exhausts and can be used only in a test cell because of its large size.

5.9 Vortex Shedding Sensors

A bluff body in a flow stream will shed vortices alternately on either side at a frequency proportional to the fluid velocity. This is a principle known as the Van Karman effect. A vortex shedding meter measures the slight vibrations of the carefully designed bluff body to produce a wide range, linear flow measurement instrument.

Vortex shedding sensors are sensitive to vibration-induced errors near their natural oscillation frequency. However, a frequency of about 160 kHz is reported for one commercially available vortex shedding sensor and the only typical sources of vibration noise in this frequency range would be turbocharger vane transients or turbocharger shaft speeds.

A commercially available product for engine exhaust streams is available from J-TEC and can tolerate temperatures up to 538°C (1000°F). This company currently only produces 2" and 3" devices with a maximum throughput of 450 cfm, but they have demonstrated the feasibility in an exhaust stream device with a range of 45:1. The device's rated repeatability of $\pm 1\%$ of full-scale could indicate significant errors at the lowest flow rates. It has a 300 ms response time for analog output or 10 ms response time for frequency output.

A general vortex shedding sensor from Omega Engineering requires that the minimal flow velocity correspond to a Reynolds number of 5,000. The repeatability is 0.2% of reading but the maximum temperature of 300°C (572°F) restricts usage to the air intake.

A second vortex shedding sensor from J-TEC which has not been hardened for use in an exhaust stream characterizes itself as "Lo-flo." Its rangeability is 70:1 going from 43 m/s (140 ft/s) down to 0.6 m/s (2 ft/s), and has a repeatability of 0.5%.

5.10 Hot Wire Anemometers

A wire heated by electrical current in a flowing stream of cold fluid will tend to be cooled, thereby changing the resistance of the wire. Through the use of an electrical circuit, either the current through the wire is maintained constant and the resistance is measured or the resistance (and hence the wire temperature) is maintained constant and the current is measured; either result can be related to velocity of the fluid stream. The rangeability can vary from 0.15 m/s (0.5 ft/s) to supersonic with transient responses of about 10 μ s. The response time and the ruggedness of the sensor represent a trade-off since a very thin wire is necessary for the highest response times. Fairly rugged quick response systems are commercially available with the latest trend being toward mass integrated flow sensors that already compensate for varying temperature and pressure. The cooling principle limits the usage of hot wire anemometry to the intake.

A very precise instrument with pressure and temperature options is available from Omega with a repeatability of 0.2% of full-scale. It has a fairly quick response time of 500 ms. It is currently packaged as a portable instrument that would need to be modified for mounting in a pipe.

5.11 Estimation From Engine Parameters

It is possible to estimate mass flow through the engine if speed, displacement, and intake air density are known, but the method is sensitive to exhaust back pressure, which governs the mass of burned gas retained in the cylinder and the cylinder wall temperature, which alters volumetric efficiency due to heat transfer. In addition, volumetric efficiency varies from engine to engine and there is a need to measure both manifold air temperature and manifold air pressure with sufficient accuracy. The method is therefore approximate and requires intrusion into the engine.

5.12 Preferred Technology

Experimental efforts at West Virginia University (Fuller, 2001; Meyer, 2001) have confirmed that flow measurement is most accurate using either a venturi or annubar, with measurement of temperature, pressure, and differential pressure. The venturi may be favored where blocking of the annubar ports by PM is an issue.

6 ISSUES OF PORTABILITY

Of possible concern to the I&M program is the ease with which the equipment can be transported, erected or installed. The bulk of AC and DC dynamometer units precludes their use in portable application. The need for water-cooling will prove an encumbrance if water-cooled eddy-current units or water brake dynamometers are chosen, or if AC or DC dynamometers require water-cooled resistor banks. These issues favor the use of air-cooled eddy-current power absorbers in portable or transportable applications. The power requirements and size of full-scale dilution tunnels does not recommend them for portable or transportable use, unless true research grade data are required. Choice of analyzer type is not influenced by transportation concerns. Both I&M grade and research grade analyzers can be transported without harm if reasonable care is taken to prevent impact.

7 RECOMMENDATIONS

This section presents material as a preamble to the recommendations, and then provides prescriptions for two heavy-duty I&M systems.

7.1 Reported Units

If a vehicle and a chassis dynamometer are employed for the emissions measurement, the values for the test can be readily expressed in units of grams/cycle, grams/mile, grams/axle-hp-hr (g/ahp-hr), based upon integrated energy delivered to the rollers provided that the actual total mass of each emissions species is determined. Methods for obtaining accurate mass emissions measurements have been presented in Section 4 of this report. Units of g/mile are to be favored where the data are to have a secondary importance in inventory applications.

There is, however, an option of determining an average emissions level over a cycle in units of g/gallon of fuel. This is readily found by integrating the concentration of each regulated species over the cycle, and the concentration of CO₂ (or CO₂ plus CO plus HC) as a surrogate for fuel consumed, and dividing the species integrated concentration by the CO₂ integrated concentration. Although this will yield an average that is not properly weighted by exhaust mass flow rate, it will provide an excellent tool for the identification of high emitters, and weighting can be achieved a priori in formulating the test cycle. Similar weighting strategies are employed today in steady state multi mode cycle formulations. The advantage of this g/gallon approach is that no exhaust mass measurement need be made. It is interesting to note that the g/gallon data may still be used in an inventory context if vehicle fuel consumption is estimated.

If a modern vehicle has a standard data protocol output, that yields what is sometimes termed “broadcast torque” or “load percent”, or a fuel use rate, data can be processed to yield values in g/bhp-hr or g/gallon of fuel from this method. However, processing of “load percent” into brake power requires knowledge of the engine torque map. Attempts to download information from the vehicle will frustrate the program. Numerous different protocols exist, the information is absent on older vehicles, these signals may or may not account for idle load, fan and auxiliaries loads are unknown and the broadcast values are not necessarily very accurate. Therefore, for a high throughput of vehicles on an I&M system, use of emissions values gained without downloading information from the vehicle is essential.

It is also possible to estimate emissions in units of g/bhp-hr based upon a translation from g/gallon with an assumed engine fuel conversion efficiency, or from g/ahp-hr with an assumed drivetrain and tire loss efficiency. Translation from g/gallon becomes unreliable at light load, where engine frictional and pumping losses dominate. Translation from g/ahp-hr is made difficult because fan and auxiliary losses must be considered and because drivetrain efficiencies vary substantially. These approaches are at best approximate and limited to application at higher power levels.

7.2 Comments on Test Cycle

Three options exist in performing the I&M test.

1. The vehicle may be driven through a speed-time schedule, which is a well-documented practice. In this way the vehicle would employ gears during the test, reflecting realistic shifting emissions.
2. The driver may correspond to screen commands, such as a command to accelerate to a set speed as fast as possible, and then maintain that speed. This is similar to the concept of a test route now used widely in field evaluations for research purposes.
3. The vehicle may be operated through the test in a single gear, being brought to a test starting speed with the chosen gear selected before emissions are logged. This seeks to exercise the engine, rather than the vehicle, through a schedule, and is similar to work on test certification cycle mimicry performed previously at West Virginia University (McKain et al., 1998). It will not work as a procedure for most automatic transmission vehicles and, if engine based, will require torque maps or preliminary torque evaluations prior to execution.

For I&M purposes, if an inspector were to drive the vehicle, option (2) would be favored because it could be configured to elicit emissions closer to real life operation. However, it is likely that the vehicle's operator will drive the test. For this reason, and for ease of public understanding and acceptability, a simple speed-time trace, as in (1) should be favored. Option (3) is well suited as a tool for certification compliance screening, but will prove cumbersome to execute in practice and difficult for the public to understand.

It is likely, if (1) is chosen, that study will be required to yield a cycle for I&M. If there is a need to produce data that can be used directly for inventory evaluations, then the cycle should yield results expressed in g/mile, to avoid confusion with certification values. The cycle should be chosen to yield g/mile values that reasonably reflect real use, so that conflict with inventory is not perceived.

I&M compliance could also be assessed in the “not to exceed” engine operating zone, but it would be necessary to verify engine torque for this purpose. There is also interest in I&M “short tests” that seek to find high emitters rapidly on the dynamometer. For this thrust, it is first necessary to identify modes that most commonly precipitate high emissions. NO_x emissions are well characterized in all modes of operation, because for present day engines NO_x is nearly linearly proportional to fuel consumed. One exception is the case of “off-cycle” NO_x, which

may be elicited using a steady cruise period of sufficient length. PM emissions associated with over fueling arise during full load operation and during transients associated with rapidly increasing load. These modes may also be included separately in a “short test”, or may be elicited using a full power acceleration with shifting.

In the case where the only intent is to find high emitters, g/gallon remains an option.

Tests should be commenced and ended with idle operation to minimize time alignment concerns. Idle emissions length may be adjusted to reflect reality.

7.3 Proposed Systems

This section will present the proposed dynamometer and emissions measurement equipment for the heavy-duty I&M program. Two systems are recommended below. The first system is suitable for I&M and for inventory applications and requires exhaust mass flow measurement. The second is applicable particularly to I&M high emitter detection, and does not include exhaust mass flow measurement.

Both systems require identical chassis dynamometer hardware and analyzer hardware.

A suitable dynamometer system must be able to load the vehicle over a wide speed range and mimic both inertia and road load. It is suggested that two pathways are followed to achieve this goal.

Case (1):

A basic design for new dynamometer construction may be proposed, allowing some latitude for interpretation of the design.

Case (2):

Specifications for the performance of the chassis dynamometer design in (1) may be promulgated. In this way, existing dynamometers may be configured to meet the specifications, and may be enabled for I&M purposes with the addition of an analytic train for the emissions.

Case (2) would permit research grade dynamometers to be used immediately for I&M purposes, with just software added, and would allow research grade dynamometers to mimic the performance of the new design proposed in (1).

The design in (1) should be configured using air-cooled eddy-current power absorbers which allow transient cycle operation and dissipate heat with low utility requirements. Although flywheels are desirable in some applications, the need to couple and decouple flywheels to correspond with test weights is undesirable. Power should be taken from the wheels with rollers of 16 to 20 inch diameter to avoid wheel slipping at low roller diameters. Larger diameter rollers are desirable for reduction of tire deformation, but increase the height of a dynamometer to a degree that would challenge portability. At least two major dynamometer manufacturers (Clayton Dynamometer and Mustang Dynamometer) have produced heavy-duty dynamometers meeting these criteria, and clearly many additional manufacturers are capable of doing so.

Existing heavy-duty chassis dynamometer products, designed to handle both single and tandem axle configurations, employ six rollers, with four rollers employed for the only or forward-rear axle, and two for the rear-rear axles. The four forward rollers cradle the drive wheels permitting rapid vehicle positioning, and the power absorbers are driven by the rollers. Without flywheels, full retarding torque may not be applied at very low speeds, but it will be sufficient for loading over an acceleration ramp likely to be present in the final I&M test schedule.

The heavy-duty chassis dynamometers that are already produced include hardware to prompt the driver for the cycle, log data and control the eddy-current power absorbers.

Current BAR emissions measurement devices are unsuited to direct application in the heavy-duty diesel arena. Analyzers should be research grade, sampling from dilute exhaust gas. Clearly the gases that must be measured are NO_x (because NO_x emissions from diesel vehicles are high on an energy-specific basis) and HC (because of toxics concern), but it is likely that CO will be measured even though CO emissions from diesel engines are usually very low in value. It is recommended that CO₂ should be measured. There are at least four major manufacturers of research grade gaseous emissions instruments. The CO and CO₂ analyzers employ NDIR technology, the HC analyzers employ FID and the NO_x analyzers employ chemiluminescent sensors. The use and reliability of these analyzers is well established.

PM should be measured using a TEOM. Filters record mass emitted directly, but cannot be handled in a timely fashion. Other PM analysis instruments may measure aspects of PM, but it is difficult to infer PM mass from their measurements for a broad range of vehicle types, model years and fuel types. The TEOM is the only instrument considered that provides a continuous output of PM mass collected from a stream. The TEOM should sample from dilute exhaust.

The difference between the two systems proposed lies in the exhaust dilution. Figure 8.2-1 shows the arrangement (System 1) that should be used when actual mass emissions must be known, where units of g/mile are required, and when the results might have direct inventory application. In this case a commercially available proportionally sampling mini-dilution tunnel should be used. Such a dilution system is complex, but schematically it includes the exhaust mass flow measurement device, controller, mass flow controllers and dilution tunnel illustrated in Figure 8.2-1. Data from this system can be given in g/mile. The commercially available mini-dilution tunnels presently marketed base their proportional sampling on flow rates of engine intake air and fuel. For the I&M application, it is desirable to connect only to the truck exhaust pipe, and so exhaust flow must be used for proportional flow control of the slipstream. In this case, exhaust flow should be measured using a venturi. This decision was made based upon recent studies conducted by the investigators and their co-workers. Since exhaust flow rates will vary widely, it will prove necessary to have flow measuring devices configured for different ranges and selectable by the operator according to engine displacement or power rating.

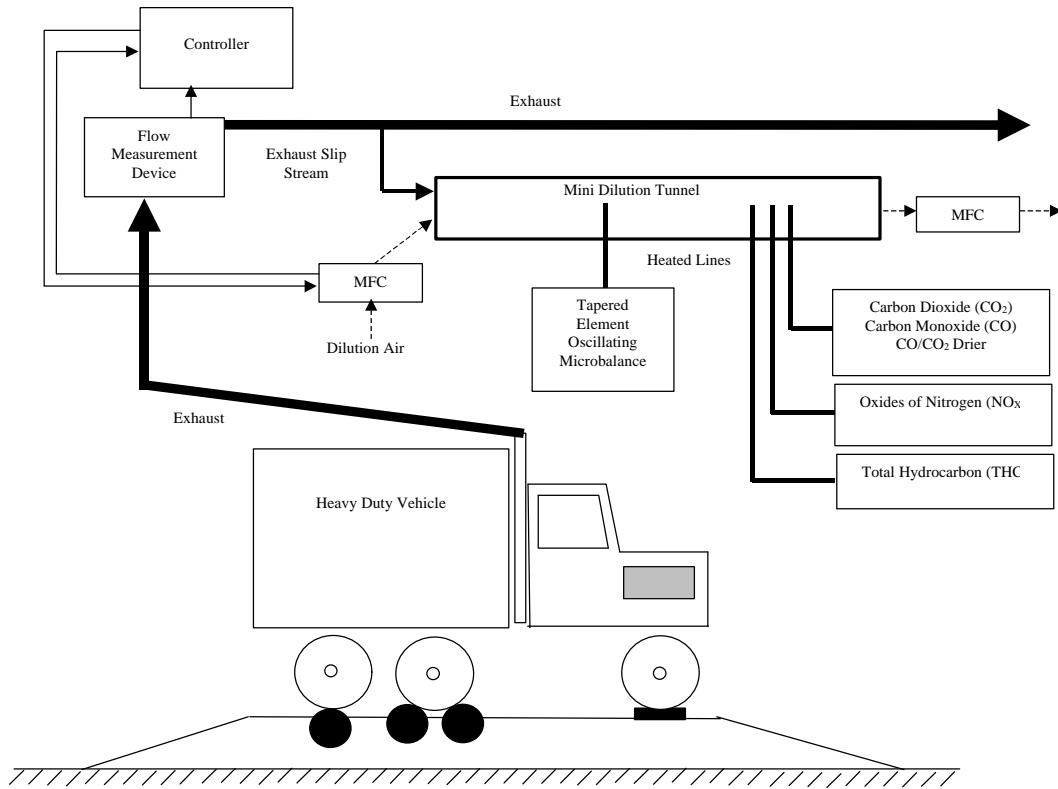


Figure 8.2-1. System 1 includes the exhaust mass flow measurement device, controller, mass flow controllers and dilution tunnel.

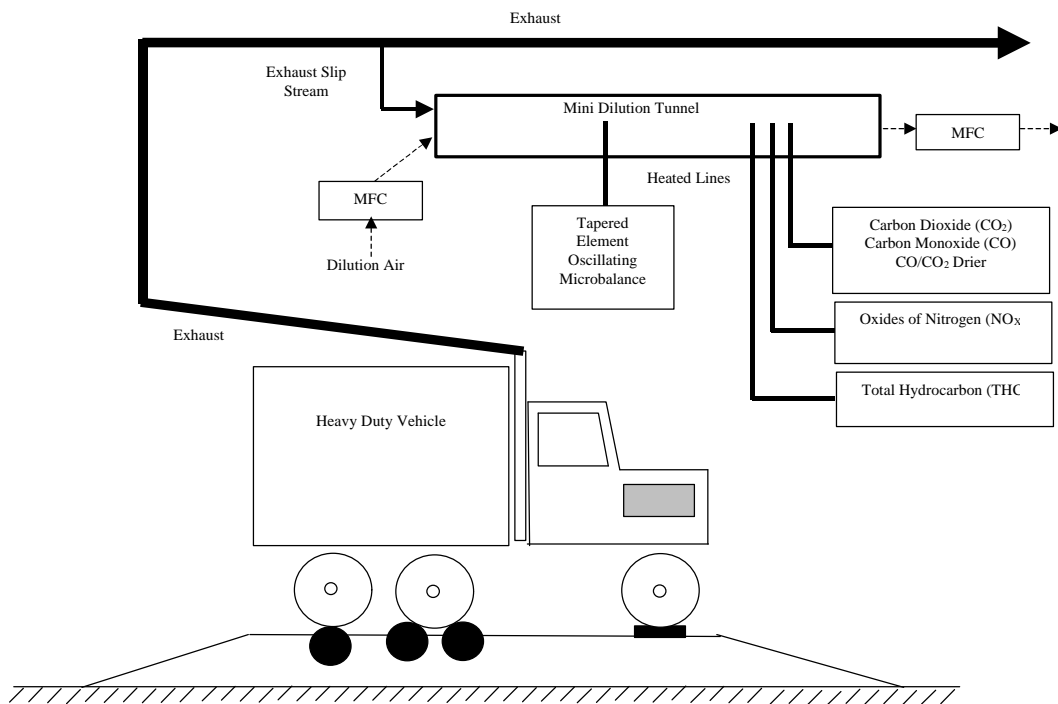


Figure 8.2-2. System 2 does not incorporate any mass flow measurement device in the exhaust. The mini-dilution tunnel is of the constant dilution ratio type, with two mass flow controllers setting fixed flow rates for dilute exhaust and dilution air.

The second system (System 2), illustrated in Figure 8.2-2, does not incorporate any mass flow measurement device in the exhaust. The mini-dilution tunnel is of the constant dilution ratio type, with two mass flow controllers setting fixed flow rates for dilute exhaust and dilution air. Exhaust slipstream mass flow rate is therefore fixed. Results would be in units of g/gallon, computed from averages of regulated emissions and CO₂ concentrations over the cycle.

8 COST ESTIMATION FOR I&M SYSTEMS

Data from two dynamometer manufacturers were selected for the final cost comparison. Their systems were found to be comparable. The dynamometers are able to absorb up to 750 and 1200 horsepower respectively. Each system utilizes two, eddy-current power absorbers for loading the test vehicle. Each system uses a split six-roller configuration (4 rollers for the drive axle) to accommodate both single axle and tandem axle trucks. A maximum weight of 26,000 pounds per axle is observed. The dynamometers are capable of speeds greater than 100 mph. Each system employs motor systems for vehicle coast down and system calibration. Each system requires 80 psi shop air for operation. The systems require 110 VAC, 220 VAC single phase and 220 VAC three phase electrical services.

Each system provides a computer for dynamometer control and data acquisition. Software to control the dynamometer is included with each package. The capacity of the computer system is sufficient to integrate a proportional sampling system control and data acquisition.

8.1 System Price Totals

Costs of the two integrated dynamometer and sampling systems are presented for comparison below. System 1 includes the integration of the selected dynamometer test bed and a proportional sampling system. A complete emissions analysis bench has been selected and included in each system. Analyzers have been priced individually. Cost of flow measurement has been estimated from known component costs. Cost of system integration, including software preparation, is difficult to estimate, but was set at \$25,000 based on the assumption of a minimum production of 10 units. The itemized costs were determined in May 2001.

System 1

Prop. Sampling System	\$ 100,000
Dynamometer Test Bed	\$ 80,000
TEOM	\$ 33,000
Carbon Dioxide (CO₂)	\$ 12,000
Carbon Monoxide (CO)	\$ 12,000
CO₂ / CO Dryer	\$ 1,500
Oxides of Nitrogen (NO_x)	\$ 12,500
Hydrocarbon	\$ 26,000
Heated lines and Probes	\$ 10,000
Exhaust Piping	\$ 1,500
Flow Measurement	\$ 8,000
Analyzer Bench Integration	\$ 10,000
System Integration	\$ 25,000
<i>System 1 Total</i>	\$ 331,500

Table 8.1-1. Cost itemization of System 1 as of May 2001.

8.1.1 System 2

System 2 is designed without the integration of the Sierra Proportional Sampling System. For this system, a proportional sampling system will be constructed from off the shelf components and a simple mini-tunnel design. Assembling the system will require mass flow controllers, a full flow exhaust measurement system, and the fabrication of the simple mini-tunnel. The development of a control system for the mass flow controllers, flow data acquisition, and dynamometer system has been included.

Dynamometer Test Bed	\$ 80,000
Mini-Tunnel	\$ 10,000
Mass Flow Controllers	\$ 5,000
Flow Control	\$ 2,500
TEOM	\$ 33,000
Carbon Dioxide (CO₂)	\$ 12,000
Carbon Monoxide (CO)	\$ 12,000
CO₂ / CO Dryer	\$ 1,500
Oxides of Nitrogen (NO_x)	\$ 12,500
Hydrocarbon	\$ 26,000
Heated lines and Probes	\$ 10,000
Exhaust Piping	\$ 1,500
Analyzer Bench Integration	\$ 10,000
System Integration	\$ 25,000
<i>System 2 Total</i>	<i>\$ 241,000</i>

Table 8.1-2. Cost itemization of System 2 as of May 2001.

REFERENCES

Abdul-Khalek, S. I. and Kittelson, D. B., "Diesel Trap Performance: Particle Size Measurements and Trends" *SAE Technical Paper 982599*, 1998.

Abramowitz, M. and Stegun, I. A., "Handbook of Mathematic Functions", Applied Mathematics Series 55, *U.S. Department of Commerce, National Bureau of Standards*, March 1965.

Adachi et al., "Measurement of Exhaust Flow Rate: Helium Trace Method with a Mass Spectrometer," SAE Paper 971020, 1997.

Bischof, O.F., "The SMPS, the Most Widely Used Nanoparticle Sizer", ETH Workshop, 7 August 1998.

Burtscher, H. and Siegmann, H. C., "Aerosols, Large Clusters In Gas Suspensions", *Springer Series in Chemical Physics*, n 56, p 272-289, 1994.

Butler, J. W., Gierczak, C. A., Jesion, G., Stedman, D. H., and Lesko, J. M., "On-Road NOx Emissions Intercomparison of On-Board Measurements and Remote Sensing," Final Report, Coordinating Research Council, Inc., Atlanta, GA, CRC Report No. VE-11-6, 1994.

Byrd, R. L., 1996, "Measurement of Smoke Opacity and Particulate Matter from Heavy Duty In-Use Diesel Powered Vehicles", M.S. Thesis, Dept. of Mech. and Aero. Eng., West Virginia University, Morgantown, WV.

Clark, N. N., Jarrett, J. P., Atkinson, C. M., "Field Measurements of Particulate Matter Emissions, Carbon Monoxide, and Exhaust Opacity from Heavy-Duty Diesel Vehicles," Journal of the Air & Waste Management Assoc., Vol. 107, pp. 84-93, 1999.

Coulson, J. M., Richardson, J. F.; "Chemical Engineering", *Pergamon Press, New York, NY 10010*, Vol. 1, Third Edition (SI Units), 1977. pp 268-74.

Dalzell, W. H.; Sarofim, A. F., "Optical Constants of Soot and Their Application to Heat-Flux Calculations", *ASME Journal of Heat Transfer*, 1969, vol. 91, no. 1, p 100-104.

Environmental Protection Agency, Code of Federal Regulations, Title 40 Part 86 Subpart N, Office of the Federal Register National Archives and Records Administration, July 1,1998.

Fuller, A. D., 2001, "Flow Rate Measurement System for a Mobile Emissions Measurement Syster", M.S. Thesis, Dept. of Mech. and Aero. Eng., West Virginia University, Morgantown, WV.

Gautam, M., Mehta, S., Clark, N.N., Lyons, D., "Size Distribution of In-use Heavy-duty Particulate Emissions", Final Report to NREL, Sub-contract No. XCI-8-17077-01, 1999.

Gautam, M., Byrd, R.L., Carder, D.K., Banks, P.D. and Lyons, D.; "Particulate Matter and Smoke Emissions from In-Use Heavy-Duty Vehicles", *Journal of Environmental Science and Health*, Part A, A35 (4), pp. 557-573, 2000.

Gilbert, M. S. and Clark, N. N., "Measurement of Particulate Matter From Diesel Engine Exhaust Using a Tapered Element Oscillating Microbalance", in review.

Graze, R. R. Jr., "Development of a Miniaturized, Dilution-Based Diesel Engine Particulate Sampling System for Gravimetric Measurement of Particulates", *SAE Technical Paper 931190*, 1993.

Hunt, A.J.; Quinby-Hunt, M.S.; and Shepherd, I.G., "Diesel Exhaust Particle Characterization by Polarized Light Scattering", *SAE Technical Paper 982629*, 1998.

Jarrett, R. P., Clark, N. N., Gilbert, M. S. and Ramamurthy R., "Evaluation and Correction of Moisture Adsorption and Desorption From A Tapered Element Oscillating Microbalance", *Journal of Powder Technology*, in press, 2001.

Jarrett, R. J., 2000, "Evaluation of Opacity, Particulate Matter, and Carbon Monoxide From Heavy-Duty Diesel Transient Chassis Tests", M.S. Thesis, Dept. of Mech. and Aero. Eng., West Virginia University, Morgantown, WV.

Jones, B. L.; Stollery, J. D.; Clifton, M. J.; and Wylie, T. F., "In-Service Smoke and Particulate Measurements", *SAE Technical Paper 970748*, 1997.

Kelly, N. A. and Groblicki, P. J., "Real-world emissions from a modern production vehicle driven in Los Angeles," *Journal of the Air & Waste Management Association*, Vol. 43, No. 10, 1993.

McKain, D. L., Clark, N. N., McDaniel, T. I., and Hoppie, J. A., "Chassis Test Cycle Development for Heavy-Duty Engine Emissions Test Compliance," *SAE Technical Paper No. 980407*, 1998.

Meyer, E. T., 2001, "Evaluation of Exhaust Flow Rate Measurement Techniques for a Mobile Emissions Monitoring System", M.S. Thesis, Dept. of Mech. and Aero. Eng., West Virginia University, Morgantown, WV.

Modest, M. F., *Radiative Heat Transfer*; McGraw Hill, Inc.; New Jersey, 1993, p 385-400.

Okrent, D. A., "Optimization of a Third Generation TEOM Monitor for Measuring Diesel Particulate in Real-Time," *SAE Paper 980409*, 1998.

Rickeard, D. J.; Bateman, J. R.; Kwon, Y. K., "Exhaust Particulate Size Distribution: Vehicle and Fuel Influences in Light Duty Vehicles", *SAE Technical Paper 96198*, 1996.

Roetzer et al., "Measurement of the Contribution of a Single Plant to Air Pollution using the SF₆ Tracer," International Conference on Air Pollution-Proceedings Monitoring, Simulation and Control Proceedings of the 1996 4th International Conference on Air Pollution, Computational Mechanics, Inc., Billerica, MA, 1996. pp. 527-536.

SAE Surface Vehicle Recommended Practice, "Snap-Acceleration Smoke Test Procedure for Heavy-Duty Diesel Powered Vehicles", *SAE J1667*, 1996.

Shore, P. R., Cuthbertson, R. D., "Application of a Tapered Element Oscillating Microbalance to Continuous Diesel Particulate Measurement," *SAE Paper* 850405, 1985.

Stephens, R. D., Mulawa, P. A., Giles, M. T., Kennedy, K. G., Groblicki, P. J., Cadle, S. H., and Knapp, K. T., "An Experimental Evaluation of Remote Sensing-Based Hydrocarbon Measurements: A Comparison to FID Measurements," *Journal of Air & Waste Management*, Vol. 46., No. 2, 1996.

Van de Hulst, H. C., "Light Scattering by Small Particles", *John Wiley & Sons, Inc.* New York, 1957.

Whitby, R., Gibbs, R., Johnson, R., Hill, B., Shimpi, S. Jorgeson, R., "Real-Time Diesel Particulate Measurement using a Tapered Element Oscillating Microbalance," *SAE Paper* 820463, 1982.

Wiscombe, W. J., "Improved Mie Scattering Algorithms", *Applied Optics*, 1980, vol. 19, p 1505-1509.

9 ACKNOWLEDGEMENTS

This research was performed under contract with the California Air Resources Board for support under ARB contract #94-347. The statements and conclusions in this paper are those of WVU and not necessarily those of the California Air Resources Board. The mention of commercial products, their sources, or their use in connection with material reported herein is not to be construed as actual or implied endorsement of such products. Several West Virginia University researchers, including Gregory Thompson, Ronald Jarrett and Daniel Carder, contributed to the research and writing that constitute this report, and their contributions are acknowledged.